Mapping the Spacetime Metric with a Global Navigation Satellite System – extension of study: Recovering of orbital constants using inter-satellites links

Final Report

Authors: Andrej Čadež[1], Uroš Kostić[1], Pacôme Delva[2] and Sante Carloni[3]
Affiliation: [1]Faculty of Mathematics and Physics, University of Ljubljana
[2]SYRTE, Paris Observatory, Pierre and Marie Curie University
[3]Advanced Concepts Team, European Space Agency

Date: January 11th, 2011

Contacts:

Andrej Čadež
Tel: +38(0)14766533
Fax: +38(0)12517281
e-mail: andrej.cadez@fmf.uni-lj.si

Advanced Concepts Team
Tel: +31(0)715654192
Fax: +31(0)715658018
e-mail: act@esa.int

Available on the ACT website
http://www.esa.int/act

Ariadna ID: 09/1301 CCN
Study Type: Standard
Contract Number: 22709 CCN

Contents

List of Figures

1 Introduction

The need for defining our position in space and time is an ancient one and its realization has developed in millennium according to human understanding of the world and according to technology available to further such understanding. The commonly used global coordinates, the geographic longitude and latitude, or the astronomical right ascension and declination were carefully defined with respect to Earth rotation axis and a point on the equator, conveniently chosen in such a way that it can be most easily and accurately realized by observation. Much later, with the development of dynamics, the height was recognized as the third coordinate, dynamically equivalent to the two horizontal coordinates, but singled out as the coordinate in the direction of gravity. Finally, time became a full fledged coordinate only about a hundred years ago with the development of general relativity. Until 1998, the fundamental catalogues of stars used as fiducial points were a realization of a dynamical reference frame, based on a dynamical theory of motion in the Solar System. However, since 1998, the recommended reference system is a kinematic reference frame, based on the observation of extra-galactic radio sources. This reference frame proved to be closer to an inertial frame than the previous one. The noise floor of ICRF2 has been shown to be around 40 μas, and its stability within 10 μas (Petit et al. 2010). This corresponds to around 20 cm accuracy at typical GNSS altitude. Ephemerides still contribute to build reference frames, and are now aligned with ICRF2.

However, the dynamical reference frame, based on motion of planets and probes in the Solar System suffers some difficulties. First of all observations are done from Earth, so one needs a model of Earth rotation and deformations to reduce the data. Moreover, some parameters are not well-known, like the mass of asteroids. We propose to construct a dynamical reference system based on the motion of satellites around Earth (GNSS constellation) and electromagnetic links between them. This construction will be sufficient to solve the problem of positioning, and at the same time determining the spacetime geometry around Earth.

In this report, we study the relation between some preferred global coordinates and dynamically defined coordinates. We will show that Autonomous Basis of Coordinates (ABC) can precisely be defined within a framework consisting of dynamical description of GNSS system satellites and the description of light propagation between satellites.

Autonomous Basis of Coordinates can be extended in space via emission coordinates, if dynamics of light propagation is known throughout space. The dynamics of satellites of a GNSS constellation is well understood, since they move in the local gravitational field, dominated by that of the Earth, including contributions from other external bodies, such as the Moon, Sun and planets, while their mutual interaction may be neglected due to their very small mass compared to the Earth and to other perturbing bodies. Furthermore, it was shown in the previous report that stochastic forces acting on satellites can be considered as small. Therefore, it is possible to accurately describe satellite dynamics by Hamilton's formalism, where the system Hamiltonian is the sum of non-interacting Hamiltonians, having the same form for each satellite. Thus, the motion of the constellation through space-time can be considered as a Hamiltonian flow, where each member of the flow is characterized by seven constants of motion. The flow is completely specified, if all the constants are known.

The application of the above approach requires the Hamiltonian to be expressed in specific generalized coordinates, such as those tied to extra-galactic radio sources (ICRS). Therefore, the scale of validity of such application depends on the accuracy by which the Hamiltonian can be written with respect to coordinates defined outside dynamical framework. Here we propose an original approach to the definition of coordinates: inter-satellites links continuously refine orbital information, thus improving the hamiltonian and constants of motion of satellites, and finally the global coordinates.

The two main ingredients of this framework are constants of Hamiltonian flow and the Hamiltonian itself. In a relativistic framework the Hamiltonian applies to both satellite dynamics and propagation of light. The Hamiltonian describing the dynamics of GNSS satellites is rather well known, especially from the point of view of Newtonian and post-Newtonian description. On the other hand, the constants of motion of satellites are relatively much less accurate, because they depend on launching conditions and must be measured and remeasured after satellites are put in orbit and may also change after a period of time due to stochastic perturbations on satellites or even due to small unknown perturbations in the Hamiltonian producing secular terms. Therefore, this report focuses on a mechanism for determining constants of motion of a constellation of satellites moving in a given gravitational field. We study three examples:

i) satellites move and light propagates in Minkowski space-time,

ii) satellites move according to Kepler's laws, light propagates with velocity c with respect to the Keplerian frame and,

iii) satellites move and light propagates in the Schwarzschild space time.

We justify this step by step approach by noting the result of dynamical perturbation analysis, which states that solutions of equations of motion with a perturbed Hamiltonian can be expressed in terms of solutions of a simpler unperturbed Hamiltonian in such a way that the constants of motion of the unperturbed Hamiltonian become slowly varying functions of time. It will become clear, however, how the slow variance of constants of motion can be detected and used to construct ever more precise Hamiltonian.

The ABC concept 2

A GNSS is a system of satellites in space emitting precise timing signals, often called emission coordinates (Coll and Pozo 2006; Coll et al. 2009), for the purpose of providing a local inertial coordinate basis in space-time. In order to determine his space-time position with respect to this basis, an observer must receive four proper times emitted by four different satellites, his emission coordinates, at a particular moment of his time, and be able to calculate the local inertial coordinates of the four satellites as a function of their emission coordinates. If more than four emission coordinates are received by an observer, then the positioning problem is over determined. In order for the GNSS system basis to be self consistent, all combinations of emission coordinates, received at any event in space time, must give the same four local inertial coordinates for this event. As emphasized above, the main constraint on self consistency of a GNSS system comes from the precision of constants of motion. Here we propose that the constants of motion be determined and checked internally by the GNSS system in such a way that each satellite checks its own position as any other observer with respect to all the other satellites, i.e. in addition to emitting its proper time, each satellite also receives other satellite's emission coordinates and makes its information available to the central GNSS control (Arona et al. 2006; Rodríguez-Pérez et al. 2011).

2.1 Notations

The following notation, illustrated in Fig. 2.1 will be used:

$S^i[k]$	future light cone of k-th signal sent by satellite i
$\bar{\tau}^i[k]$	proper time of satellite i when $S^i[k]$ was created
$\tau_i^j[k]$	proper time of satellite j when its world line crosses $S^i[k]$
$P^{ij} = \{\bar{\tau}^i[k], \tau_i^j[k]\}$	Pair of emission and reception proper times between satellites i and j (i emitter and j receptor).

The complete spacetime manifold will be denoted by $\mathcal{M}$, and submanifolds of $\mathcal{M}$ will be denoted by script letters $\mathcal{M}_4$ for a four dimensional submanifold, $\mathcal{V}$ for a three dimensional

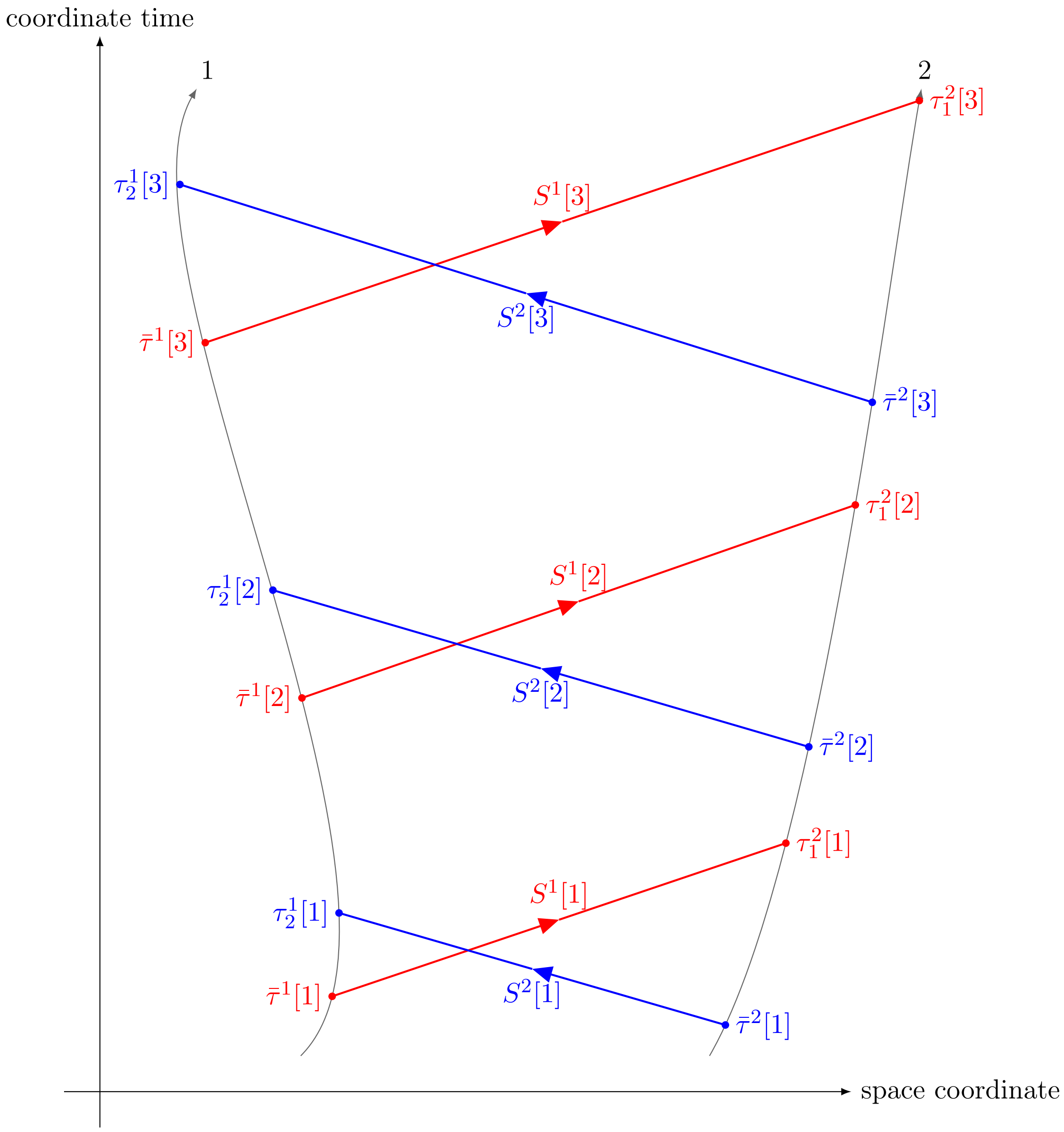

Figure 2.1: Signals sent and received by satellites labelled 1 and 2. The signals trajectories are located on the future light cones of the emission events. Red dots and blue dots denote equidistant proper time intervals when respectively signals $S^1[k]$ and $S^2[k]$ are emitted. $P^{ij}[k]$ represents the pair of emission and reception proper times between satellites 1 and 2, e.g. $P^{12}[3] = \{\bar{\tau}^1[3], \tau_1^2[3]\}$.

spacelike submanifold, $\mathcal{A}$ for a two dimensional submanifold, and $\mathcal{C}$ for curves in $\mathcal{M}$. Coordinates in $\mathcal{M}$ will be denoted by x^μ for $\mu = 0 \cdots 3$ and the metric in $\mathcal{M}$ will generally be given by the metric tensor $g_{\mu\nu}(x^\lambda)$. The Minkowski metric tensor will be used with the convention $\eta_{00} = -1$, $\eta_{0i} = 0$ and $\eta_{ij} = \delta_{ij}$, where roman indices run from 1 to 3. In the coordinate representation events $\mathcal{P}$ are expressed by the matrix of four coordinates as $\underline{x} = \{x^0, x^1, x^2, x^3\}$; curves $\mathcal{C}$ are expressed by a matrix of four coordinates as functions of a parameter (usually proper time) along the curve $\mathcal{C}$: $\underline{\xi}(\tau) = \{x^0(\tau), x^1(\tau), x^2(\tau), x^3(\tau)\}$; two dimensional submanifolds are expressed by a matrix of four coordinates as functions of two parameters; etc... Vectors, which can be thought of as tangents to curves, are generally written as $d\mathcal{C}/d\tau$, and in the coordinate representation they are expressed as $\underline{v} = \{\frac{dx^0}{d\tau}, \frac{dx^1}{d\tau}, \frac{dx^2}{d\tau}, \frac{dx^3}{d\tau}\}$. If the spacetime is foliated into 3-dimensional space and time, the vectors in the three dimensional foil $\mathcal{V}(t)$ are denoted as $\vec{a}$, or $\hat{e}$, if they are of unit length.

2.2 Minkowski space-time

In this section we illustrate the ABC concept with the simplest possible case: consider a GNSS constellation established very far from large masses, so that its satellites and light can be considered as moving in a Minkowski space-time. First we show how to retreive satellites mutual constants of motion from observations of emission coordinates. Then we define a procedure to construct a global inertial reference system based upon the emission coordinates for this simple case. Finally we give a geometrical interpretation that illustrates how this concept leads to a mesure of spacetime curvature. The more complex case involving gravitation and non-gravitational perturbations will contain small deviations from this procedure. A different but complementary approach has been defined in (Coll et al. 2010a,b).

2.2.1 Mutual constants of motion

The system Hamiltonian is the sum of terms

$$H = \frac{1}{2m}\left(-p_0^2 + p_x^2 + p_y^2 + p_z^2\right) \tag{2.1}$$

for each satellite. Each term is a constant of motion and it's value is $-\frac{1}{2}mc^2$. The motion of photons – signals propagating emission coordinates – is governed by the same Hamiltonian (2.1), that is also a constant of motion with value zero.

This Hamiltonian predicts linear motion of satellites and light:

$$ct = -\frac{p_0}{m}\tau + t_0 \ , \ x = \frac{p_x}{m}\tau + x_0 \ , \ y = \frac{p_y}{m}\tau + y_0 \ , \ z = \frac{p_z}{m}\tau + z_0 \tag{2.2}$$

with 7 independent constants of motion: t_0, x_0, y_0, z_0, p_x, p_y, p_z, while the conserved momentum p_0/m is determined by the constraint $H = -\frac{1}{2}mc^2$ for satellites or $H = 0$ for photons.

Consider two satellites i and j with constants of motion: ${}^it_0$, ${}^ix_0$, ${}^iy_0$, ${}^iz_0$, ${}^ip_x$, ${}^ip_y$, ${}^ip_z$, and ${}^jt_0$, ${}^jx_0$, ${}^jy_0$, ${}^jz_0$, ${}^jp_x$, ${}^jp_y$, ${}^jp_z$. One can always tie the local inertial frame to one of them. In this frame the satellite's at rest constants of motion are all zero: ${}^it_0 = 0$ – time is synchronized with proper time, ${}^ix_0 = 0$, ${}^iy_0 = 0$, ${}^iz_0 = 0$ – the satellite is at the origin of Minkowski frame, ${}^ip_x = 0$, ${}^ip_y = 0$, ${}^ip_z = 0$ – the satellite is at rest with respect to the frame chosen. This defines the temporal axis of the chosen Minkowski frame, but spatial axes have no preferred direction with respect to satellite i at rest. So the choice of spatial axes is left to the observer. One may, without loss of generality, choose the z axis in the direction of the 3-velocity of the next satellite j having non-zero velocity with respect to origin. The other spatial directions x and y, are perpendicular to j's velocity and to each other. Since the velocity of j is only in the direction z, the x and y coordinates of j's orbit must remain the same at all times. So we can again, without loss of generality, choose the orientation of axes x and y so, that y coordinate of j is zero. In this inertial frame the trajectories of satellites i and j can be expressed as follows:

$$\mathcal{C}_i : \underline{r}_i(\tau^i) = \{c\tau^i, 0, 0, 0\} \tag{2.3}$$

$$\mathcal{C}_j : \underline{r}_j(\tau^j) = \{c(\gamma_{ij}\tau^j + t_{ij}), x_{ij}, 0, \gamma_{ij}v_{ij}\tau^j + z_{ij}\} \tag{2.4}$$

where $\gamma_{ij} = (1 - {v_{ij}}^2/c^2)^{-1/2}$. It is convenient to introduce $v_{ij} = c\ \tanh(\xi_{ij})$, so that $\gamma_{ij} = \cosh(\xi_{ij})$.

The satellite i sends pairs of numbers $P^{ij}[k] = \{\bar{\tau}[k], \tau[k]\}$ to the central processing unit where, we repeat, $\bar{\tau}[k] = \bar{\tau}^j[k]$ is the proper time of satellite j when it emits signal $S^j[k]$, and $\tau[k] = \tau^i[k]$ is the proper time of satellite i when this signal is received; indices i and j on τ are ommited to keep the notation transparent. According to Eqs. (2.3) – (2.4), the event of emission of proper time $\bar{\tau}[k]$ has coordinates: $\mathcal{P}_{emiss} = \{c(\cosh(\xi_{ij})\bar{\tau}[k] + t_{ij}), x_{ij}, 0, \sinh(\xi_{ij})\bar{\tau}[k] + z_{ij}\}$, and the event of detection $\mathcal{P}_{det} = \{c\tau[k], 0, 0, 0\}$. Since these two events are on a light-like trajectory, their spatial distance is c times the temporal difference. So we can write:

$$c(\tau[k] - \cosh(\xi_{ij})\bar{\tau}[k] - t_{ij}) = \left(x_{ij}^2 + (\sinh(\xi_{ij})c\bar{\tau}[k] + z_{ij})^2\right)^{1/2} . \tag{2.5}$$

Squaring both sides, and grouping the terms, we obtain:

$$\begin{aligned} &\tau[k]^2 + \bar{\tau}[k]^2 - 2\cosh(\xi_{ij})\tau[k]\bar{\tau}[k] - \\ &\qquad - 2t_{ij}\tau[k] + 2\left(\cosh(\xi_{ij})t_{ij} - \sinh(\xi_{ij})\frac{z_{ij}}{c}\right)\bar{\tau}[k] + t_{ij}^2 - \frac{x_{ij}^2 + z_{ij}^2}{c^2} = 0 \ , \end{aligned} \tag{2.6}$$

a quadratic form with respect to variables $\bar{\tau}[k]$ and $\tau[k]$, i.e. the graph τ versus $\bar{\tau}$ is a hyperbola. Fitting all pairs $P = \{\bar{\tau}[k], \tau[k]\}$ to 2.5, one obtains the four coefficients ξ_{ij}, t_{ij}, x_{ij} and z_{ij}, which we call the four **mutual constants of motion**.

2.2.2 Construction of a reference system

The mutual constants of motion determine curves 2.4, which are edges of a two manifold $\mathcal{A}_{ij}$ spanned by light-like geodesics connecting the two satellites. Mutual constants of motion can be obtained for all $\binom{n}{2}$ pairs of n satellites in the constellation and thus determine $\binom{n}{2}$ 2-manifolds. All the 2-manifolds are joined along common edges, and can form a boundary of a four dimensional sub-manifold $\mathcal{M}_4$, as illustrated in Fig. 2.2 for a 2+1 dimensional case. Four satellites support 6 2-manifolds, that enclose a four dimensional volume. Coordinates

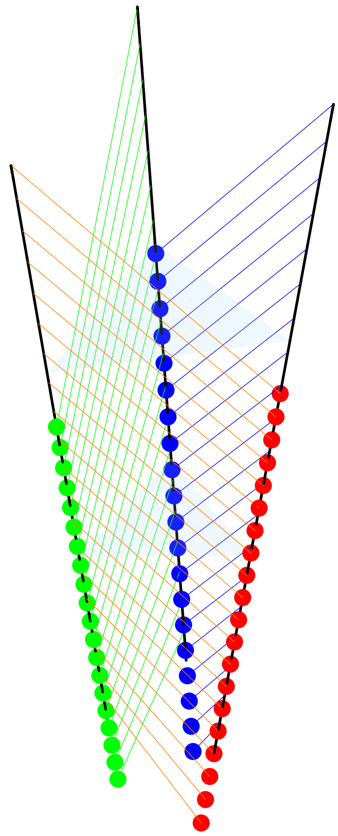

Figure 2.2: The three 2-manifolds formed by light-like geodesics connecting world lines of three satellites moving in 2+1 dimensional Minkowski space. The three 2-manifolds enclose the 3-manifold, which consists of triangles with the three satellites at their edges as they move in time.

of a GNSS must cover this volume and the metric must be such, that the geometry on the six bordering 2-manifolds $\mathcal{A}_{ij}$ agrees with the geometry determined by mutual constants of motion. Since we are assuming a flat space-time, it is most convenient to cover it with Minkowski coordinates. The temporal axis of a such common Minkowski frame may, without loss of generality, be chosen along the 4-velocity of one satellite, call it satellite 0, so that $t \equiv \tau^0$. This choice naturally foliates spacetime with 3-manifolds $\mathcal{V}(t)$, so that the 4-trajectories of other three satellites can be written in the global frame as:

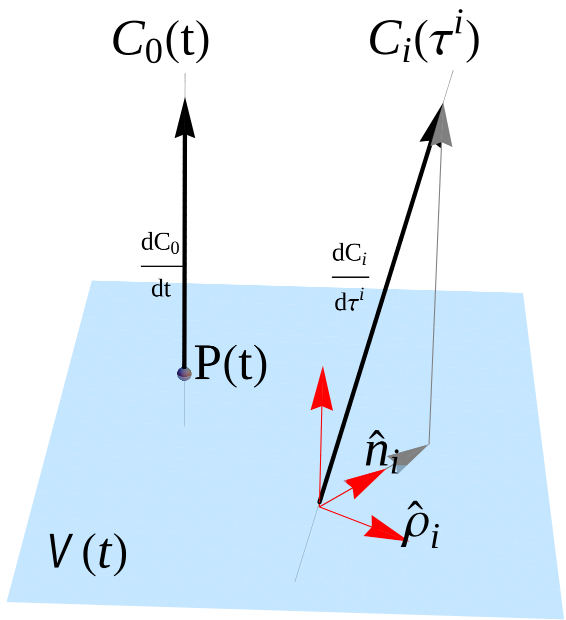

Figure 2.3: Spacetime is naturally foliated with 3-manifolds $\mathcal{V}(t)$, when considering satellite 0 as giving the time direction: $t \equiv \tau^0$. The 4-velocity of satellite i, $\frac{d\mathcal{C}_i}{d\tau^i}$, has a spatial part in $\mathcal{V}(t)$, along which we choose the unit vector $\hat{n}_i$. We choose the unit vector $\hat{\rho}_i$ so that it is contained in the 2-manifold $\mathcal{A}(0) \in \mathcal{V}(0)$ defined by $(P(0), \hat{n}_i)$, orthogonal to $\hat{n}_i$ and on $P(0)$ side.

$$\underline{r}_i(\tau^i) = \{c(\gamma_i \tau^i + t_i), x_i \hat{\rho}_i + \hat{n}_i \left(\gamma_i v_i \tau^i + z_i\right)\}, \tag{2.7}$$

where $\hat{n}_i$ is the unit vector along i's 3-velocity in $\mathcal{V}(t)$, and $\hat{\rho}_i \in \mathcal{V}(t)$ is orthonormal to $\hat{n}$ (see fig. 2.3). Note that $v_i = \tanh \xi_i$, x_i, z_i and t_i are mutual constants of motion of satellite i with respect to the origin, thus they are calculable on board of satellite 0 from data pairs

$P^{i0}[k]$. However the directions $\hat{n}_i$ and $\hat{\rho}_i$ can only be specified with respect to directions to other satellites. Their relations can be determined by the central processing unit, which has access to all data available in the system. In the common Minkowski frame the equation 2.5 can be written in the form (again omitting indices i and j on τ):

$$\begin{aligned}
&\tau[k]^2 + \overline{\tau}[k]^2 - 2\tau[k]\overline{\tau}[k]\left[\cosh\xi_i \cosh\xi_j + \sinh\xi_i \sinh\xi_j \hat{n}_i \cdot \hat{n}_j\right] \\
&+ 2\tau\left[\cosh\xi_i\left(t_i - t_j\right) + \sinh\xi_i \frac{1}{c}\left(x_j\hat{\rho}_j\cdot\hat{n}_i + z_j\hat{n}_i\cdot\hat{n}_j - z_i\right)\right] \\
&+ 2\overline{\tau}\left[\cosh\xi_j\left(t_j - t_i\right) + \sinh\xi_j \frac{1}{c}\left(x_i\hat{\rho}_i\cdot\hat{n}_j + z_i\hat{n}_i\cdot\hat{n}_j - z_j\right)\right] \\
&+ \left(t_i - t_j\right)^2 - \frac{1}{c^2}\left[x_i^2 + x_j^2 + z_i^2 + z_j^2 - 2x_i\hat{\rho}_i\cdot\left(x_j\hat{\rho}_j + z_j\hat{n}_j\right) - 2z_i\hat{n}_i\cdot\left(x_j\hat{\rho}_j + z_j\hat{n}_j\right)\right] = 0
\end{aligned} \tag{2.8}$$

Equations 2.6 and 2.8 express the same truth in two different systems of coordinates, therefore they represent the same hyperbola between τ and $\overline{\tau}$. Thus, the coefficients of quadratic forms 2.6 and 2.8 must be the same, which requires the following four equations for each pair $i-j$ to be satisfied:

$$\begin{cases}
\cosh(\xi_{ij}) = \cosh(\xi_i)\cosh(\xi_j) + \sinh(\xi_i)\sinh(\xi_j)\hat{n}_i\cdot\hat{n}_j \\
t_{ij} = \cosh(\xi_i)\left(t_j - t_i\right) - \frac{1}{c}\left[(x_j\hat{\rho}_j + z_j\hat{n}_j)\cdot\hat{n}_i - z_i\right]\sinh(\xi_i) \\
\cosh(\xi_{ij})t_{ij} - \frac{1}{c}\sinh(\xi_{ij})z_{ij} = \cosh(\xi_j)\left(t_j - t_i\right) + \frac{1}{c}\left[(x_i\hat{\rho}_i + z_i\hat{n}_i)\cdot\hat{n}_j - z_j\right]\sinh(\xi_j) \\
t_{ij}^2 - \frac{1}{c^2}\left(x_{ij}^2 + z_{ij}^2\right) = \left(t_i - t_j\right)^2 - \frac{1}{c^2}\left[x_i^2 + x_j^2 + z_i^2 + z_j^2\right. \\
\qquad\qquad \left. -2x_i\hat{\rho}_i\cdot\left(x_j\hat{\rho}_j + z_j\hat{n}_j\right) - 2z_i\hat{n}_i\cdot\left(x_j\hat{\rho}_j + z_j\hat{n}_j\right)\right] ,
\end{cases}$$

The unknowns, scalar products: $\hat{n}_i\cdot\hat{n}_j$, $\hat{n}_i\cdot\hat{\rho}_j$, $\hat{n}_j\cdot\hat{\rho}_i$ and $\hat{\rho}_i\cdot\hat{\rho}_j$, can be calculated from these equations. Finally one can choose the spacelike triade of orthonormal unit vectors along the Minkowski basis and express all $\hat{\rho}_i$ and $\hat{n}_i$ in this basis.

2.2.3 Toward a measurement of spacetime curvature

One can also look at the problem of reconstruction of constants of motion from a more geometrical point of view. The orbits (3-trajectories) of satellites can be expressed in the common frame as position vectors with respect to common time t:

$$\vec{r}_i(t) = x_i\hat{\rho}_i + \hat{n}_i\left(v_i(t - t_i) + z_i\right) , \tag{2.9}$$

where $\hat{\rho}_i$ and $\hat{n}_i$ are constant, orthogonal unit vectors.

Consider three satellites: 1, 2, and 3, defining a triangle contained in $\mathcal{V}(t)$ at each moment

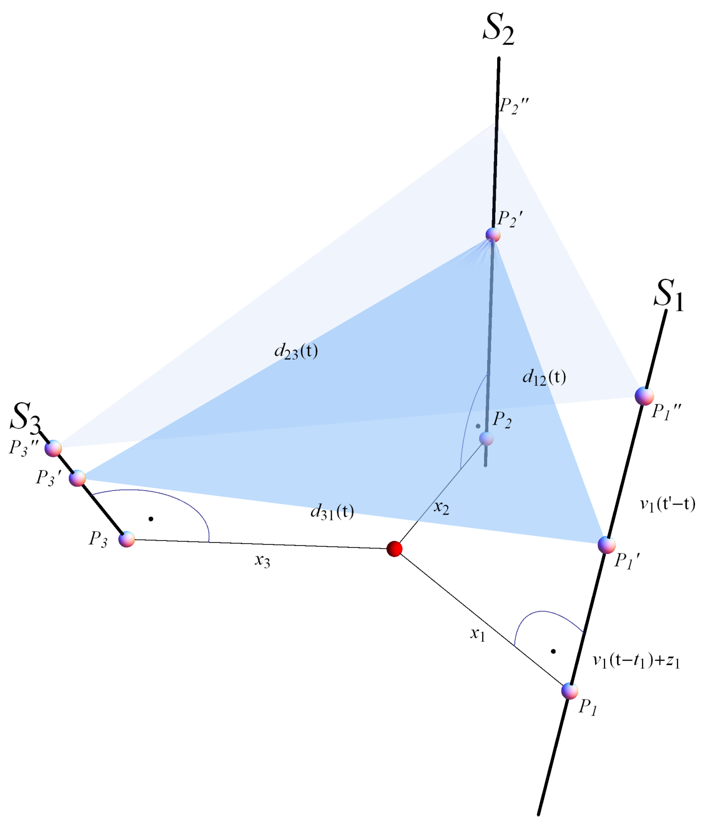

Figure 2.4: Orbits of satellites S_1, S_2 and S_3 with respect to satellite S_0 (red sphere), which is at rest with respect to the global Minkowski frame. Triangles $\mathcal{P}_1'$, $\mathcal{P}_2'$, $\mathcal{P}_3'$ and $\mathcal{P}_1''$, $\mathcal{P}_2''$, $\mathcal{P}_3''$ connect the positions of the three satellites as they are at moments t and t', respectively, with respect to the global Minkowski time. Distances x_1, x_2 and x_3 are the closest approach distances of satellites 1,2 and 3 to satellite 1. The sides $v_1(t-t_1)+z_1$ ... $v_1(t-t_3)+z_3$ and $v_1(t'-t)$ ... $v_3(t'-t)$ are also determined by mutual constants of motion.

of global time t (see Fig. 2.4). The mutual constants of these satellites with respect to 0 give the parameters x_1, x_2, x_3, z_1, z_2, z_3, t_1, t_2, z_3 and v_1, v_2, v_3, with their geometric meaning illustrated in Fig. 2.4. Mutual constants of satellite 1 with respect to 2 give the length $\bar{d}_{12}(\tau^1)$, the distance from satellite 1 to 2 in the local rest frame of satellite 2. The length $\bar{d}_{12}(\tau^1)$ is different than $d_{12}(t)$ because it is observed in a different Lorentz frame. The side $d_{12}(t)$ can be obtained from $\bar{d}_{12}(\tau^1)$ by expressing $\tau_1 = \frac{t-t_1}{\gamma_1}$ in terms of t, using mutual constants of motion, and then projecting $\bar{d}_{12}$ onto the local rest frame of satellite 0. (frame, where satellite 0 is at rest.) The result of such transformation can be written in the form:

$$d_{12}(t) = \bar{d}_{12}\left(\frac{t-t_1}{\gamma_1}\right)\frac{1}{\sqrt{1-(\frac{v_1}{c}\gamma_1\cos\delta_{12})^2}}, \tag{2.10}$$

where δ_{12} is the angle between the mutual 3-velocity vector of 2 with respect to 1, and the

3-vector in direction from 1 to 2 at time t, both expressed in the frame of 0. The angle δ_{12} cannot be calculated from mutual constants of motion, however, the v_1^2/c^2 term can be neglected compared to 1 for small velocities, so that to first order $d_{12}(t) \sim \overline{d}_{12}(t-t_1)$.

Using the same approximation for the other two sides $d_{23}(t)$ and $d_{31}(t)$ and three more sides $d_{12}(t\prime)$, $d_{23}(t')$, $d_{31}(t')$, one can determine the first approximation for the geometric structure with vertices $\mathcal{O}$, $\mathcal{P}_1$, $\mathcal{P}_2$, $\mathcal{P}_3$, $\mathcal{P}_1'$, $\mathcal{P}_2'$, $\mathcal{P}_3'$, $\mathcal{P}_1''$, $\mathcal{P}_2''$, $\mathcal{P}_3''$. One then ties global spatial axes to this structure and determines the missing angles and recalculates the better approximations for points $\mathcal{O}, \cdots \mathcal{P}_3''$. This procedure can be repeated until the points converge to the final position with required accuracy, or simply use the algebraic solution described above. Finally one ties Cartesian spatial axes to the geometric structure, for example $\vec{e}_1$, $\vec{e}_2$, may be in the plane of the triangle $\mathcal{P}_1'$, $\mathcal{P}_2'$, $\mathcal{P}_3'$, and the third one perpendicular to it.

If the Hamiltonian, describing the motion of satellites and light, has been chosen correctly, then the mutual constants of motion, determined at any later time interval, will remain the same, and successive motion of satellites will be describable as uniform. Note that, for a short enough period of time, every motion can be considered as uniform, so that the above procedure always gives a locally Minkowski structure for a sufficiently short time interval $\{t, t\prime\}$. This short time interval may be succeeded by another short time interval, in which the triangle $\mathcal{P}_1$, $\mathcal{P}_2$, $\mathcal{P}_3$ will fit the preceding triangle $\mathcal{P}_1'$, $\mathcal{P}_2'$, $\mathcal{P}_3'$, but the vertices of the new $\mathcal{P}_1'$, $\mathcal{P}_2'$, $\mathcal{P}_3'$ may not be exactly on straight lines S_1, S_2, S_3, determined in the first step. The deviation of vertices from expected positions is the geodetic deviation, which is the measure of the Riemann tensor - the curvature of spacetime. Thus, by strategically placing satellites, and measuring their mutual motion, it is possible to use the above mechanism for mapping the Riemann tensor of space-time. Thus, it is possible, in principle, to use emission coordinate pairs $P^{ij}[k]$ for constructing a map of the stationary space-time, covered by the constellation, and, on the basis of such data, to construct the complete Hamiltonian, that would describe dynamics (provided there are no non-gravitational perturbations) with increasing accuracy.

The mechanism just described, demonstrates the intimate connection between geometry and dynamics established by covariant emission coordinates and serves as an important demonstration of the ABC concept. Nevertheless, the space-time around the Earth is dominated by the gravitational field of the Earth, therefore, it is convenient to start the refinement of dynamical description from spherically symmetric Hamiltonians, which include the gravitational field of the Earth.

2.3 Keplerian motion

As the next illustration, let us consider a constellation where satellite dynamics is describable by a Keplerian Hamiltonian

$$H = \frac{p^2}{2m} - G\frac{Mm}{r} \ , \tag{2.11}$$

where M is the mass of the Earth, much larger than the mass of the satellite m. We assume that light propagates on straight lines with the speed c. Satellites belonging to a GNSS constellation will generally be on bound (usually almost circular) orbits - ellipses that obey the third law of Kepler. This introduces a natural distance scale, which becomes observable through the sinodic period of two satellites.

The spherical symmetry of the Hamiltonian suggests the introduction of spherical coordinates, centred at the gravity centre of M and oriented in fixed directions with respect to distant stars. The constants of motion of each satellite are: a (main axis of ellipse), ε (eccentricity), ι (inclination with respect to x-y plane), Ω (longitude of ascending node), ω (longitude of perigee), t^{peri} (time of perigee passage). We use the notation $MC_i = \{a_i, \varepsilon_i, \iota_i, \Omega_i, \omega_i, t_i^{peri}\}$ for this set of constants, where the index i reffers to satellite label. The motion of each satellite can be expressed in global Cartesian coordinates as

$$\vec{r}(t|a, \varepsilon, \iota, \Omega, \omega, t^{peri}) = \mathbf{R}_z(\omega) \cdot \mathbf{R}_x(\iota) \cdot \mathbf{R}_z(\Omega) \cdot \vec{\rho}(E(t - t^{peri})|a, \varepsilon) \ , \tag{2.12}$$

where $\mathbf{R}_z(\alpha)$ and $\mathbf{R}_x(\alpha)$ are rotation matrices about z and x by α. $E(t)$ is the eccentric anomaly, which can be expressed with a Fourier series

$$E(t) = \left(\frac{GM}{a^3}\right)^{1/2} t + \sum_{k=1}^{\infty} \frac{2}{k} J_k(k\varepsilon) \sin\left(k\left(\frac{GM}{a^3}\right)^{1/2} t\right) \ , \tag{2.13}$$

where $J_k(x)$ are Bessel functions. In the orbital plane

$$\vec{\rho}(E|a, \varepsilon) = \left(a\cos E - \varepsilon, a\sqrt{1-\varepsilon^2}\sin E, 0\right) \ . \tag{2.14}$$

The pairs $P^{ij}[k] = \{\bar{\tau}^i[k],\ \tau_i^j[k]\}$ obey, for all k, the equation

$$\tau_i^j + \Delta t_{ij} - \bar{\tau}^i = \frac{1}{c}\left|\vec{r}(\bar{\tau}^i|MC_i) - \vec{r}(\tau_i^j + \Delta t_{ij}|MC_j)\right| \ , \tag{2.15}$$

where, in the case considered, τ is the proper time of satellites, running with the same rate as universal time, and Δt_{ij} is the difference in time origin of the clocks of i and j. Obviously, the relation between $\bar{\tau}$ and τ can only depend on relative orientation of orbits i and j. Therefore, we again introduce mutual constants of motion by choosing a local coordinate frame, such that one satellite is oriented with respect to the other: t^{peri} for the sending satellite is zero, the $\vec{e'}_1$ axis points toward the perigee of the sending satellite and the $\vec{e'}_3$ axis is perpendicular to its orbital plane. The mutual constants of motion, necessary to describe the relative motion of satellites i and j, are: $MC_{ii} = \{a_i, \varepsilon_i, 0, 0, 0, 0\}$ and $MC_{ij} = \{a_j, \varepsilon_j, \iota_{ji}, \Omega_{ji}, \omega_{ji}, t^{peri}_{ji}\}$. For brevity of notation it is useful to join them in a common array $Mc_{ij} = \{a_i, a_j, \varepsilon_i, \varepsilon_j, \iota_{ji}, \Omega_{ji}, \omega_{ji}, t^{peri}_{ji}\}$ — the main axes and eccentricities of both orbits, the relative inclination of orbits, the longitude of the line of nodes with respect to the perigee of the sending satellite, the longitude of receiving satellite with respect to line of nodes, and perigee passage time of the receiving satellite.

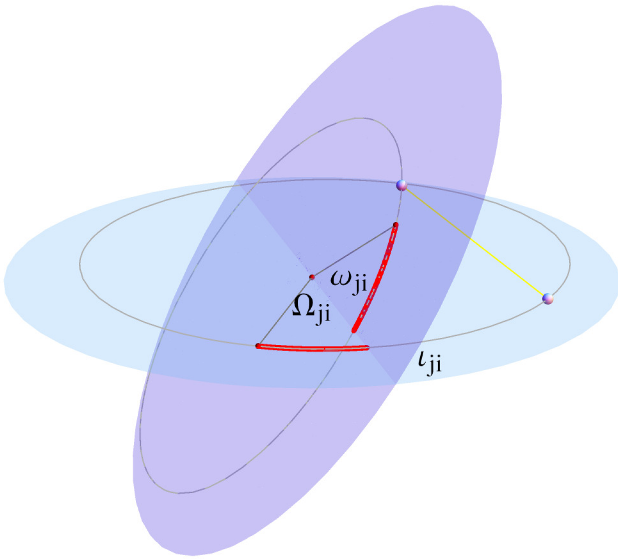

Figure 2.5: Mutual constants of motion for two satellites on Keplerian orbits: $Mc_{ij} = \{a_i, a_j, \varepsilon_i, \varepsilon_j, \iota_{ji}, \Omega_{ji}, \omega_{ji}, t^{peri}_{ji}\}$.

The pairs $P^{0j}[k] = \{\bar{\tau}^0[k], \tau^j_0[k]\} = \{\bar{\tau}[k], \tau[k]\}$, where index 0 refers to the sending satellite, now obey equation (2.15) with $\iota_i = 0$, $\Omega_i = 0$, $\omega_i = 0$, $t^{peri}_i = 0$; the remaining constants $a_i = a$, $\varepsilon_i = \varepsilon$, $a_j = a'$, $\varepsilon_j = \varepsilon'$, $\iota_j = \iota_{ji} = \iota$, $\Omega_j = \Omega_{ij} = \Omega$, $\omega_j = \omega_{ji} = \omega$, $t^{peri}_j = t^{peri}_{ji} = t^{peri}$ are mutual constants of motion Mc. They can be determined by least square fitting the data on the left of equation (2.15) to functions on the right of this equation, where mutual constants of motion are parameters of the fit. In other words, we construct an action:

$$\mathcal{S}[Mc, \Delta t] = \sum_{k=1}^{N} \left[\tau[k] + \Delta t - \bar{\tau}[k] \; - \; \left| \vec{r}(\bar{\tau}[k]|a, \varepsilon, 0, 0, 0, 0) - \vec{r}(\tau[k] + \Delta t|a', \varepsilon', \iota, \Omega, \omega, t^{peri}) \right| \right]^2 \tag{2.16}$$

and minimize it with respect to the parameters. It is obvious, that the solution with parameters corresponding to a small value of $\mathcal{S}$, would describe well the mutual dynamics during the time interval covered by the pairs $P^{0j}[k],\ k = 1 \cdots N$. It was found numerically that the minimization of this action actually recovers the correct mutual constants of motion if the interval $\tau[k]$ covers a few mutual periods. Yet, it is worth mentioning that the minimization of (2.16) is a highly non-linear problem – the action as a function of mutual constants of motion has many local minima or saddle points, so that minimization procedures that are based on gradient methods may be caught in one of the local minima. It was found by numerical experiments, that the global minimum is deeper and narrower for larger numbers of data points N (see Chap. 3). Therefore, the minimization procedure should start with not too many points covering the time interval in question. Minimizing scarce data, one obtains a good first approximation for mutual constants of motion. These constants are then used in the next minimization step with finer resolution to obtain the final best solution for the mutual constants of motion. In this way one builds the mutual constants of motion of all satellite pairs. In order to refer all constants of motion to the same global system of coordinates we proceed as follows:

Choose satellite labelled 0 as the one defining the global Cartesian axes $\hat{\mathbf{e}}_1$, $\hat{\mathbf{e}}_2$ and $\hat{\mathbf{e}}_3$ so that the $\hat{\mathbf{e}}_3$ axis points in the direction of his orbital angular momentum: $\vec{l}_0 = m\sqrt{GMa_0(1-\varepsilon_0^2)}\hat{\mathbf{e}}_3$, and $\hat{\mathbf{e}}_1$ in the direction of its Runge-Lenz vector: $\vec{R}_0 = \varepsilon_0 \hat{\mathbf{e}}_1$. Angular momenta $\vec{l}_i = l_i \hat{e}_3^{0i}$ and Runge-Lenz vectors $\vec{R}_i = R_i \hat{e}_1^{0i}$ of other satellites define local Cartesian frames. These frames are rotated with respect to the global frame, and the Euler rotation can be expressed with mutual constants of motion ι_{0i}, Ω_{0i} and ω_{0i} as:

$$\begin{vmatrix} \hat{e}_1^{0i} \\ \hat{e}_2^{0i} \\ \hat{e}_3^{0i} \end{vmatrix} = \mathbf{R}(\iota_{0i}, \Omega_{0i}, \omega_{0i}) \cdot \begin{vmatrix} \hat{\mathbf{e}}_1 \\ \hat{\mathbf{e}}_2 \\ \hat{\mathbf{e}}_3 \end{vmatrix} \tag{2.17}$$

where the rotation matrix is:

$$\mathbf{R}(\iota, \Omega, \omega) = \begin{vmatrix} \cos\omega\cos\Omega - \cos\iota\sin\omega\sin\Omega & \cos\iota\cos\Omega\sin\omega + \cos\omega\sin\Omega & \sin\iota\sin\omega \\ -\cos\Omega\sin\omega - \cos\iota\cos\omega\sin\Omega & \cos\iota\cos\omega\cos\Omega - \sin\omega\sin\Omega & \cos\omega\sin\iota \\ \sin\iota\sin\Omega & -\cos\Omega\sin\iota & \cos\iota \end{vmatrix}. \tag{2.18}$$

In this way all constants of motion can be defined with respect to the global frame defined by satellite 0. However, any satellite can be chosen to define the axes of the global frame.

Suppose we choose satellite k to define the global frame, then we can write:

$$\begin{aligned}\begin{vmatrix} \hat{e}_1^{ki} \\ \hat{e}_2^{ki} \\ \hat{e}_3^{ki} \end{vmatrix} &= \mathbf{R}(\iota_{ki}, \Omega_{ki}, \omega_{ki}) \cdot \begin{vmatrix} \hat{e}_1^{0k} \\ \hat{e}_2^{0k} \\ \hat{e}_3^{0k} \end{vmatrix} \\ &= \mathbf{R}(\iota_{ki}, \Omega_{ki}, \omega_{ki}) \cdot \mathbf{R}(\iota_{0k}, \Omega_{0k}, \omega_{0k}) \cdot \begin{vmatrix} \hat{\mathbf{e}}_1 \\ \hat{\mathbf{e}}_2 \\ \hat{\mathbf{e}}_3 \end{vmatrix}, \end{aligned} \tag{2.19}$$

where ι_{ki}, Ω_{ki} and ω_{ki} are mutual constants in the set Mc_{ij}. Combining (2.17) and (2.19), one arrives at the identity:

$$\mathbf{R}(\iota_{ji}, \Omega_{ji}, \omega_{ji}) = \mathbf{R}(\iota_{ki}, \Omega_{ki}, \omega_{ki}) \cdot \mathbf{R}(\iota_{jk}, \Omega_{jk}, \omega_{jk}) \tag{2.20}$$

between any three satellites i, j, k. Thus, the constants of motion MC_i for a given satellite can be calculated in many different ways from mutual constants of motion. Ideally all results should be the same, but, because of noise in the data, or because of insufficient dynamical description the constants deduced from different sets of mutual constants may not perfectly agree.

A way to get a good approximation for global constants from mutual constants, may be as follows: We note that instead of a, ε, ι, Ω, ω, t_{peri}, one can describe the orbit also by the angular momentum, Runge-Lenz vector and the time of periastron passage. The length of both vectors is obtained directly from mutual constants of motion, so for every satellite i in the constellation one obtains $n-1$ values $a_i^{(j)}$ for the main axis and similarly $n-1$ values for $\varepsilon_i^{(j)}$, where the upper index in brackets indicates the other member of the pair in which the particular value was obtained. Likewise, the direction of the two vectors can be obtained either from MC_{0i} or in two steps from MC_{ji} and MC_{0j}. So from each mutual set MC_{ij} we obtain global angular momenta $\vec{l}_i^{(j)}$ and $\vec{l}_j^{(i)}$. It seems reasonable to define the average angular momentum vector of satellite i as the average of all vectors $\vec{l}_i = \frac{1}{n-1} \sum_{j \neq i} \vec{l}_i^{(j)}$, and similarly for the Runge-Lentz vector, the time offset and periastron passage time. Some results of numerical experiments with error considerations are discussed in next sections, but a thorough analysis of error propagation is still left for further considerations.

So far in our analysis, we left out two problems that would arise in practical applications: we did not offer a tool to synchronize the clock of satellite i to $t = 0$ at the first periastron passage, and we did not offer a tool to check whether the clocks of the two satellites run at the same rate. For further reference let us call the first tool "my perigee tool" and the second one "clock rate correction tool". These tools can be integrated in the minimization procedure by introducing two new variation parameters ϕ_{peri} and η in the action as follows:

$$\mathcal{S}n[Mc_{ij}, \Delta t, \phi_{peri}, \eta] = \sum_{k=1}^{N} \left[\tau[k] + \Delta t - \bar{\tau}[k] \;-\; \left| \vec{r}((\bar{\tau}[k] - \sqrt{\frac{a^3}{GM}} \phi_{peri})|MC_{ii}) - \vec{r}(\tau[k](1+\eta) + \Delta t | MC_{ij}) \right| \right]^2 \tag{2.21}$$

This makes the global minimum search quite slow, so that the global minimum may not be found in Mathematica if the initial guess of constants of motion was too far from actual values. The solution to the problem was to minimize the action first with respect to mutual constants of motion to get values of action minimuma as function of ϕ_{peri} and η, see Figs.3.9 and 3.10. This function has a clear global minimum, which narrows down the values for the initial guess.

2.4 Schwarzschild space-time

The Schwarzschild Hamiltonian, which controls the motion of satellites and light is:

$$H = -\left(\frac{1 + \frac{r_g}{2R}}{1 - \frac{r_g}{2R}} \right)^2 + \frac{p^2}{(1 + \frac{r_g}{2R})^4} \;, \tag{2.22}$$

where $r_g = \frac{GM}{c^2}$ is the gravitational radius of the Earth, $R = \sqrt{X^2 + Y^2 + Z^2}$ and (X, Y, Z) are isotropic coordinates. The Hamiltonian is a constant of motion with value -1 for satellites and 0 for photons. Introducing the Schwarzschild radial coordinate $r = R\left(1 + \frac{r_g E}{R}\right)$ and the corresponding Cartesian coordinates x , y, z, one obtains the orbital solution in the form

$$\vec{r}(\tau | a, \varepsilon, \iota, \Omega, \omega, t^{peri}) = \mathbf{R}_z(\omega) \cdot \mathbf{R}_x(\iota) \cdot \mathbf{R}_z(\Omega) \cdot \vec{\rho}(\phi(\tau - \tau^{peri}) | a, \varepsilon) \;, \tag{2.23}$$

equivalent to (2.11), also regarding the six constants of motion: $MC_i = \{a_i, \varepsilon_i, \iota_i, \Omega_i, \omega_i, t_i^{peri}\}$. Here $\phi(\tau)$ is the true anomaly as a function of proper time, and

$$\vec{\rho}(\phi | a, \varepsilon) = \frac{2r_g}{u_2 - (u_2 - u_3) cn^2 \left(K(m) + \frac{\phi}{2n} \right)} \begin{pmatrix} \cos\phi & \sin\phi & 0 \end{pmatrix} \;. \tag{2.24}$$

It is possible to express the proper time τ as a function of true anomaly in analytic form. However, the inverse is needed. We obtain it in the following way: observe that $\phi - 2\pi \frac{\tau(\phi)}{P}$ is a periodic function in ϕ with the periode $P = 4\, K(m)$, so it can be expanded into a Fourier series with coefficients proportional to powers of ε and to powers of a/r_{gE}. For reasonably small ε this series is inverted and results in a series of the form:

$$\phi(\tau) = 2\pi\frac{\tau}{P} + \sum_{n=1}^{10} C_n(a,\varepsilon)\sin(2\pi n\tau/P)\ . \tag{2.25}$$

The coefficients $C_n(a,\varepsilon)$ are expressed in a complicated, but straightforward way as functions of a and ε, as shown on page 52. Numerical experiments with data for typical Galileo orbits ($r_g/r \sim 2\times 10^{-10}$, $\varepsilon < 0.003$) have shown that the series expansion agrees with analytical expressions to more than 24 digits; this is why we keep ten terms in Fourier expansion 2.25. The equivalent of (2.15) in the Schwarzschild case is:

$$t_j(\tau_i^j[k]) + \Delta t_{ij} - t_i(\bar\tau^i[k]) = T_f\left(\vec r\left(\bar\tau^i[k]|MC_i\right), \vec r\left(\tau_i^j[k]|MC_j\right)\right)\ , \tag{2.26}$$

where $T_f(\vec r_1, \vec r_2)$ is the time of flight of a photon in a Schwarzschild space time between points $\vec r_1$ and $\vec r_2$ and $t_k(\tau)$ is the global time of the space time position of satellite k at the moment of his proper time τ. In exactly the same way as in the Keplerian case, we can choose the orbit of i as defining the coordinate axes, and we can choose mutual constants of motion $Mc_{ij} = \{a_i, a_j, \varepsilon_i, \varepsilon_j, \iota_{ji}, \Omega_{ji}, \omega_{ji}, t_{ji}^{peri}\}$

In the space time, traced by Galileo satellites, the Riemann curvature is so small, that the time of flight can very accurately be expressed with the distance between the sender and receiver divided by the speed of light plus a very small Shapiro delay

$$T_f(\vec r_1, \vec r_2) = \frac{1}{c}|\vec r_1 - \vec r_2| + \delta t_S\ , \tag{2.27}$$

where

$$\begin{aligned}\delta t_S &= \frac{4r_g}{c}\ln\frac{2\sqrt{r_1 r_2}}{r_{min}}\\ &= 59\text{p}s \times \ln\frac{2\sqrt{r_1 r_2}}{r_{min}}\ ,\end{aligned} \tag{2.28}$$

and r_{min} is the minimum distance at which a photon passes the centre of the Earth. Regarding the left hand side of (2.26), we take into account that the proper time and Schwarzschild time are almost perfectly proportional, so that $\frac{dt}{d\tau} = \left(\frac{1+\frac{r_g}{a}}{1-\frac{2r_g}{a}}\right)^{1/2} + F(\phi)$, where $F(\phi)$ is a periodic function with the period $4K(m)$, again expressed as a series in the form of (2.25), but with different (much smaller) coefficients, displayed on page 54.

From (2.26) we proceed in the same manner as from (2.15), building an action with mutual constants of motion as parameters. As before, we fit orbital solutions by minimizing the action by varying mutual constants of motion. Of course, after all is written down, it becomes clear that, because of the weakness of the gravitational field of the Earth, the

Schwarzschild action differs little from the Keplerian one. The difference, due to the factor between global time and proper time, becomes obvious after a few periods of revolution, while the Shapiro delay is a periodic effect that shows only at the level of centimetre accuracy. Building up the global constants of motion of the constellation proceeds in exactly the same way as in the Keplerian case. Some numerical examples and tests are discussed in later sections.

Numerical implementation 3

The constants of motion are calculated by minimizing 9-dimensional action $\mathcal{S} = \mathcal{S}(a_i, a_j, \varepsilon_i, \varepsilon_j, \iota, \Omega, \omega, t_{p,i}, t_{p,j})$. This action was written for Schwarzschild and flat (Kepler) space-time. Equations used to calculate the action $\mathcal{S}$ at each data point (i.e. $(t(\tau_i), \vec{r}(\tau_i))$ at each proper time τ_i along the orbit for both satellites in a pair) are given in App. A and Sec. 2.3. The proper times τ_i are the input data and are obtained as follows.

We simulated a pair of satellites in orbit around Earth using analytical equations of motion in Schwarzschild space-time from Čadež et al. (2010) and Delva et al. (2011) with a given set of constants of motion for both satellites. At each time-step i of the simulation a pair of proper times $\{\overline{\tau}^2[i], \tau_2^1[i]\}$ is obtained: $\tau_2^1[i]$ is the proper time of the first satellite at the moment of reception of the i-th signal $\overline{\tau}^2[i]$ from the second satellite. These pairs of proper times $\{\overline{\tau}^2[i], \tau_2^1[i]\}$ are then used to calculate the action (2.16) with equations given in Sec. 2.3 and App. A. In what follows, the indices 2 and 1 can be omitted as on p. 8.

The algorithm for Keplerian case was coded with Mathematica, while for Schwarzschild case it was coded mainly in Fortran 90. In this case, as minimizing method we used the Simplex algorithm of Nelder and Mead from *gsl* library (`gsl_multimin_fminimizer_nmsimplex2`) which was coded in C.

The algorithms for Schwarzschild case were tested on a PC with an Intel Core i7 CPU at 3.0 GHz and 8 GB RAM. The OS was Linux x86_64 with kernel 2.6.32-28-generic and Intel Fortran/C compiler 11.1. For Kepler case, they were tested on the same computer and on a PC with Intel Core i7 CPU at 3.2 GHz and 8GB RAM with 64-bit Windows 7 Professional and Mathematica 7.0.

3.1 Robustness of the method

We tested the robustness of the minimizing procedure, i.e. we checked its dependence on the choice of initial guess values, number of data points per orbit, number of orbits included in

satellite	Ω [°]	ω [°]	ι [°]	a [$\mathrm{r_g}$]	a [km]	ε	t_p [$\mathrm{r_g/c}$]
1	0	0	0	5×10^9	22182.6	5×10^{-5}	0
2	10	65	40	5×10^9	22182.6	2×10^{-5}	0

Table 3.1: Orbital parameters for two satellites: longitude of ascending node (Ω), longitude of perigee (ω), inclination (ι), major semi-axis (a), eccentricity (ε), and time of perigee passage (t_p).

the minimization, and the effect of clock errors. The true constants of motion, which were used for simulating a pair of satellites, are given in Tab. 3.1.*

Note that only values of Ω, ω, and ι of the second satellite relative to the first satellite in a pair can be found by minimizing (2.16), i.e. only the orientation of one orbit relative to the other can be found. Therefore, in the following subsections, Ω, ω, and ι always refer to the values of the second relative to the first satellite in pair. However, for simplicity, the angles Ω, ω, and ι for the first satellite are chosen in such a way (i.e. $\Omega_1 = \omega_1 = \iota_1 = 0$) that the relative angles for the second satellite (found by the minimizing procedure) are the same as absolute angles (i.e. the values in Table 3.1). A method for regaining the absolute values for non-zero values of Ω_1, ω_1, and ι_1 is given in Sec. 3.2.

3.1.1 Local/global minimum

Since we are using a minimization method designed for finding local minima, it is necessary to check the behaviour of $\mathcal{S}$ near the global minimum (which should exist for true values of orbital parameters). We do this by plotting the cross-sections of the 9-dimensional action: to check $\mathcal{S}$ for one orbital parameter, e.g. major semi-axis a, we keep other parameters fixed at their true values (from Table 3.1) and vary a around its true value.

As an example, we simulated the satellites with orbital parameters from Tab. 3.1 for 8 orbits and 50 points per orbit (i.e. 400 data points). The resulting cross-sections of $\mathcal{S}$ are in Fig. 3.1.

Clearly, the minimum exists, however, for a_1 and a_2 there are also other local minima near the global one, as confirmed in Fig. 3.2, where the same action for a_1 is plotted in linear scale, to better show the region near the global minimum. For this reason, it is necessary to either make sure that the initial "best-guess" coordinates are close enough to the global minimum or to use a minimization method that searches for a global minimum.

*If we choose a very small value for eccentricity, e.g. $\varepsilon = 10^{-9}$, the minimization procedure fails, therefore we chose a more reasonable value of $\varepsilon = 10^{-5}$.

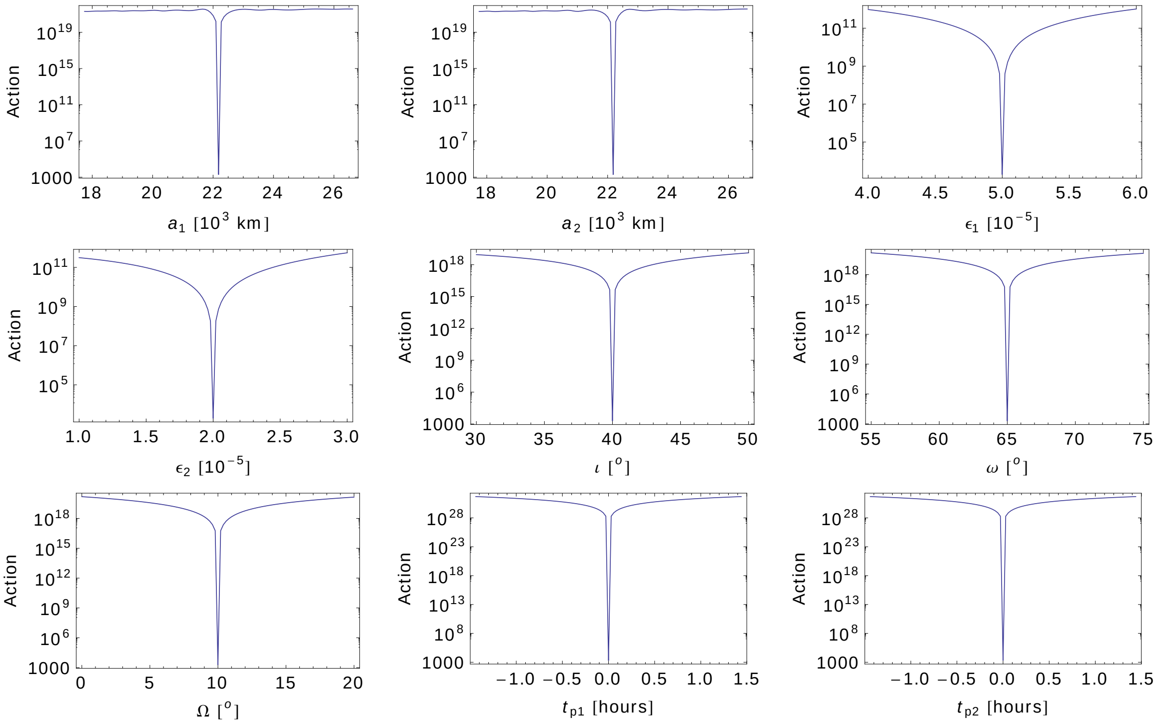

Figure 3.1: The action (2.16) near minimum point for $N = 50$ points per orbit and 8 orbits (400 data points).

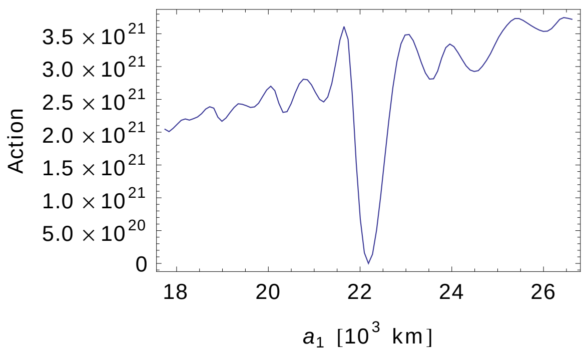

Figure 3.2: The action (2.16) near minimum point for different values of a_1 shown in linear scale.

3.1.2 Number of points per orbit

We checked the dependence of $\mathcal{S}$ and minimizing procedure on the number of points per orbit. The results of minimization are in Tab. 3.2. In all cases, the orbital parameters were the same as in Tab. 3.1 and the number of orbits was 8; only the number of points per orbit was different. The initial best-guess values for orbital parameters were obtained by multiplying the true value by 1.01.

N	$\frac{\Delta\Omega}{\Omega}$	$\frac{\Delta\omega}{\omega}$	$\frac{\Delta\iota}{\iota}$	$\frac{\Delta a_1}{a_1}$	$\frac{\Delta a_2}{a_2}$	$\frac{\Delta\varepsilon_1}{\varepsilon_1}$	$\frac{\Delta\varepsilon_2}{\varepsilon_2}$	Δt_{p1}	Δt_{p2}	$\frac{\mathcal{S}_{\ in}}{\mathcal{S}_{\ fin}}$	toc $[s]$
50	10^{-6}	10^{-6}	10^{-7}	10^{-10}	10^{-10}	10^{-4}	10^{-3}	22	22	10^{-14}	643
90	10^{-7}	10^{-8}	10^{-8}	10^{-13}	10^{-12}	10^{-6}	10^{-6}	17	17	10^{-17}	1038
180	4	0.6	1.3	0.03	0.03	2	6	93	66	0.4	2116
360	4	0.6	0.5	0.01	0.01	1	0.1	384	80	0.4	3094
720	4	0.6	0.7	0.01	0.01	1	0.7	135	100	0.5	5962

Table 3.2: The results of minimization for 2 satellites, 8 orbits and true values of parameters from Tab. 3.1: number of points along an orbit (N), relative errors after minimization for Ω, ω, ι, a_1, a_2, ε_1, and ε_2, absolute error in perigee passage time (Δt_{p1}, Δt_{p2}) in μs, the ratio of the final and the initial value of action ($\mathcal{S}_{\ in}/\mathcal{S}_{\ fin}$), and time needed to minimize $\mathcal{S}$ (toc). Absolute error of few μs in Δt_{p1} and Δt_{p2} should be compared to orbital period which is about 9.13 hours.

As can be seen in Tab. 3.2, the minimum of $\mathcal{S}$ is found only in the first two examples, with $N = 50$ and $N = 90$ points per orbit. To clear up on this, the minimizing process for $N = 50$ and $N = 720$ points per orbit is shown in Fig. 3.3 and Fig. 3.4. In the $N = 50$ case, the minimization proceeds "normally", i.e. the procedure starts from best-guess values of parameters (which are 1% higher than the true values) and converges close to true values. Also, the action and the simplex size drop in 3700 steps by 16 and 15 orders of magnitude, respectively. Surprisingly, in $N = 720$ case however, the minimization never converges to true values. It starts as in the $N = 50$ case, but soon appears to stray in different local minima.

To check for the existence of minimum, the action's cross-sections are plotted in Fig. 3.5 as in Sec. 3.1.1. There should be no problems as far as angles, eccentricities, and times are concerned, however since it has already turned out before (Fig. 3.2) that $\mathcal{S}$ for parameter a may have many local minima, we checked $\mathcal{S}$ close to its minimum in Fig. 3.6. In fact, not only many local minima still exist, but also the global minimum appears to be narrower in this case, so it is more easily missed if the initial best-guess values are too different from true values. This is confirmed in Fig. 3.7, where the same plot is shown for all the examples from Tab. 3.2: the global minimum narrows as the number of points per orbit increases, and the number of local minima increases as well. When improving the initial best-guess values (by

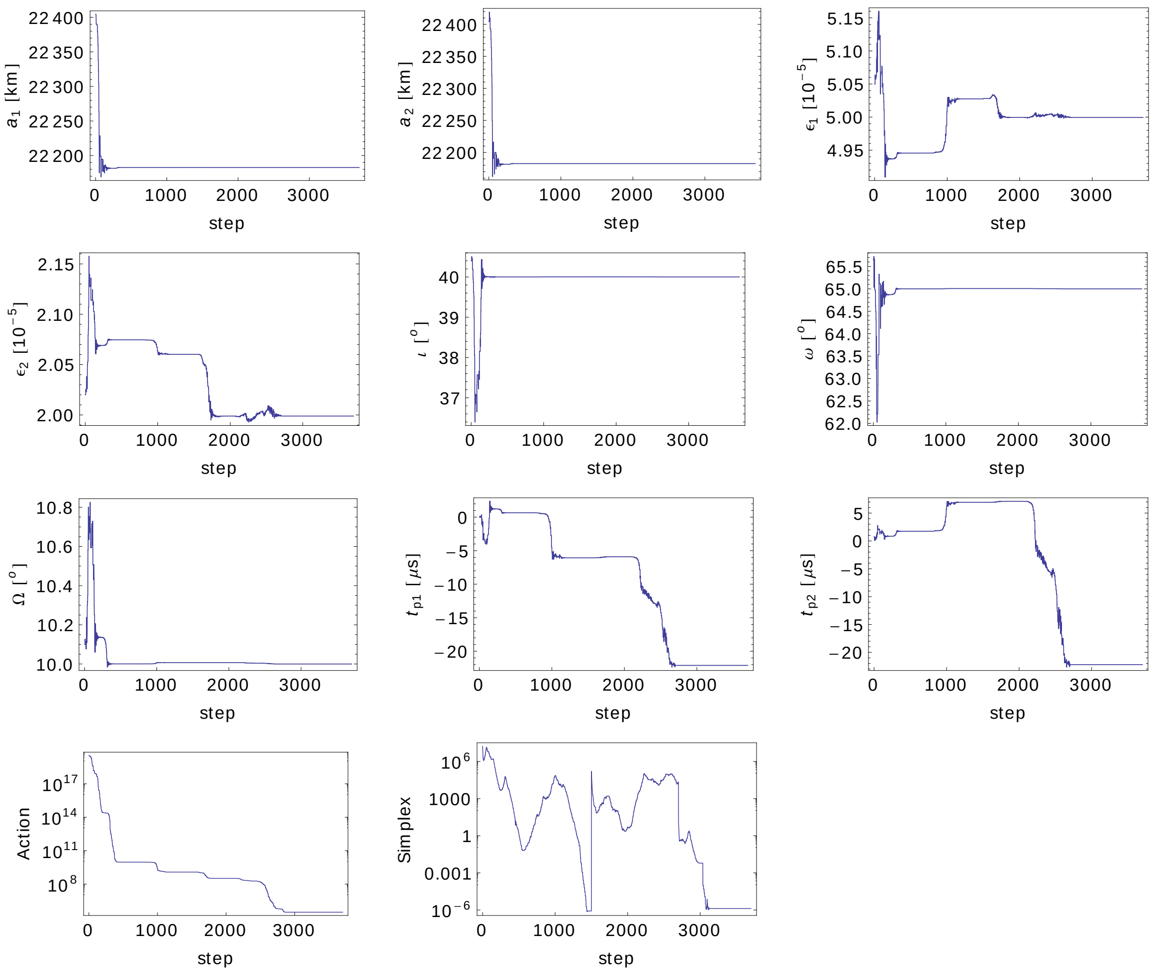

Figure 3.3: Progress of minimization for $N = 50$ points per orbit.

multiplying the true value by 1.001 instead of 1.01), the minimization converges normally in every but $N = 180$ case.

Having in mind that it is more easily to miss the global minimum and that calculation time increases significantly with increasing number of points per orbit, it is desirable to keep this number within reasonable limits, e.g. about ~ 100, since the accuracy obtained is the same in all cases.* In any case, the success of the minimization can be easily checked with the final value of $\mathcal{S}$ after minimization, which should be *many* orders of magnitude smaller than the initial value.

*The accuracy depends on the accuracy of the minimization algorithm from *gsl*, which was coded in double precision.

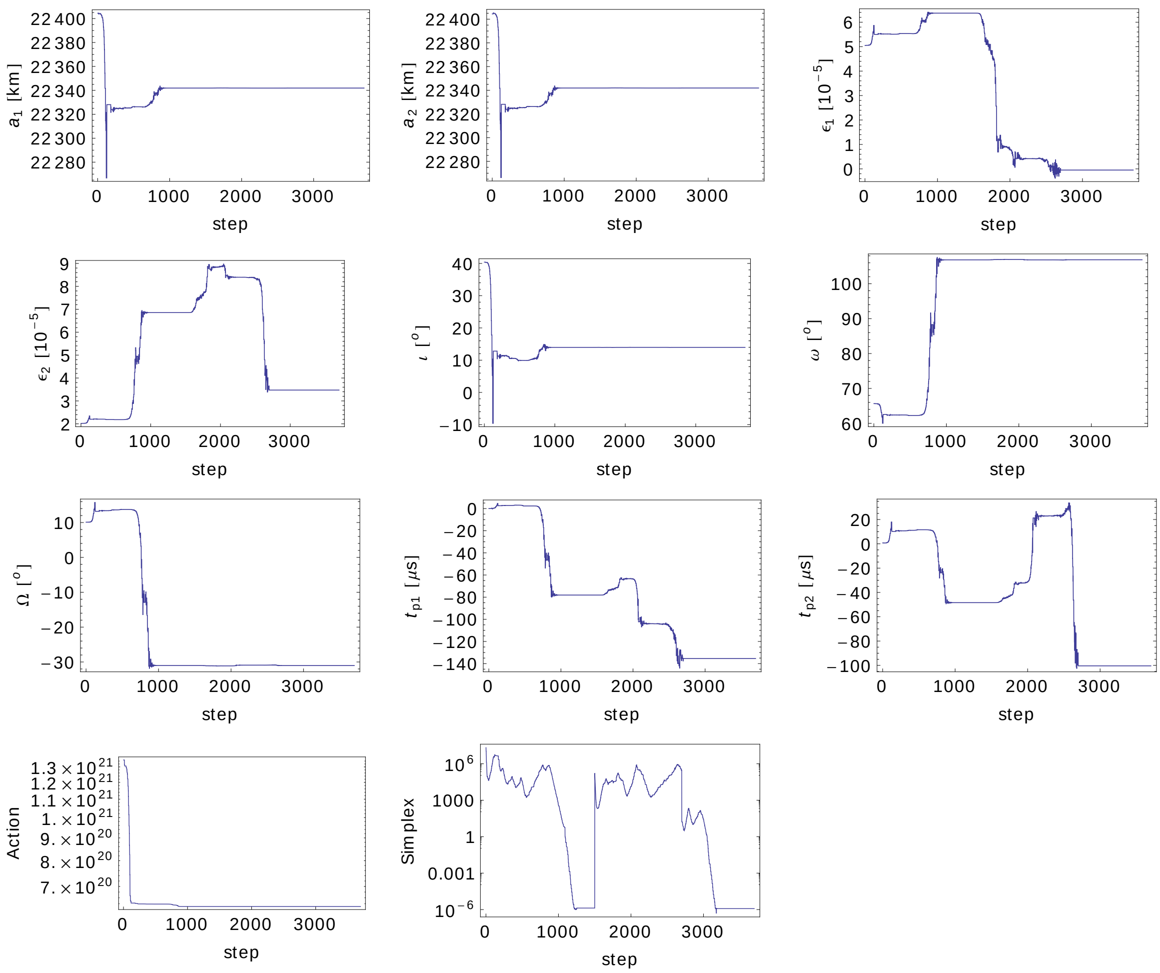

Figure 3.4: Progress of minimization for $N = 720$ points per orbit.

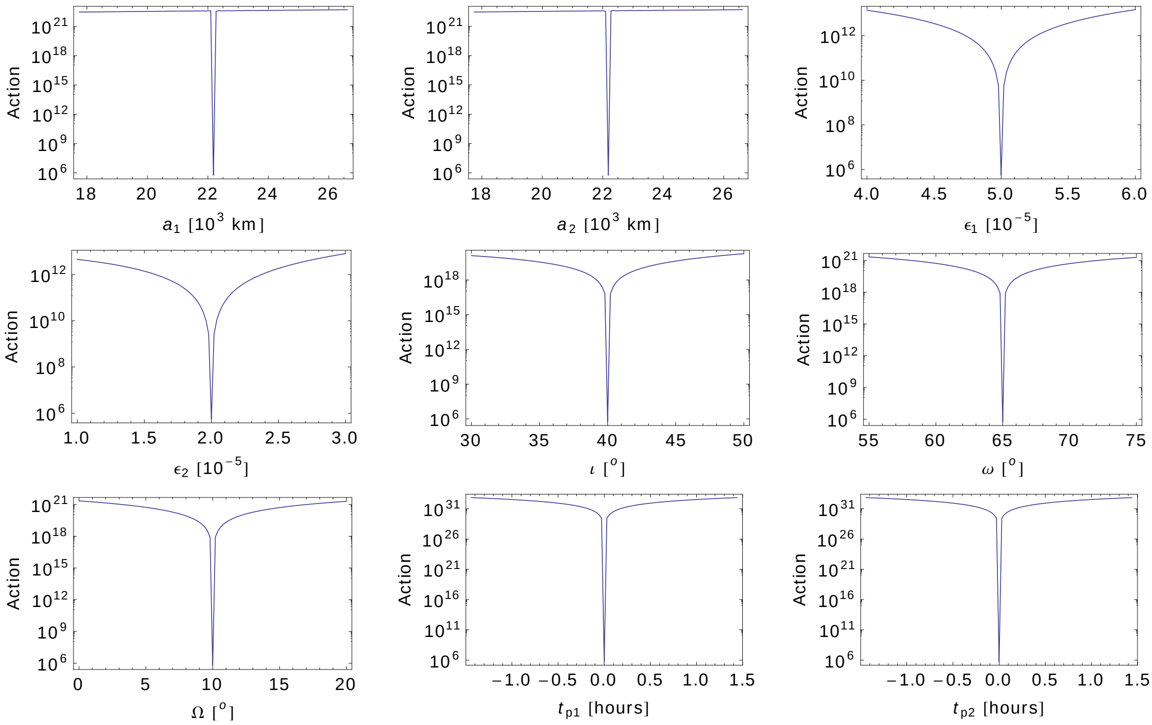

Figure 3.5: The action (2.16) near minimum point for $N = 720$ points per orbit and 8 orbits (5760 data points).

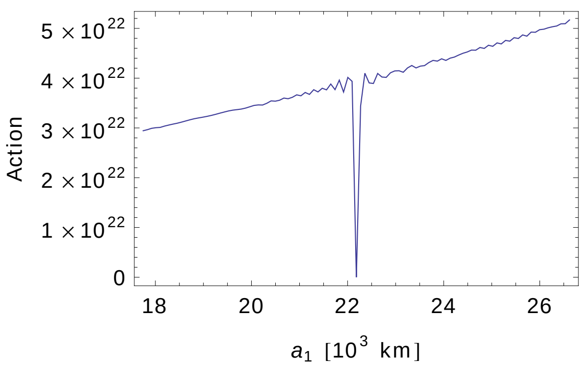

Figure 3.6: The action (2.16) near minimum point for $N = 720$ points per orbit as a function of a_1 shown in linear scale.

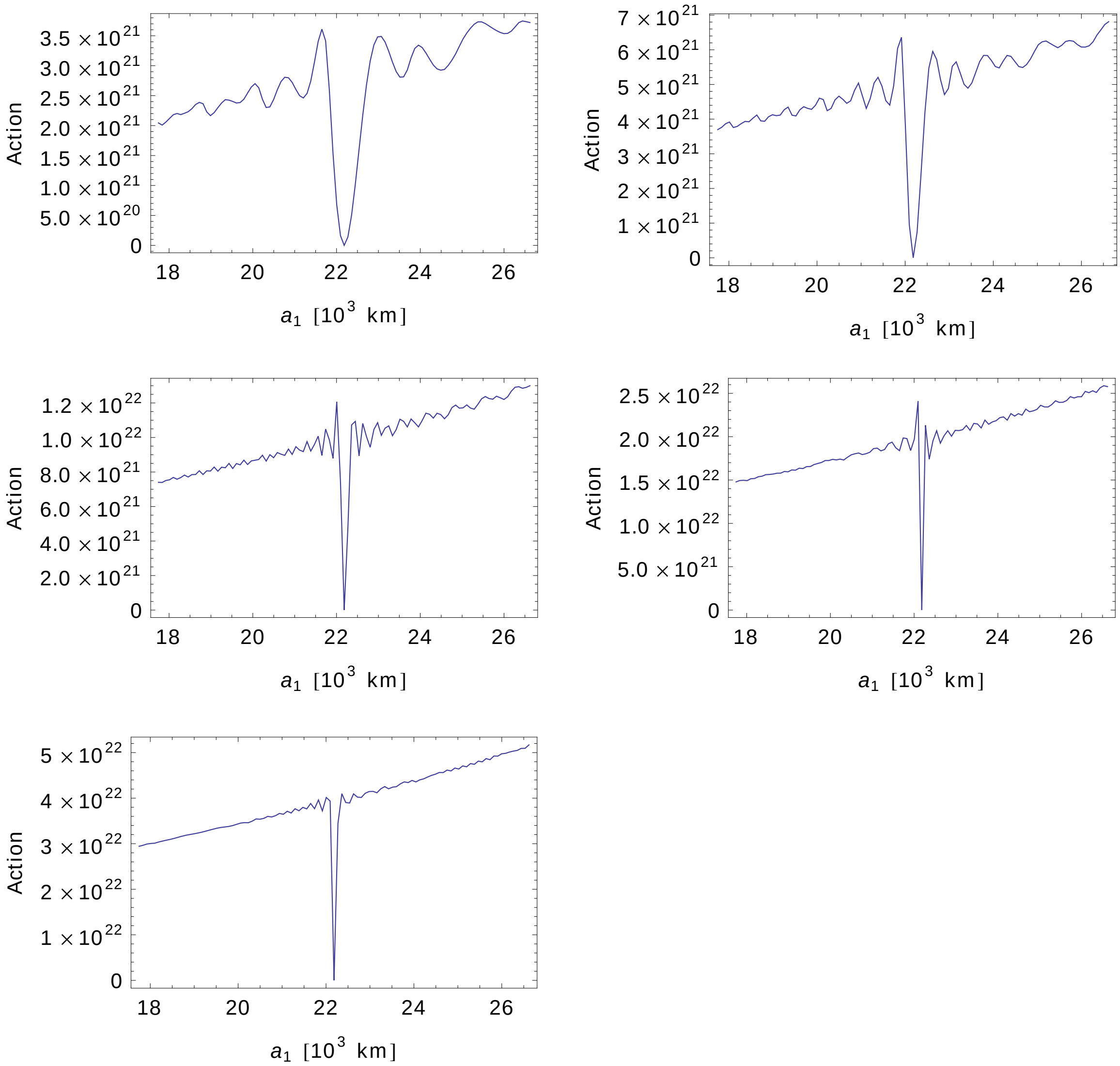

Figure 3.7: The action (2.16) near minimum point for $N = 50, 90, 180, 360, 720$ points per orbit and 8 orbits (5760 data points).

3.1.3 Number of orbits

Here we check the minimization procedure with respect to number of orbits, keeping the number of orbits constant at N=50 per orbit. The results in Tab. 3.3 show that results weakly depend on the number of orbits, and the accuracy is somewhat higher for $N_o \sim 4$ orbits. As expected, the calculation times increase with $\mathrm{N_o}$.

$\mathrm{N_o}$	$\frac{\Delta\Omega}{\Omega}$	$\frac{\Delta\omega}{\omega}$	$\frac{\Delta\iota}{\iota}$	$\frac{\Delta a_1}{a_1}$	$\frac{\Delta a_2}{a_2}$	$\frac{\Delta\varepsilon_1}{\varepsilon_1}$	$\frac{\Delta\varepsilon_2}{\varepsilon_2}$	Δt_{p1}	Δt_{p2}	$\frac{\mathcal{S}_{\ in}}{\mathcal{S}_{\ fin}}$	toc $[s]$
1	10^{-7}	10^{-8}	10^{-8}	10^{-10}	10^{-10}	10^{-6}	10^{-5}	3	3	10^{-17}	89
2	10^{-8}	10^{-9}	10^{-9}	10^{-13}	10^{-13}	10^{-8}	10^{-7}	3	3	10^{-18}	150
4	10^{-8}	10^{-8}	10^{-8}	10^{-13}	10^{-14}	10^{-8}	10^{-7}	2	2	10^{-18}	214
8	10^{-6}	10^{-6}	10^{-7}	10^{-10}	10^{-10}	10^{-4}	10^{-3}	22	22	10^{-14}	643

Table 3.3: The results of minimization for 2 satellites, 50 points per orbit and true values of parameters from Tab. 3.1: number of orbits ($\mathrm{N_o}$), relative errors after minimization for Ω, ω, ι, a_1, a_2, ε_1, and ε_2, absolute error in perigee passage time (Δt_{p1}, Δt_{p2}) in μs, the ratio of the final and the initial value of action ($\mathcal{S}_{\ in}/\mathcal{S}_{\ fin}$), and time needed to minimize $\mathcal{S}$ (toc). Absolute error of few μs in Δt_{p1} and Δt_{p2} should be compared to orbital period which is about 9.13 hours.

We also tested the same dependence by using Keplerian set of equations for $\mathcal{S}$ in Mathematica, where we could increase the precision of data (but not minimization algorithm) to as high as 60 digits (in Fortran we were limited to double precision of the *gsl* library). It turns out, that the accuracy does not increase with number of digits and we have no reason to doubt that the same would happen also for the Schwarzschild set of equations.*

3.1.4 Clock noise

To test the effects of clock noise on the minimization procedure, we assumed a value for Allan deviation σ_A of satellite clocks for the duration of the experiment (considering only shot noise) and added random noise $\delta\tau$ ($\delta\tau$ is uniformly distributed on the interval Δt) to each proper time $\overline{\tau}[k]$ and $\tau[k]$ in such a way, that $\sigma_A = \Delta t\sqrt{N}/(t_N - t_1)$, where N is the number of time intervals. The modified τ's are then used in the minimization routine. The results for different values of σ_A are in Tab. 3.4.

The minimization finds the constants of motion: as σ_A increases, the relative errors of constants of motion increase linearly, while the final value of action increases quadratically. Even though the assumed values for σ_A were unreasonably large,† the minimization still successfully finds the constants of motion.

*We were unable to test the Schwarzschild set of equations on Mathematica, because the calculation times were too long.

†Allan deviation for Galileo GNSS clocks at 1 day is 0.86 ns/day = 6×10^{-15}.

σ_A	$\frac{\Delta\Omega}{\Omega}$	$\frac{\Delta\omega}{\omega}$	$\frac{\Delta\iota}{\iota}$	$\frac{\Delta a_1}{a_1}$	$\frac{\Delta a_2}{a_2}$	$\frac{\Delta\varepsilon_1}{\varepsilon_1}$	$\frac{\Delta\varepsilon_2}{\varepsilon_2}$	Δt_{p1}	Δt_{p2}	$\frac{\mathcal{S}_{in}}{\mathcal{S}_{fin}}$	toc
10^{-15}	10^{-6}	10^{-6}	10^{-7}	10^{-11}	10^{-11}	10^{-5}	10^{-4}	3	4	10^{-15}	549
10^{-14}	10^{-7}	10^{-8}	10^{-8}	10^{-11}	10^{-12}	10^{-7}	10^{-6}	10	10	10^{-15}	793
10^{-13}	10^{-6}	10^{-7}	10^{-7}	10^{-11}	10^{-10}	10^{-6}	10^{-5}	0.15	0.2	10^{-13}	723
10^{-12}	10^{-5}	10^{-6}	10^{-6}	10^{-8}	10^{-8}	10^{-4}	10^{-4}	0.85	0.5	10^{-11}	697
10^{-11}	10^{-4}	10^{-5}	10^{-5}	10^{-8}	10^{-9}	10^{-3}	10^{-3}	1	5	10^{-9}	822
10^{-10}	10^{-3}	10^{-4}	10^{-4}	10^{-7}	10^{-7}	0.01	0.06	33	38	10^{-7}	512
10^{-9}	10^{-2}	10^{-3}	10^{-3}	10^{-6}	10^{-6}	0.08	0.5	83	250	10^{-5}	512

Table 3.4: The results of minimization for 2 satellites, 8 orbits and true values of parameters from Tab. 3.1: Allan deviation (σ_A), relative errors after minimization for Ω, ω, ι, a_1, a_2, ε_1, and ε_2, absolute error in perigee passage time (Δt_{p1}, Δt_{p2}) in μs, the ratio of the final and the initial value of action ($\mathcal{S}_{in}/\mathcal{S}_{fin}$), and time needed to minimize $\mathcal{S}$ (toc) in seconds. Absolute error of few μs in Δt_{p1} and Δt_{p2} should be compared to orbital period which is about 9.13 hours.

3.2 Construction of a constellation

To construct a constellation of satellites we used Kepler equations (Sec. 2.3) to generate 200 data pairs $(\overline{\tau}[i], \tau[i])$ along 4 orbits and to minimize the action (2.16). The action was minimized with the Mathematica routine `FindMinimum`. The true constants of motion, which were used for simulating a pair of satellites, are given in Tab. 3.5.

satellite	Ω [°]	ω [°]	ι [°]	a [km]	ε	t_p [s]
1	0	0	0	22322	0.01	0
2	40.1	11.5	45	22324	0.005	0

Table 3.5: Orbital parameters for two satellites: longitude of ascending node (Ω), longitude of perigee (ω), inclination (ι), major semi-axis (a), eccentricity (ε), and time of perigee passage (t_p).

Figure 3.8 presents the results of this experiment, where the abscissa value shows Allan deviation σ_A, while the ordinate gives the value of the action and absolute values of the difference between the calculated constant of motion and its value used to calculate the dynamics of satellites.

One can see that the error in constants of motion increases linearly and the action quadratically with timing noise amplitude, as expected. The minimization procedure always found a solution and the error is always below or near a predictable value indicated by light grey lines in Fig. 3.8. Other experiments produce very similar results. Although the experiments were not exhaustive, we feel that they give grounds to believe that the proposed minimization procedure is an effective mechanism for obtaining mutual constants of motion

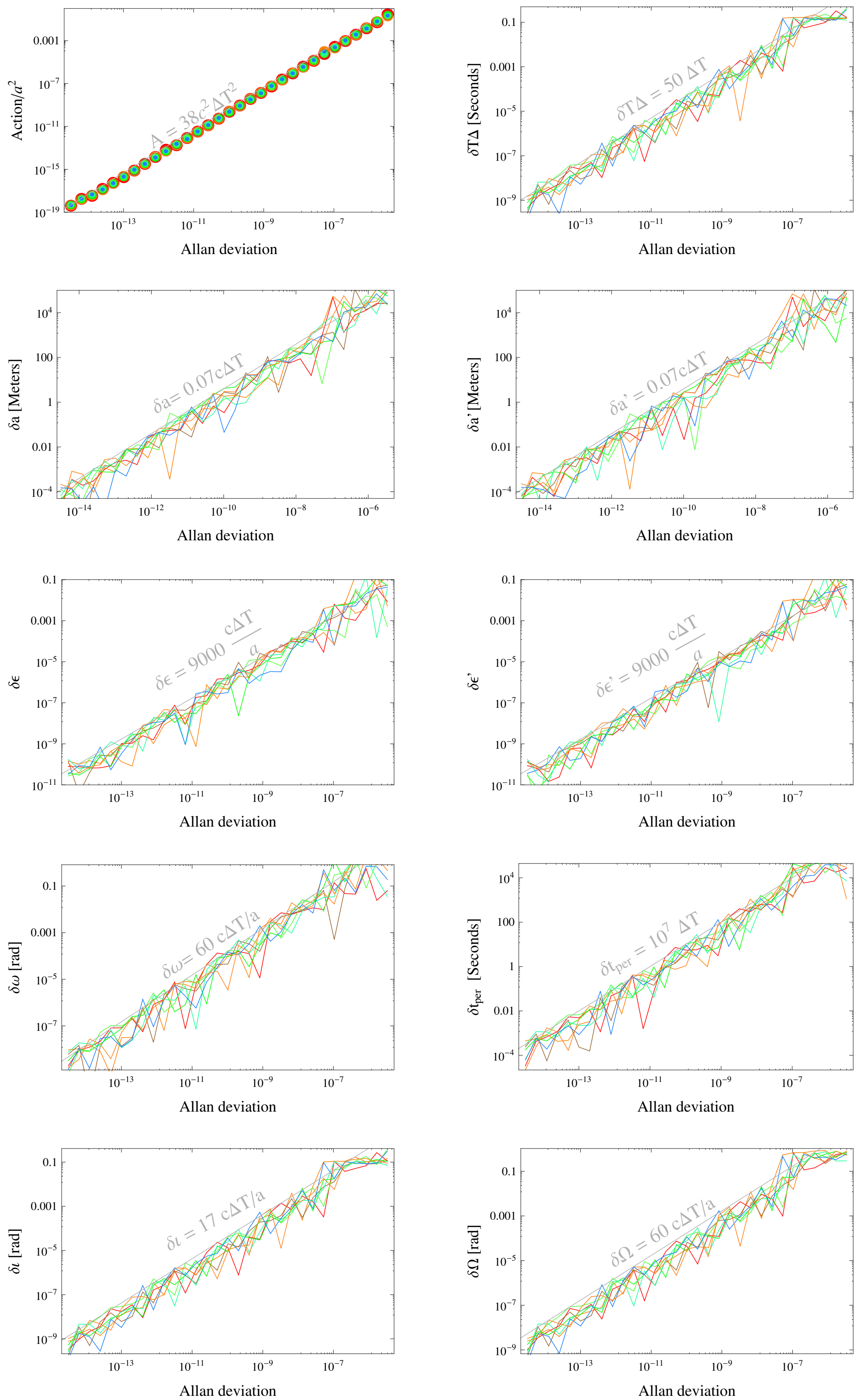

Figure 3.8: Uncertainty of constants of motion due to timing errors. For this experiment $\sigma_A = 3.5\Delta t$ (Δt is defined as in previous section). Light grey lines and corresponding formulae indicate the expected level of uncertainty in corresponding values.

between two satellites which can read the partner's emission coordinates and their own proper time.

In the "my perigee tool" we proceed as follows: starting from the set (t_k, t'_k), $k = 1 \ldots N$ we generate sets $S_l = t_k - \tau_l$, t'_k, $k = 1 \ldots N$, where the discrete values τ_l cover the interval where the correct value of perigee time is expected to be found. The action is minimized for each set S_l and the rough value of τ where the action is minimal is found. Such steps are repeated with finer and finer divisions for τ_l intervals until the diminishing of action stops. Results of applying this tool in one of such experiments are illustrated in Fig. 3.9.

The "clock rate correction tool" works in a similar way. We start with a set $S_\eta = ((1+\eta)t_k, t'_k)$, which is assumed to be the result of an exact solution of the two satellite communication problem, with the exception that the time t increases at a rate not 1 but $1+\eta$. Fig. 3.10 shows what happens with the action and the constants of motion if they are calculated from a set S_η.

Let us illustrate the meaning of these results with respect to Galileo satellites moving at $\sim$ 23000 km from the Earth and taking $\sim$ 12 hours (43200 s) to make a full circle. Suppose that the clock rate error is 8.6 ns/day, which translates into $\eta = 10^{-13}$. Assuming no other errors are present in the exchange of emission coordinates, one reads in Tab. 3.6 the following error estimates for orbital constants from Fig. 3.10:

Orbital constant	Error ($\eta = 10^{-13}$)
$T\Delta$ (clock sinhr. diff.)	$\pm$4ns
a, a' (major axes)	$\pm$50mm
ε, ε' (orbital eccentricities)	$\pm 2 \times 10^{-9}$
ι (mutual inclination)	$\pm 2 \times 10^{-9}$
Ω (longitude line of nodes)	$\pm 2 \times 10^{-9}$
ω (longitude of perige)	$\pm 2 \times 10^{-9}$
t_{peri} (time of emitters perigee pass)	0.43ms

Table 3.6: The error estimates for orbital constants from Fig. 3.10.

From mutual to global constants of motion

To test the method from Sec. 2.3 to determine constants of motion that refer to the same global system we simulated three satellites with constants of motion from Tab. 3.7. These constants $MC_i = \{a_i, \varepsilon_i, \iota_i, \Omega_i, \omega_i, t_{pi}\}$ $(i = 1,2,3)$ were used to calculate Runge-Lenz $(\vec{R}_i)$ and angular momentum $(\vec{l}_i)$ vectors of satellites in a global system of reference. After minimization, Runge-Lenz $(\vec{R}_{ij})$ and angular momentum $(\vec{l}_{ij})$ vectors of satellite i with respect to satellite j were obtained and used to calculate mutual constants of motion $\{a_i, a_j, \varepsilon_i, \varepsilon_j, \iota_{ij}, \Omega_{ij}, \omega_{ij}, t_{pi}, t_{pj},\}$ $(i \neq j = 1,2,3)$. Finally, after applying algorithm from

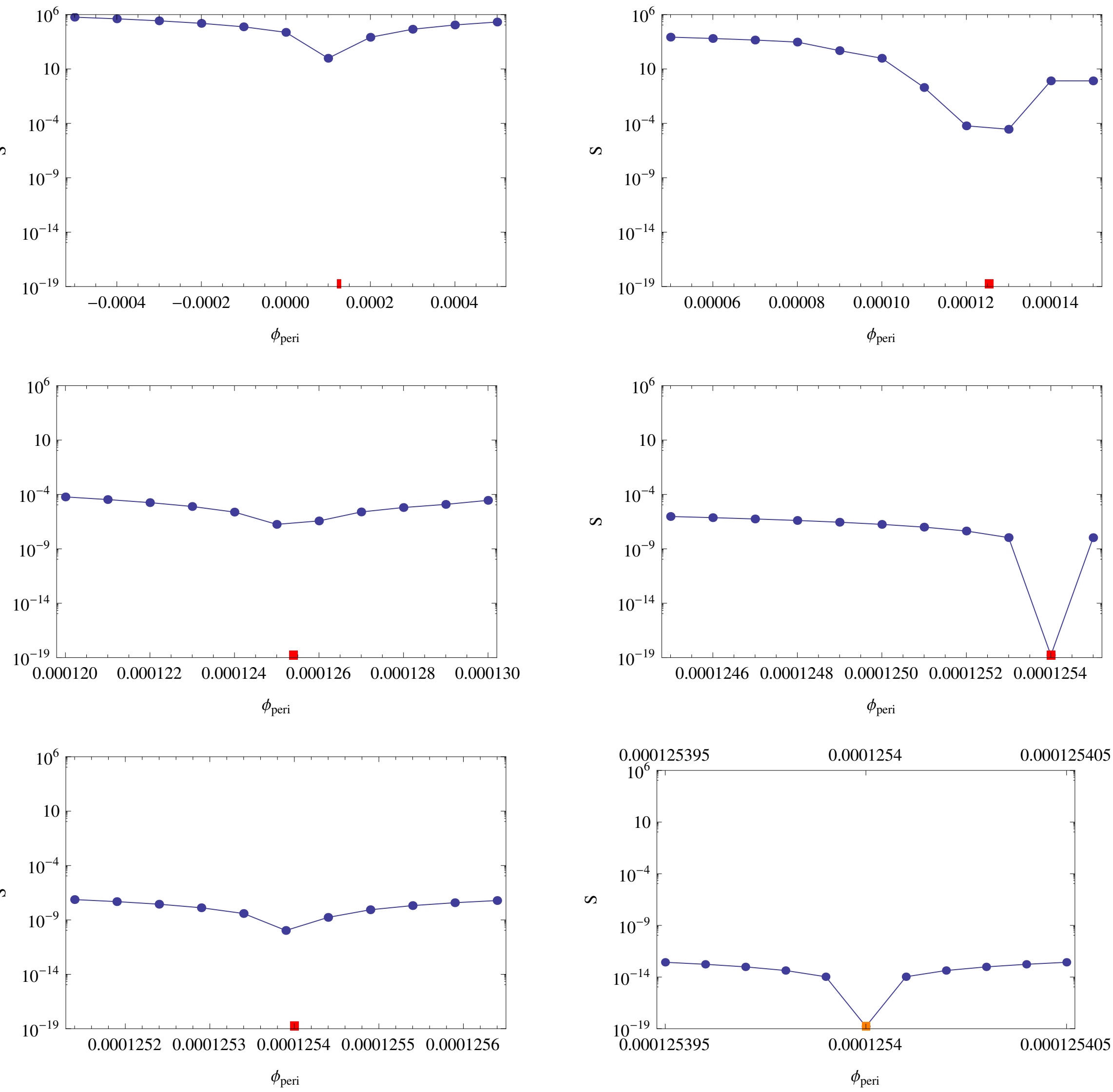

Figure 3.9: Finding the moment of perigee passage for satellite i: diagrams show the action (2.16) for discrete values τ_l; at each next step the numerical resolution is increased by a factor 10.

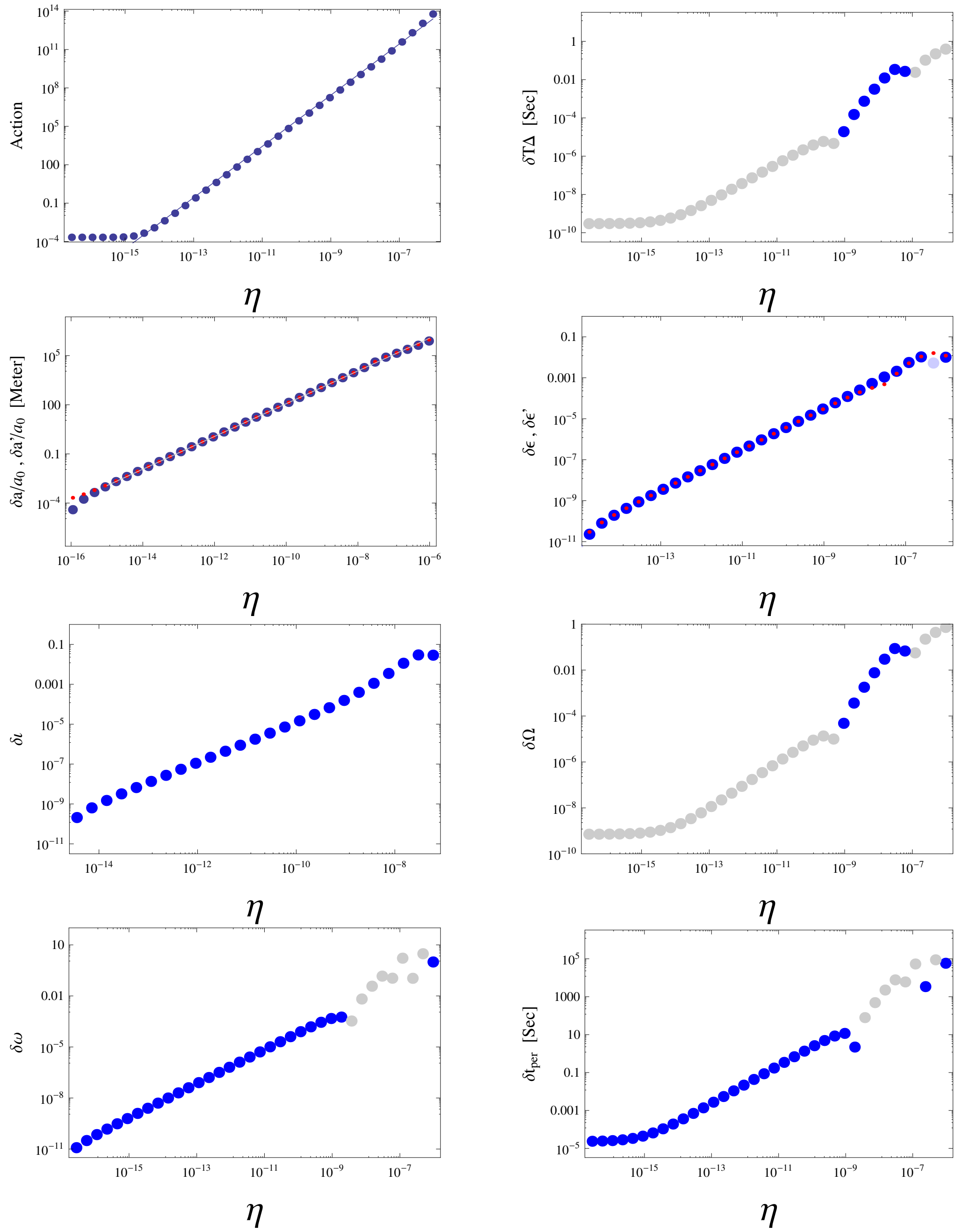

Figure 3.10: The action and the error in calculating constants of motion if clock of i drifts with respect to j's clock. The errors are plotted in the log-log scale – if they are positive with respect to the labels the corresponding points are blue (or red), otherwise they are light grey.

Sec. 2.3 (see also App. B) vectors $\vec{R'}_i$ and $\vec{l'}_i$ in a global system of reference are expressed and used to calculate global constants of motion MC'_i.

The results are in Tab. 3.8, where the differences $\vec{R'}_i - \vec{R}_i$ and $\vec{l'}_i - \vec{l}_i$ are shown, and in Tab. 3.9 where the differences $MC_i - MC'_i$ between global constants of motion are shown. As expected, the algorithm finds global constants of motion with a small error, as long as inclinations of both satellites are different. If, however, $\iota_i \approx \iota_j$ (as in case $(i, j) = (1, 3)$ and $(3, 1)$), i.e. mutual inclination equals to zero ($\iota_{13} = 0$), the algorithm still manages to find the constants but the error increases many orders of magnitude since the system of equations becomes degenerate – the line of nodes is not well defined. This and some other special cases must be treated separately, but they can clearly be resolved using parameters from non-degenerate mutual relations.

i	Ω_i [°]	ω_i [°]	ι_i [°]	a_i [km]	ε_i	t_{pi} [hour]
1	60	47	40	22322	0.002	2.77
2	35	27	10	23438	0.001	1.98
3	60	47	40	22322	0.0015	6.94

Table 3.7: Orbital parameters for three satellites: longitude of ascending node (Ω), longitude of perigee (ω), inclination (ι), major semi-axis (a), eccentricity (ε), and time of perigee passage (t_p).

i	j	$(\vec{l'}_j - \vec{l}_j)/\lvert\vec{l}_j\rvert$	$(\vec{R'}_j - \vec{R}_j)/a$
1	2	$(-10^{-13}, -2.7\ 10^{-13}, -2.6\ 10^{-14})$	$(3.4\ 10^{-16}, -1.4\ 10^{-15}, 7\ 10^{-17})$
2	1	$(2.8\ 10^{-14}, 6\ 10^{-14}, 5.7\ 10^{-15})$	$(-10^{-14}, -2.5\ 10^{-14}, -1.6\ 10^{-15})$
1	3	$(2.2\ 10^{-6}, -1.4\ 10^{-6}, -3.3\ 10^{-6})$	$(-7\ 10^{-5}, 4\ 10^{-4}, 2\ 10^{-4})$
3	1	$(-2\ 10^{-7}, 2.7\ 10^{-7}, 2.8\ 10^{-8})$	$(2\ 10^{-10}, -7\ 10^{-11}, 3\ 10^{-10})$

Table 3.8: Relative differences between true and calculated Runge-Lenz $(\vec{R'}_j - \vec{R}_j)/a$ and angular momentum $(\vec{l'}_j - \vec{l}_j)/|\vec{l}_j|$ vectors for satellites i and j. Vectors $\vec{R}'_j$ and $\vec{l}'_j$ are expressed in a (cartesian) system where satellite i's constants of motion are MC_i, i.e. $\vec{R'}_i = \vec{R}_i$ and $\vec{l'}_j = \vec{l}_j$. Note that for the last two examples $\iota_1 = \iota_3$, therefore it is not possible to determine (well) the corresponding vectors $\vec{l'}_j$ and $\vec{R'}_j$.

i	j	$\Omega'_j - \Omega_j$	$\omega'_j - \omega_j$	$\iota'_j - \iota_j$
1	2	-1.4×10^{-12}	5×10^{-13}	1.5×10^{-13}
2	1	10^{-13}	9×10^{-12}	-8.8×10^{-15}
1	3	-2.3×10^{-7}	-1.8×10^{-6}	4×10^{-6}
3	1	-5.1×10^{-7}	3.9×10^{-7}	-4.3×10^{-8}

Table 3.9: Differences between true and calculated angles $\Omega'_j - \Omega_j$, $\omega'_j - \omega_j$, and $\iota'_j - \iota_j$ for satellites i and j. The angles Ω'_j, ω'_j, and ι'_j are expressed in a system where satellite i's constants of motion are MC_i, i.e. $\Omega'_i = \Omega_i$, $\omega'_i = \omega_i$, and $\iota'_i = \iota_i$. Note that for the last two examples $\iota_1 = \iota_3$, therefore it is not possible to determine (well) the corresponding angles Ω'_j, ω'_j, and ι'_j.

Conclusion 4

The concept **A**utonomous **B**asis of **C**oordinates (ABC) is introduced. It is a natural extension of general relativistic description of dynamics of non-interacting bodies, described by geodesics in space-time. Since light, propagating along geodesics as well, spreads emission coordinates throughout space-time, it is possible to describe dynamics in terms of emission coordinates. The ABC concept provides a means to translate dynamical information, described by emission coordinates, into the conventional representation based on local stationary frame coordinates. Dynamical information, expressed in terms of emission coordinates, gives direct information about the Riemannian structure of space-time, and thus allows the construction of local stationary frame with coordinates and metric that provides a precise definition of equations of motion.

The mechanism of ABC concept is first illustrated in the Minkowski space-time. This illustration shows how perturbations, in the form of Riemann tensor, can be detected on the basis of dynamical information provided by emission coordinates, i.e. how deviations from assumed dynamics lead to improvement of dynamical description. In sections 2.3 and 2.4 we have shown how dynamical information, provided by emission coordinates, can be used in more realistic space-times – Keplerian and Schwarzschild – to build the complete dynamical model of the constellation.

The results of numerical ABC models are presented in Sec. 3: the input code generates sets of pairs of emission coordinates $P^{ij} = \{\bar{\tau}^i[k], \tau_i^j[k]\}$ (see (2.1)) for the given dynamical model, corresponding to an exact model scenario. The output code takes input data and attempts to reconstruct constants of motion used to construct the input data. It was demonstrated, that the reconstruction is robust, and accurately returns the constants of motion, so that positions of satellites, calculated from reconstructed data, usually agree to 15 significant figures with those calculated from input code constants. This accuracy is limited by the internal precision of minimization procedures used to determine constants of motion. Some exceptions to such precision have been noted, but detailed analysis of degenerate cases still needs to be performed. Accuracy limitations imposed by clock noise were evaluated. Clock noise is modelled as random phase noise characterized by typical timing error with respect to uniformly running proper time plus a small drift resulting in a small difference between the rate of the clock and the rate of proper time. We find that the rate error and resulting timing synchronization errors can be averaged out on sets of data covering a few orbital periods (see Figs. 3.8 and 3.10). The remaining timing phase error is determined in absolute terms by the Allan deviation of the clock on time scale of only a few orbital periods. Theoretically the average timing phase error goes to zero with increasing number of observations, meaning that, for time scales longer then a few orbital periods the measure of time is gauged by dynamics and not by clocks.

The ABC concept establishes a local inertial frame, which is based solely on dynamics of GNSS satellites, and is thus completely independent of a terrestrial reference. Natural distance and time scales are firmly defined by the gravitational radius of the Earth and the speed of light, therefore, the translation from emission coordinates to local inertial coordinates involves no other physical scale. Only the accuracy of defining emission coordinate labels depends on the accuracy of on-board clocks. Therefore, the relative position error of dynamical prediction is limited by relative (not absolute) clock error – by Allan deviation over the period of a few orbits in which constants of motion of satellites can be determined. Preliminary analysis, presented in this report, indicate that proposed Galileo on-board clocks, with Allan deviation of 1 ns per day, would allow average satellite relative position errors ($\delta r = |\vec{r} - \vec{r}_{calc}|$) to be below $1.5 \times 10^{-10} a \approx 4$ mm at any time. The global constants of motion, which are averages of mutual ones, are expected to be defined with accordingly higher accuracy. The accuracy of average values is expected to increase with time, as the dynamical model will include higher order stationary perturbations in the system Hamiltonian. The ultimate accuracy of the ABC frame is eventually limited by stochastic perturbations, that cannot be included in the Hamiltonian.

This preliminary study of the ABC concept can end in a rather optimistic tone. Our analysis suggests that present technology, planned to be used in the Galileo system, should be able to routinely reach millimetre accuracy with respect to an absolute local inertial frame defined independently of Earth based coordinates. At this level of accuracy it seems logical and even necessary to decouple the local inertial frame from the geodetic Earth frame, and allow the comparison of the two, to tell us fine details about Earth rotation, gravitational potential and dynamics of Earth crust.

SCHWARZSCHILD EQUATIONS A

`AllCf` and `COf` are coefficients in the expansion of

$$r^2(\Phi) = \texttt{COf} + \sum_{i=1}^{s} \left[(-1)^i \texttt{AllCf}[[i]] \cos \frac{i\pi\phi}{2n\mathrm{K}(m)} \right] , \tag{A.1}$$

where $s \leq 18$; when the coefficients are calculated, s is set to the lowest value for which the sum gives results with required accuracy. The arguments of `AllCf` and `COf` are $\alpha_0, \ldots, \alpha_4$ ... are the coefficients of expansion of $\mathrm{cn}(x|m)^2$ in a Fourier (nome expansion) series

$$\mathrm{cn}^{-2}(x|m) = \sum_{j=0}^{5} \cos \frac{j\pi x}{\mathrm{K}(m)} \alpha_j \tag{A.2}$$

and u_2, u_3 are the roots of the characteristic polynomial of the Schwarzscild orbit problem

$$u = u_2 - (u_2 - u_3)\mathrm{cn}^2(\frac{\phi}{2n}|m) . \tag{A.3}$$

If $\texttt{Fun}[\tau] = a[[1]]\tau + \sum_{i=1}^{N-1} a[[i+1]] \sin(i\tau)$, where $N = \texttt{Length}[a]$ then $\texttt{InvFun}[x\tau, a]$ is the inverse of $\texttt{Fun}[\tau]$, i.e. $\texttt{InvFun}[\texttt{Fun}[\tau], a] = \tau$. This approximation is valid if the series coefficients $a[[i]]$ go to zero sufficiently rapidly. Note that this approximation limits the domain of validity of expansion $\phi(\tau)$ below.

If `KT` and `KS` are Fourier series coefficients of two fourier series $\texttt{FT}[\psi] = \sum_j^N \texttt{KT}[[j]] \sin(j\psi)$ and $\texttt{FS}[\psi] = \sum_j^M \texttt{KS}[[j]] \sin(j\psi)$, then `Produkt` returns the $P = \min(N, M)$ Fourier coefficients of $\texttt{FT}[\psi]\texttt{FS}[\psi]$. If one of the series has few nonzero Fourier coefficients and the other one needs more terms to describe the function, give the value zero to the small terms in order not to truncate the output series too soon.

AllCf[{α_0, α_1, α_2, α_3, α_4}, u_2, u_3][[1]]

$$
\begin{aligned}
&\frac{1}{16\,u_3^8}\,(u_2-u_3)\,\Big(15\,(u_2-u_3)^4\,\alpha_1^5\,(4\,u_3+7\,(u_2-u_3)\,(-4+4\,\alpha_0+3\,\alpha_2))\,+\\
&\quad 15\,(u_2-u_3)^4\,\alpha_1^4\,(10\,u_3+7\,(u_2-u_3)\,(-10+10\,\alpha_0+11\,\alpha_2))\,\alpha_3\,+\\
&\quad 2\,(u_2-u_3)^2\,\alpha_1^3\,\Big(24\,u_3^3+40\,(u_2-u_3)\,u_3^2\,(-3+3\,\alpha_0+2\,\alpha_2)\,+\\
&\qquad 105\,(u_2-u_3)^3\,\Big(2\,(-2+2\,\alpha_0+\alpha_2)\,\Big(2\,(-1+\alpha_0)^2+3\,(-1+\alpha_0)\,\alpha_2+2\,\alpha_2^2\Big)+3\,(-4+4\,\alpha_0+3\,\alpha_2)\,\alpha_3^2\Big)\,+\\
&\qquad 30\,(u_2-u_3)^2\,u_3\,\Big(12\,(-2+\alpha_0)\,\alpha_0-16\,\alpha_2+16\,\alpha_0\,\alpha_2+7\,\alpha_2^2+6\,\Big(2+\alpha_3^2\Big)\Big)\Big)\,+\\
&\quad 6\,(u_2-u_3)\,\alpha_2\,\alpha_3\,\Big(8\,u_3^4+8\,(u_2-u_3)\,u_3^3\,(-4+4\,\alpha_0+\alpha_2)+20\,(u_2-u_3)^2\,u_3^2\\
&\qquad\Big(4+4\,\alpha_0^2+2\,\alpha_0\,(-4+\alpha_2)+(-2+\alpha_2)\,\alpha_2+\alpha_3^2\Big)+10\,(u_2-u_3)^3\,u_3\,\Big(16\,\alpha_0^3+12\,\alpha_0^2\,(-4+\alpha_2)\,+\\
&\qquad\quad 2\,(-8+\alpha_2\,(6+(-6+\alpha_2)\,\alpha_2))+3\,(-4+\alpha_2)\,\alpha_3^2+12\,\alpha_0\,\Big(4+(-2+\alpha_2)\,\alpha_2+\alpha_3^2\Big)\Big)\,+\\
&\qquad 35\,(u_2-u_3)^4\,\Big(8+8\,\alpha_0^4+8\,\alpha_0^3\,(-4+\alpha_2)-8\,\alpha_2+12\,\alpha_2^2-4\,\alpha_2^3+\alpha_2^4+4\,\alpha_0\,(-8+\alpha_2\,(6+(-6+\alpha_2)\,\alpha_2))\,+\\
&\qquad\quad 6\,\alpha_0\,(-4+\alpha_2)\,\alpha_3^2+3\,(4+(-2+\alpha_2)\,\alpha_2)\,\alpha_3^2+\alpha_3^4+12\,\alpha_0^2\,\Big(4+(-2+\alpha_2)\,\alpha_2+\alpha_3^2\Big)\Big)\Big)\,+\\
&\quad 6\,(u_2-u_3)^2\,\alpha_1^2\,\alpha_3\,\Big(8\,u_3^3+20\,(u_2-u_3)\,u_3^2\,(-2+2\,\alpha_0+3\,\alpha_2)+30\,(u_2-u_3)^2\,u_3\\
&\qquad\Big(4+4\,(-2+\alpha_0)\,\alpha_0-12\,\alpha_2+12\,\alpha_0\,\alpha_2+5\,\alpha_2^2+\alpha_3^2\Big)+35\,(u_2-u_3)^3\,\Big(-8+8\,\alpha_0^3+12\,\alpha_0^2\,(-2+3\,\alpha_2)\,-\\
&\qquad\quad 6\,\alpha_3^2+6\,\alpha_0\,\Big(4+\alpha_2\,(-12+5\,\alpha_2)+\alpha_3^2\Big)+\alpha_2\,\Big(10\,(-3+\alpha_2)\,\alpha_2+9\,\Big(4+\alpha_3^2\Big)\Big)\Big)\Big)\,+\\
&\quad 2\,\alpha_1\,\Big(16\,u_3^5+24\,(u_2-u_3)\,u_3^4\,(-2+2\,\alpha_0+\alpha_2)+48\,(u_2-u_3)^2\,u_3^3\\
&\qquad\Big(2+2\,\alpha_0^2+2\,\alpha_0\,(-2+\alpha_2)+(-2+\alpha_2)\,\alpha_2+\alpha_3^2\Big)+20\,(u_2-u_3)^3\,u_3^2\,\Big(8\,\alpha_0^3+12\,\alpha_0^2\,(-2+\alpha_2)\,+\\
&\qquad\quad 12\,\alpha_0\,\Big(2+(-2+\alpha_2)\,\alpha_2+\alpha_3^2\Big)+3\,\alpha_2\,\Big((-2+\alpha_2)^2+2\,\alpha_3^2\Big)-4\,\Big(2+3\,\alpha_3^2\Big)\Big)+30\,(u_2-u_3)^4\,u_3\\
&\qquad\Big(8+8\,\alpha_0^4+16\,\alpha_0^3\,(-2+\alpha_2)+\alpha_2\,(-16+3\,\alpha_2\,(8+(-4+\alpha_2)\,\alpha_2))+24\,\alpha_3^2+3\,\alpha_2\,(-8+5\,\alpha_2)\,\alpha_3^2\,+\\
&\qquad\quad 3\,\alpha_3^4+24\,\alpha_0^2\,\Big(2+(-2+\alpha_2)\,\alpha_2+\alpha_3^2\Big)+4\,\alpha_0\,\Big(3\,\alpha_2\,\Big((-2+\alpha_2)^2+2\,\alpha_3^2\Big)-4\,\Big(2+3\,\alpha_3^2\Big)\Big)\Big)\,+\\
&\qquad 21\,(u_2-u_3)^5\,\Big(16\,\alpha_0^5+40\,\alpha_0^4\,(-2+\alpha_2)+80\,\alpha_0^3\,\Big(2+(-2+\alpha_2)\,\alpha_2+\alpha_3^2\Big)-16\,\Big(1+5\,\alpha_3^2\Big)\,+\\
&\qquad\quad 10\,\alpha_0\,\Big(8+\alpha_2\,(-16+3\,\alpha_2\,(8+(-4+\alpha_2)\,\alpha_2))+24\,\alpha_3^2+3\,\alpha_2\,(-8+5\,\alpha_2)\,\alpha_3^2+3\,\alpha_3^4\Big)\,+\\
&\qquad\quad 5\,\Big(\alpha_2\,(8+(-4+\alpha_2)\,\alpha_2\,(4+(-2+\alpha_2)\,\alpha_2))+2\,\alpha_2\,(12+\alpha_2\,(-15+4\,\alpha_2))\,\alpha_3^2+3\,(-2+\alpha_2)\,\alpha_3^4\Big)\,+\\
&\qquad\quad 20\,\alpha_0^2\,\Big(3\,\alpha_2\,\Big((-2+\alpha_2)^2+2\,\alpha_3^2\Big)-4\,\Big(2+3\,\alpha_3^2\Big)\Big)\Big)\Big)\Big)
\end{aligned}
$$

```
AllCf[{α0, α1, α2, α3, α4}, u2, u3][[2]]
```

$$
\begin{aligned}
&\frac{1}{32\,u_3^8}\,(u_2-u_3)\\
&\Big(120\,(u_2-u_3)^4\,(u_3+7\,(u_2-u_3)\,(-1+\alpha_0))\,\alpha_2^5+525\,(u_2-u_3)^5\,\alpha_2^4\,\big(2\,\alpha_1^2+4\,\alpha_1\,\alpha_3+\alpha_3^2\big)+48\,(u_2-u_3)^2\,\alpha_2^3\\
&\quad\big(2\,u_3^3+10\,(u_2-u_3)\,u_3^2\,(-1+\alpha_0)+35\,(u_2-u_3)^3\,(-1+\alpha_0)\,\big(2+2\,(-2+\alpha_0)\,\alpha_0+3\,\alpha_1^2+4\,\alpha_1\,\alpha_3+3\,\alpha_3^2\big)+\\
&\quad 5\,(u_2-u_3)^2\,u_3\,\big(6+6\,(-2+\alpha_0)\,\alpha_0+3\,\alpha_1^2+4\,\alpha_1\,\alpha_3+3\,\alpha_3^2\big)\big)+60\,(u_2-u_3)^3\,\alpha_2^2\,\big(21\,(u_2-u_3)^2\,\alpha_1^4+\\
&\quad 70\,(u_2-u_3)^2\,\alpha_1^3\,\alpha_3+3\,\alpha_1\,\alpha_3\,\big(4\,u_3^2+24\,(u_2-u_3)\,u_3\,(-1+\alpha_0)+21\,(u_2-u_3)^2\,\big(4\,(-1+\alpha_0)^2+\alpha_3^2\big)\big)+\\
&\quad \alpha_3^2\,\big(2\,u_3^2+12\,(u_2-u_3)\,u_3\,(-1+\alpha_0)+7\,(u_2-u_3)^2\,\big(6\,(-1+\alpha_0)^2+\alpha_3^2\big)\big)+\\
&\quad 6\,\alpha_1^2\,\big(u_3^2+6\,(u_2-u_3)\,u_3\,(-1+\alpha_0)+7\,(u_2-u_3)^2\,\big(3\,(-1+\alpha_0)^2+2\,\alpha_3^2\big)\big)\big)+\\
&\quad (u_2-u_3)\,\alpha_1\,\big(105\,(u_2-u_3)^4\,\alpha_1^5+462\,(u_2-u_3)^4\,\alpha_1^4\,\alpha_3+60\,(u_2-u_3)^2\,\alpha_1^2\,\alpha_3\\
&\qquad \big(4\,u_3^2+24\,(u_2-u_3)\,u_3\,(-1+\alpha_0)+21\,(u_2-u_3)^2\,\big(4\,(-1+\alpha_0)^2+\alpha_3^2\big)\big)+\\
&\qquad 5\,(u_2-u_3)^2\,\alpha_1^3\,\big(16\,u_3^2+96\,(u_2-u_3)\,u_3\,(-1+\alpha_0)+21\,(u_2-u_3)^2\,\big(16\,(-1+\alpha_0)^2+9\,\alpha_3^2\big)\big)+\\
&\qquad 12\,\alpha_3\,\big(8\,u_3^4+32\,(u_2-u_3)\,u_3^3\,(-1+\alpha_0)+20\,(u_2-u_3)^2\,u_3^2\,\big(4\,(-1+\alpha_0)^2+\alpha_3^2\big)+40\,(u_2-u_3)^3\,u_3\\
&\qquad\quad (-1+\alpha_0)\,\big(4\,(-1+\alpha_0)^2+3\,\alpha_3^2\big)+35\,(u_2-u_3)^4\,\big(8\,(-1+\alpha_0)^4+12\,(-1+\alpha_0)^2\,\alpha_3^2+\alpha_3^4\big)\big)+\\
&\qquad 6\,\alpha_1\,\big(8\,u_3^4+32\,(u_2-u_3)\,u_3^3\,(-1+\alpha_0)+40\,(u_2-u_3)^2\,u_3^2\,\big(2\,(-1+\alpha_0)^2+\alpha_3^2\big)+80\,(u_2-u_3)^3\\
&\qquad\quad u_3\,(-1+\alpha_0)\,\big(2\,(-1+\alpha_0)^2+3\,\alpha_3^2\big)+35\,(u_2-u_3)^4\,\big(8\,(-1+\alpha_0)^4+24\,(-1+\alpha_0)^2\,\alpha_3^2+3\,\alpha_3^4\big)\big)\big)+\\
&\quad 4\,\alpha_2\,\big(16\,u_3^5+48\,(u_2-u_3)\,u_3^4\,(-1+\alpha_0)+48\,(u_2-u_3)^2\,u_3^3\,\big(2+2\,(-2+\alpha_0)\,\alpha_0+\alpha_1^2+\alpha_1\,\alpha_3+\alpha_3^2\big)+\\
&\qquad 80\,(u_2-u_3)^3\,u_3^2\,(-1+\alpha_0)\,\big(2+2\,(-2+\alpha_0)\,\alpha_0+3\,\big(\alpha_1^2+\alpha_1\,\alpha_3+\alpha_3^2\big)\big)+15\,(u_2-u_3)^4\,u_3\\
&\qquad \big(16-64\,\alpha_0^3+16\,\alpha_0^4+7\,\alpha_1^4+20\,\alpha_1^3\,\alpha_3+12\,\alpha_1\,\alpha_3\,\big(4+\alpha_3^2\big)+6\,\alpha_3^2\,\big(8+\alpha_3^2\big)+48\,\alpha_0^2\,\big(2+\alpha_1^2+\alpha_1\,\alpha_3+\alpha_3^2\big)+\\
&\qquad\quad 6\,\alpha_1^2\,\big(8+5\,\alpha_3^2\big)-32\,\alpha_0\,\big(2+3\,\big(\alpha_1^2+\alpha_1\,\alpha_3+\alpha_3^2\big)\big)\big)+21\,(u_2-u_3)^5\,(-1+\alpha_0)\\
&\qquad \big(16-64\,\alpha_0^3+16\,\alpha_0^4+80\,\alpha_1^2+5\,\big(7\,\alpha_1^4+4\,\alpha_1\,\big(4+5\,\alpha_1^2\big)\,\alpha_3+2\,\big(8+15\,\alpha_1^2\big)\,\alpha_3^2+12\,\alpha_1\,\alpha_3^3+6\,\alpha_3^4\big)-\\
&\qquad\quad 32\,\alpha_0\,\big(2+5\,\big(\alpha_1^2+\alpha_1\,\alpha_3+\alpha_3^2\big)\big)+16\,\alpha_0^2\,\big(6+5\,\big(\alpha_1^2+\alpha_1\,\alpha_3+\alpha_3^2\big)\big)\big)\big)\Big)
\end{aligned}
$$

$\mathbf{AllCf[\{\alpha_0, \alpha_1, \alpha_2, \alpha_3, \alpha_4\}, u_2, u_3][[3]]}$

$$
\begin{aligned}
&\frac{1}{16\, u_3^8} (u_2 - u_3) \\
&((u_2 - u_3)\, \alpha_1\, (2\, (u_2 - u_3)\, \alpha_1^2\, (8\, u_3^3 + 40\, (u_2 - u_3)\, u_3^2\, (-1 + \alpha_0) + 15\, (u_2 - u_3)^2\, u_3\, (8\, (-1 + \alpha_0)^2 + \alpha_1^2) + \\
&\quad 35\, (u_2 - u_3)^3\, (-1 + \alpha_0)\, (8\, (-1 + \alpha_0)^2 + 3\, \alpha_1^2)) + \\
&\quad 3\, (16\, u_3^4 + 64\, (u_2 - u_3)\, u_3^3\, (-1 + \alpha_0) + 40\, (u_2 - u_3)^2\, u_3^2\, (4\, (-1 + \alpha_0)^2 + \alpha_1^2) + 80\, (u_2 - u_3)^3\, u_3 \\
&\quad (-1 + \alpha_0)\, (4\, (-1 + \alpha_0)^2 + 3\, \alpha_1^2) + 7\, (u_2 - u_3)^4\, (80\, (-1 + \alpha_0)^4 + 120\, (-1 + \alpha_0)^2\, \alpha_1^2 + 11\, \alpha_1^4))\, \alpha_2 + \\
&\quad 12\, (u_2 - u_3)\, (4\, u_3^3 + 20\, (u_2 - u_3)\, u_3^2\, (-1 + \alpha_0) + 35\, (u_2 - u_3)^3\, (-1 + \alpha_0)\, (4\, (-1 + \alpha_0)^2 + 5\, \alpha_1^2) + \\
&\quad 5\, (u_2 - u_3)^2\, u_3\, (12\, (-1 + \alpha_0)^2 + 5\, \alpha_1^2))\, \alpha_2^2 + \\
&\quad 20\, (u_2 - u_3)^2\, (6\, u_3^2 + 36\, (u_2 - u_3)\, u_3\, (-1 + \alpha_0) + 7\, (u_2 - u_3)^2\, (18\, (-1 + \alpha_0)^2 + 5\, \alpha_1^2))\, \alpha_2^3 + \\
&\quad 120\, (u_2 - u_3)^3\, (u_3 + 7\, (u_2 - u_3)\, (-1 + \alpha_0))\, \alpha_2^4 + 210\, (u_2 - u_3)^4\, \alpha_2^5) + \\
&\quad (32\, u_3^5 + 96\, (u_2 - u_3)\, u_3^4\, (-1 + \alpha_0) + 96\, (u_2 - u_3)^2\, u_3^3\, (2 + 2\, (-2 + \alpha_0)\, \alpha_0 + \alpha_1^2 + \alpha_2^2) + \\
&\quad 40\, (u_2 - u_3)^3\, u_3^2\, (8\, (-1 + \alpha_0)^3 + 12\, (-1 + \alpha_0)\, \alpha_1^2 + 6\, \alpha_1^2\, \alpha_2 + 12\, (-1 + \alpha_0)\, \alpha_2^2 + \alpha_2^3) + \\
&\quad 21\, (u_2 - u_3)^5\, (32\, (-1 + \alpha_0)^5 + 160\, (-1 + \alpha_0)^3\, \alpha_1^2 + 60\, (-1 + \alpha_0)\, \alpha_1^4 + 15\, \alpha_1^2\, (16\, (-1 + \alpha_0)^2 + 3\, \alpha_1^2)\, \alpha_2 + \\
&\quad 20\, (-1 + \alpha_0)\, (8\, (-1 + \alpha_0)^2 + 15\, \alpha_1^2)\, \alpha_2^2 + 40\, ((-1 + \alpha_0)^2 + 2\, \alpha_1^2)\, \alpha_2^3 + 60\, (-1 + \alpha_0)\, \alpha_2^4 + 5\, \alpha_2^5) + \\
&\quad 60\, (u_2 - u_3)^4\, u_3\, (8 - 32\, \alpha_0^3 + 8\, \alpha_0^4 + 3\, \alpha_1^4 + 24\, \alpha_0^2\, (2 + \alpha_1^2 + \alpha_2^2) + 4\, \alpha_0 \\
&\quad (-8 + 6\, \alpha_1^2\, (-2 + \alpha_2) + (-12 + \alpha_2)\, \alpha_2^2) + \alpha_2^2\, (24 + \alpha_2\, (-4 + 3\, \alpha_2)) + 3\, \alpha_1^2\, (8 + \alpha_2\, (-8 + 5\, \alpha_2)))) \\
&\quad \alpha_3 + 90\, (u_2 - u_3)^3\, \alpha_1\, (2\, (u_2 - u_3)\, (u_3 + 7\, (u_2 - u_3)\, (-1 + \alpha_0))\, \alpha_1^2 + \\
&\quad (4\, u_3^2 + 24\, (u_2 - u_3)\, u_3\, (-1 + \alpha_0) + 21\, (u_2 - u_3)^2\, (4\, (-1 + \alpha_0)^2 + \alpha_1^2))\, \alpha_2 + \\
&\quad 6\, (u_2 - u_3)\, (u_3 + 7\, (u_2 - u_3)\, (-1 + \alpha_0))\, \alpha_2^2 + 21\, (u_2 - u_3)^2\, \alpha_2^3)\, \alpha_3^2 + \\
&\quad 4\, (u_2 - u_3)^2\, (12\, u_3^3 + 60\, (u_2 - u_3)\, u_3^2\, (-1 + \alpha_0) + 90\, (u_2 - u_3)^2\, u_3\, (2 + 2\, (-2 + \alpha_0)\, \alpha_0 + \alpha_1^2 + \alpha_2^2) + \\
&\quad 35\, (u_2 - u_3)^3\, (12\, (-1 + \alpha_0)^3 + 18\, (-1 + \alpha_0)\, \alpha_1^2 + 9\, \alpha_1^2\, \alpha_2 + 18\, (-1 + \alpha_0)\, \alpha_2^2 + 2\, \alpha_2^3))\, \alpha_3^3 + \\
&\quad 1050\, (u_2 - u_3)^5\, \alpha_1\, \alpha_2\, \alpha_3^4 + 60\, (u_2 - u_3)^4\, (u_3 + 7\, (u_2 - u_3)\, (-1 + \alpha_0))\, \alpha_3^5)
\end{aligned}
$$

AllCf[{α_0, α_1, α_2, α_3, α_4}, u_2, u_3][[4]]

$$
\begin{aligned}
&\frac{1}{32\,u_3^8}\,(u_2-u_3)^2\,\Big(105\,(u_2-u_3)^4\,\alpha_2^6+120\,(u_2-u_3)^3\,(u_3+7\,(u_2-u_3)\,(-1+\alpha_0))\,\alpha_2^3\,(2\,\alpha_1+\alpha_3)\,(2\,\alpha_1+3\,\alpha_3)+\\
&\quad 2\,\alpha_1\,\Big((u_2-u_3)^2\,\alpha_1^3\,\Big(10\,u_3^2+60\,(u_2-u_3)\,u_3\,(-1+\alpha_0)+21\,(u_2-u_3)^2\,\Big(10\,(-1+\alpha_0)^2+\alpha_1^2\Big)\Big)+\\
&\qquad 6\,\Big(8\,u_3^4+32\,(u_2-u_3)\,u_3^3\,(-1+\alpha_0)+20\,(u_2-u_3)^2\,u_3^2\,\Big(4\,(-1+\alpha_0)^2+\alpha_1^2\Big)+40\,(u_2-u_3)^3\,u_3\\
&\qquad\quad (-1+\alpha_0)\,\Big(4\,(-1+\alpha_0)^2+3\,\alpha_1^2\Big)+35\,(u_2-u_3)^4\,\Big(8\,(-1+\alpha_0)^4+12\,(-1+\alpha_0)^2\,\alpha_1^2+\alpha_1^4\Big)\Big)\,\alpha_3+\\
&\qquad 15\,(u_2-u_3)^2\,\alpha_1\,\Big(4\,u_3^2+24\,(u_2-u_3)\,u_3\,(-1+\alpha_0)+21\,(u_2-u_3)^2\,\Big(4\,(-1+\alpha_0)^2+\alpha_1^2\Big)\Big)\,\alpha_3^2+\\
&\qquad 30\,(u_2-u_3)^2\,\Big(4\,u_3^2+24\,(u_2-u_3)\,u_3\,(-1+\alpha_0)+21\,(u_2-u_3)^2\,\Big(4\,(-1+\alpha_0)^2+\alpha_1^2\Big)\Big)\,\alpha_3^3+\\
&\qquad 210\,(u_2-u_3)^4\,\alpha_1\,\alpha_3^4+210\,(u_2-u_3)^4\,\alpha_3^5\Big)+10\,(u_2-u_3)^2\,\alpha_2^4\\
&\quad \Big(8\,u_3^2+48\,(u_2-u_3)\,u_3\,(-1+\alpha_0)+21\,(u_2-u_3)^2\,\Big(8+8\,(-2+\alpha_0)\,\alpha_0+4\,\alpha_1^2+7\,\alpha_1\,\alpha_3+4\,\alpha_3^2\Big)\Big)+\\
&\quad 48\,(u_2-u_3)\,\alpha_2\,\Big(5\,(u_2-u_3)^2\,(u_3+7\,(u_2-u_3)\,(-1+\alpha_0))\,\alpha_1^4+\\
&\qquad 20\,(u_2-u_3)^2\,(u_3+7\,(u_2-u_3)\,(-1+\alpha_0))\,\alpha_1^3\,\alpha_3+\alpha_3^2\,\Big(2\,u_3^3+10\,(u_2-u_3)\,u_3^2\,(-1+\alpha_0)+\\
&\qquad\quad 35\,(u_2-u_3)^3\,(-1+\alpha_0)\,\Big(2\,(-1+\alpha_0)^2+\alpha_3^2\Big)+5\,(u_2-u_3)^2\,u_3\,\Big(6\,(-1+\alpha_0)^2+\alpha_3^2\Big)\Big)+\\
&\qquad 2\,\alpha_1^2\,\Big(u_3^3+5\,(u_2-u_3)\,u_3^2\,(-1+\alpha_0)+15\,(u_2-u_3)^2\,u_3\,\Big((-1+\alpha_0)^2+\alpha_3^2\Big)+\\
&\qquad\quad 35\,(u_2-u_3)^3\,(-1+\alpha_0)\,\Big((-1+\alpha_0)^2+3\,\alpha_3^2\Big)\Big)+\alpha_1\,\alpha_3\,\Big(4\,u_3^3+20\,(u_2-u_3)\,u_3^2\,(-1+\alpha_0)+\\
&\qquad\quad 15\,(u_2-u_3)^2\,u_3\,\Big(4\,(-1+\alpha_0)^2+\alpha_3^2\Big)+35\,(u_2-u_3)^3\,(-1+\alpha_0)\,\Big(4\,(-1+\alpha_0)^2+3\,\alpha_3^2\Big)\Big)\Big)+\\
&\quad 6\,\alpha_2^2\,\Big(8\,u_3^4+32\,(u_2-u_3)\,u_3^3\,(-1+\alpha_0)+40\,(u_2-u_3)^2\,u_3^2\,\Big(2+2\,(-2+\alpha_0)\,\alpha_0+(\alpha_1+\alpha_3)^2\Big)+\\
&\qquad 80\,(u_2-u_3)^3\,u_3\,(-1+\alpha_0)\,\Big(2+2\,(-2+\alpha_0)\,\alpha_0+3\,(\alpha_1+\alpha_3)^2\Big)+\\
&\qquad 35\,(u_2-u_3)^4\,\Big(8-32\,\alpha_0^3+8\,\alpha_0^4+4\,\alpha_1^2\,\Big(6+\alpha_1^2\Big)+16\,\alpha_1\,\Big(3+\alpha_1^2\Big)\,\alpha_3+3\,\Big(8+7\,\alpha_1^2\Big)\,\alpha_3^2+\\
&\qquad\quad 14\,\alpha_1\,\alpha_3^3+3\,\alpha_3^4+24\,\alpha_0^2\,\Big(2+(\alpha_1+\alpha_3)^2\Big)-16\,\alpha_0\,\Big(2+3\,(\alpha_1+\alpha_3)^2\Big)\Big)\Big)\Big)
\end{aligned}
$$

AllCf[{α_0, α_1, α_2, α_3, α_4}, u_2, u_3][[5]]

$$
\begin{aligned}
&\frac{1}{16\,u_3^8}\,(u_2-u_3)^2\,\Big(30\,(u_2-u_3)^3\,(u_3+7\,(u_2-u_3)\,(-1+\alpha_0))\,\alpha_2^4\,(4\,\alpha_1+\alpha_3)+105\,(u_2-u_3)^4\,\alpha_2^5\,(\alpha_1+2\,\alpha_3)+\\
&\quad \alpha_2\,\Big(5\,(u_2-u_3)^2\,\alpha_1^3\,\Big(8\,u_3^2+48\,(u_2-u_3)\,u_3\,(-1+\alpha_0)+21\,(u_2-u_3)^2\,\Big(8\,(-1+\alpha_0)^2+\alpha_1^2\Big)\Big)+\\
&\qquad 3\,\Big(16\,u_3^4+64\,(u_2-u_3)\,u_3^3\,(-1+\alpha_0)+80\,(u_2-u_3)^2\,u_3^2\,\Big(2\,(-1+\alpha_0)^2+\alpha_1^2\Big)+160\,(u_2-u_3)^3\,u_3\\
&\qquad\quad (-1+\alpha_0)\,\Big(2\,(-1+\alpha_0)^2+3\,\alpha_1^2\Big)+35\,(u_2-u_3)^4\,\Big(16\,(-1+\alpha_0)^4+48\,(-1+\alpha_0)^2\,\alpha_1^2+7\,\alpha_1^4\Big)\Big)\,\alpha_3+\\
&\qquad 60\,(u_2-u_3)^2\,\alpha_1\,\Big(2\,u_3^2+12\,(u_2-u_3)\,u_3\,(-1+\alpha_0)+21\,(u_2-u_3)^2\,\Big(2\,(-1+\alpha_0)^2+\alpha_1^2\Big)\Big)\,\alpha_3^2+\\
&\qquad 30\,(u_2-u_3)^2\,\Big(4\,u_3^2+24\,(u_2-u_3)\,u_3\,(-1+\alpha_0)+7\,(u_2-u_3)^2\,\Big(12\,(-1+\alpha_0)^2+7\,\alpha_1^2\Big)\Big)\,\alpha_3^3+\\
&\qquad 420\,(u_2-u_3)^4\,\alpha_1\,\alpha_3^4+210\,(u_2-u_3)^4\,\alpha_3^5\Big)+12\,(u_2-u_3)\,\alpha_2^2\\
&\quad \Big(15\,(u_2-u_3)^2\,(u_3+7\,(u_2-u_3)\,(-1+\alpha_0))\,\alpha_1^3+45\,(u_2-u_3)^2\,(u_3+7\,(u_2-u_3)\,(-1+\alpha_0))\,\alpha_1^2\,\alpha_3+\\
&\qquad 5\,(u_2-u_3)^2\,(u_3+7\,(u_2-u_3)\,(-1+\alpha_0))\,\alpha_3^3+4\,\alpha_1\,\Big(u_3^3+5\,(u_2-u_3)\,u_3^2\,(-1+\alpha_0)+\\
&\qquad\quad 15\,(u_2-u_3)^2\,u_3\,\Big((-1+\alpha_0)^2+\alpha_3^2\Big)+35\,(u_2-u_3)^3\,(-1+\alpha_0)\,\Big((-1+\alpha_0)^2+3\,\alpha_3^2\Big)\Big)\Big)+\\
&\quad 6\,(u_2-u_3)\,\alpha_1\,\Big((u_2-u_3)^2\,(u_3+7\,(u_2-u_3)\,(-1+\alpha_0))\,\alpha_1^4+20\,(u_2-u_3)^2\\
&\qquad (u_3+7\,(u_2-u_3)\,(-1+\alpha_0))\,\alpha_1^3\,\alpha_3+30\,(u_2-u_3)^2\,(u_3+7\,(u_2-u_3)\,(-1+\alpha_0))\,\alpha_1^2\,\alpha_3^2+\\
&\qquad 4\,\alpha_3^2\,\Big(2\,u_3^3+10\,(u_2-u_3)\,u_3^2\,(-1+\alpha_0)+35\,(u_2-u_3)^3\,(-1+\alpha_0)\,\Big(2\,(-1+\alpha_0)^2+\alpha_3^2\Big)+\\
&\qquad\quad 5\,(u_2-u_3)^2\,u_3\,\Big(6\,(-1+\alpha_0)^2+\alpha_3^2\Big)\Big)+2\,\alpha_1\,\alpha_3\,\Big(4\,u_3^3+20\,(u_2-u_3)\,u_3^2\,(-1+\alpha_0)+\\
&\qquad\quad 15\,(u_2-u_3)^2\,u_3\,\Big(4\,(-1+\alpha_0)^2+\alpha_3^2\Big)+35\,(u_2-u_3)^3\,(-1+\alpha_0)\,\Big(4\,(-1+\alpha_0)^2+3\,\alpha_3^2\Big)\Big)\Big)+\\
&\quad 10\,(u_2-u_3)^2\,\alpha_2^3\,\Big(42\,(u_2-u_3)^2\,\alpha_1^3+147\,(u_2-u_3)^2\,\alpha_1^2\,\alpha_3+\\
&\qquad 3\,\alpha_3\,\Big(4\,u_3^2+24\,(u_2-u_3)\,u_3\,(-1+\alpha_0)+21\,(u_2-u_3)^2\,\Big(4\,(-1+\alpha_0)^2+\alpha_3^2\Big)\Big)+\\
&\qquad \alpha_1\,\Big(4\,u_3^2+24\,(u_2-u_3)\,u_3\,(-1+\alpha_0)+21\,(u_2-u_3)^2\,\Big(4\,(-1+\alpha_0)^2+5\,\alpha_3^2\Big)\Big)\Big)\Big)
\end{aligned}
$$

$\mathbf{AllCf}[\{\alpha_0, \alpha_1, \alpha_2, \alpha_3, \alpha_4\}, \mathbf{u_2}, \mathbf{u_3}][[\mathbf{6}]]$

$$
\begin{aligned}
&\frac{1}{32\, u_3^8} (u_2-u_3)^2 \Big((u_2-u_3) \Big(7 (u_2-u_3)^3 \alpha_1^6 + 60 (u_2-u_3)^2 (u_3 + 7 (u_2-u_3) (-1+\alpha_0)) \alpha_1^4 \alpha_2 + \\
&\qquad 60 (u_2-u_3) \alpha_1^2 \Big(2 u_3^2 + 12 (u_2-u_3) u_3 (-1+\alpha_0) + 7 (u_2-u_3)^2 \Big(6 (-1+\alpha_0)^2 + \alpha_1^2\Big)\Big) \alpha_2^2 + \\
&\qquad 16 \Big(2 u_3^3 + 10 (u_2-u_3) u_3^2 (-1+\alpha_0) + 15 (u_2-u_3)^2 u_3 \Big(2 (-1+\alpha_0)^2 + \alpha_1^2\Big) + \\
&\qquad\quad 35 (u_2-u_3)^3 (-1+\alpha_0) \Big(2 (-1+\alpha_0)^2 + 3 \alpha_1^2\Big)\Big) \alpha_2^3 + \\
&\qquad 525 (u_2-u_3)^3 \alpha_1^2 \alpha_2^4 + 60 (u_2-u_3)^2 (u_3 + 7 (u_2-u_3) (-1+\alpha_0)) \alpha_2^5\Big) + \\
&\quad 2 (u_2-u_3) \alpha_1 \Big(5 (u_2-u_3) \alpha_1^2 \Big(8 u_3^2 + 48 (u_2-u_3) u_3 (-1+\alpha_0) + 21 (u_2-u_3)^2 \Big(8 (-1+\alpha_0)^2 + \alpha_1^2\Big)\Big) + \\
&\qquad 24 \Big(4 u_3^3 + 20 (u_2-u_3) u_3^2 (-1+\alpha_0) + 15 (u_2-u_3)^2 u_3 \Big(4 (-1+\alpha_0)^2 + \alpha_1^2\Big) + \\
&\qquad\quad 35 (u_2-u_3)^3 (-1+\alpha_0) \Big(4 (-1+\alpha_0)^2 + 3 \alpha_1^2\Big)\Big) \alpha_2 + \\
&\qquad 30 (u_2-u_3) \Big(4 u_3^2 + 24 (u_2-u_3) u_3 (-1+\alpha_0) + 7 (u_2-u_3)^2 \Big(12 (-1+\alpha_0)^2 + 5 \alpha_1^2\Big)\Big) \alpha_2^2 + \\
&\qquad 360 (u_2-u_3)^2 (u_3 + 7 (u_2-u_3) (-1+\alpha_0)) \alpha_2^3 + 525 (u_2-u_3)^3 \alpha_2^4\Big) \alpha_3 + \\
&\quad 6 \Big(8 u_3^4 + 32 (u_2-u_3) u_3^3 (-1+\alpha_0) + 40 (u_2-u_3)^2 u_3^2 \Big(2 + 2 (-2+\alpha_0) \alpha_0 + \alpha_1^2 + \alpha_2^2\Big) + \\
&\qquad 40 (u_2-u_3)^3 u_3 \Big(4 (-1+\alpha_0)^3 + 6 (-1+\alpha_0) \alpha_1^2 + 3 \alpha_1^2 \alpha_2 + 6 (-1+\alpha_0) \alpha_2^2 + \alpha_2^3\Big) + \\
&\qquad 35 (u_2-u_3)^4 \Big(8 - 32 \alpha_0^3 + 8 \alpha_0^4 + 3 \alpha_1^4 + 24 \alpha_0^2 \Big(2 + \alpha_1^2 + \alpha_2^2\Big) + 8 \alpha_0 \Big(-4 + 3 \alpha_1^2 (-2+\alpha_2) + (-6+\alpha_2) \alpha_2^2\Big) + \\
&\qquad\quad \alpha_2^2 (24 + \alpha_2 (-8 + 3 \alpha_2)) + 6 \alpha_1^2 (4 + \alpha_2 (-4 + 3 \alpha_2))\Big)\Big) \alpha_3^2 + \\
&\quad 80 (u_2-u_3)^3 \alpha_1 \Big(7 (u_2-u_3) \alpha_1^2 + 3 \alpha_2 (32 u_3 + 7 u_2 (-4 + 4 \alpha_0 + \alpha_2) - 7 u_3 (4 \alpha_0 + \alpha_2))\Big) \alpha_3^3 + \\
&\quad 40 (u_2-u_3)^2 \Big(2 u_3^2 + 12 (u_2-u_3) u_3 (-1+\alpha_0) + 21 (u_2-u_3)^2 \Big(2 + 2 (-2+\alpha_0) \alpha_0 + \alpha_1^2 + \alpha_2^2\Big)\Big) \alpha_3^4 + \\
&\quad 105 (u_2-u_3)^4 \alpha_3^6\Big)
\end{aligned}
$$

$\mathbf{AllCf}[\{\alpha_0, \alpha_1, \alpha_2, \alpha_3, \alpha_4\}, \mathbf{u_2}, \mathbf{u_3}][[\mathbf{7}]]$

$$
\begin{aligned}
&\frac{1}{16\, u_3^8} (u_2-u_3)^3 \Big(21 (u_2-u_3)^3 \alpha_2^5 (5 \alpha_1 + \alpha_3) + 30 (u_2-u_3)^2 (u_3 + 7 (u_2-u_3) (-1+\alpha_0)) \alpha_2^4 (\alpha_1 + 4 \alpha_3) + \\
&\quad 12 \alpha_2^2 \Big(5 (u_2-u_3)^2 (u_3 + 7 (u_2-u_3) (-1+\alpha_0)) \alpha_1^3 + 2 \Big(2 u_3^3 + 10 (u_2-u_3) u_3^2 (-1+\alpha_0) + \\
&\qquad\quad 15 (u_2-u_3)^2 u_3 \Big(2 (-1+\alpha_0)^2 + \alpha_1^2\Big) + 35 (u_2-u_3)^3 (-1+\alpha_0) \Big(2 (-1+\alpha_0)^2 + 3 \alpha_1^2\Big)\Big) \alpha_3 + \\
&\qquad 30 (u_2-u_3)^2 (u_3 + 7 (u_2-u_3) (-1+\alpha_0)) \alpha_1 \alpha_3^2 + 15 (u_2-u_3)^2 (u_3 + 7 (u_2-u_3) (-1+\alpha_0)) \alpha_3^3\Big) + \\
&\quad 6 \alpha_1 \alpha_3 \Big(5 (u_2-u_3)^2 (u_3 + 7 (u_2-u_3) (-1+\alpha_0)) \alpha_1^3 + 2 \Big(4 u_3^3 + 20 (u_2-u_3) u_3^2 (-1+\alpha_0) + \\
&\qquad\quad 15 (u_2-u_3)^2 u_3 \Big(4 (-1+\alpha_0)^2 + \alpha_1^2\Big) + 35 (u_2-u_3)^3 (-1+\alpha_0) \Big(4 (-1+\alpha_0)^2 + 3 \alpha_1^2\Big)\Big) \alpha_3 + \\
&\qquad 10 (u_2-u_3)^2 (u_3 + 7 (u_2-u_3) (-1+\alpha_0)) \alpha_1 \alpha_3^2 + 20 (u_2-u_3)^2 (u_3 + 7 (u_2-u_3) (-1+\alpha_0)) \alpha_3^3\Big) + \\
&\quad 10 (u_2-u_3) \alpha_2^3 \Big(21 (u_2-u_3)^2 \alpha_1^3 + 84 (u_2-u_3)^2 \alpha_1^2 \alpha_3 + 21 (u_2-u_3)^2 \alpha_3^3 + \\
&\qquad \alpha_1 \Big(4 u_3^2 + 24 (u_2-u_3) u_3 (-1+\alpha_0) + 21 (u_2-u_3)^2 \Big(4 (-1+\alpha_0)^2 + 5 \alpha_3^2\Big)\Big)\Big) + \\
&\quad (u_2-u_3) \alpha_2 \Big(21 (u_2-u_3)^2 \alpha_1^5 + 420 (u_2-u_3)^2 \alpha_1^4 \alpha_3 + 840 (u_2-u_3)^2 \alpha_1^3 \alpha_3^2 + \\
&\qquad 60 \alpha_1 \alpha_3^2 \Big(2 u_3^2 + 12 (u_2-u_3) u_3 (-1+\alpha_0) + 7 (u_2-u_3)^2 \Big(6 (-1+\alpha_0)^2 + \alpha_3^2\Big)\Big) + \\
&\qquad 5 \alpha_3^3 \Big(8 u_3^2 + 48 (u_2-u_3) u_3 (-1+\alpha_0) + 21 (u_2-u_3)^2 \Big(8 (-1+\alpha_0)^2 + \alpha_3^2\Big)\Big) + \\
&\qquad 30 \alpha_1^2 \alpha_3 \Big(4 u_3^2 + 24 (u_2-u_3) u_3 (-1+\alpha_0) + 7 (u_2-u_3)^2 \Big(12 (-1+\alpha_0)^2 + 5 \alpha_3^2\Big)\Big)\Big)\Big)
\end{aligned}
$$

AllCf[{α_0, α_1, α_2, α_3, α_4}, u_2, u_3][[8]]

$$\begin{aligned}
&\frac{1}{32\,u_3^8}(u_2-u_3)^3\Big(42(u_2-u_3)^3\alpha_2^6+120(u_2-u_3)^2(u_3+7(u_2-u_3)(-1+\alpha_0))\alpha_2^3(\alpha_1^2+2\alpha_1\alpha_3+3\alpha_3^2)+48\alpha_2\alpha_3\\
&\quad\Big(5(u_2-u_3)^2(u_3+7(u_2-u_3)(-1+\alpha_0))\alpha_1^3+\Big(2u_3^3+10(u_2-u_3)u_3^2(-1+\alpha_0)+15(u_2-u_3)^2u_3\\
&\quad\quad\Big(2(-1+\alpha_0)^2+\alpha_1^2\Big)+35(u_2-u_3)^3(-1+\alpha_0)\Big(2(-1+\alpha_0)^2+3\alpha_1^2\Big)\Big)\alpha_3+\\
&\quad 5(u_2-u_3)^2(u_3+7(u_2-u_3)(-1+\alpha_0))\alpha_1\alpha_3^2+5(u_2-u_3)^2(u_3+7(u_2-u_3)(-1+\alpha_0))\alpha_3^3\Big)+\\
&10(u_2-u_3)\alpha_2^4\Big(2u_3^2+12(u_2-u_3)u_3(-1+\alpha_0)+21(u_2-u_3)^2\Big(2+2(-2+\alpha_0)\alpha_0+\alpha_1^2+4\alpha_1\alpha_3+\alpha_3^2\Big)\Big)+\\
&2(u_2-u_3)\alpha_1\alpha_3\Big(21(u_2-u_3)^2\alpha_1^4+210(u_2-u_3)^2\alpha_1^3\alpha_3+210(u_2-u_3)^2\alpha_1^2\alpha_3^2+\\
&\quad 30\alpha_1\alpha_3\Big(2u_3^2+12(u_2-u_3)u_3(-1+\alpha_0)+7(u_2-u_3)^2\Big(6(-1+\alpha_0)^2+\alpha_3^2\Big)\Big)+\\
&\quad 5\alpha_3^2\Big(8u_3^2+48(u_2-u_3)u_3(-1+\alpha_0)+21(u_2-u_3)^2\Big(8(-1+\alpha_0)^2+\alpha_3^2\Big)\Big)\Big)+\\
&15(u_2-u_3)\alpha_2^2\Big(7(u_2-u_3)^2\alpha_1^4+84(u_2-u_3)^2\alpha_1^3\alpha_3+126(u_2-u_3)^2\alpha_1^2\alpha_3^2+7(u_2-u_3)^2\alpha_3^4+\\
&\quad 4\alpha_1\alpha_3\Big(4u_3^2+24(u_2-u_3)u_3(-1+\alpha_0)+7(u_2-u_3)^2\Big(12(-1+\alpha_0)^2+5\alpha_3^2\Big)\Big)\Big)\Big)
\end{aligned}$$

AllCf[{α_0, α_1, α_2, α_3, α_4}, u_2, u_3][[9]]

$$\begin{aligned}
&\frac{1}{16\,u_3^8}(u_2-u_3)^3\Big((u_2-u_3)^2\alpha_1\alpha_2^3\Big(70(u_2-u_3)\alpha_1^2+21u_2\alpha_2(-10+10\alpha_0+\alpha_2)-3u_3\alpha_2(-80+70\alpha_0+7\alpha_2)\Big)+\\
&5(u_2-u_3)\alpha_2\Big(21(u_2-u_3)^2\alpha_1^4+36(u_2-u_3)(u_3+7(u_2-u_3)(-1+\alpha_0))\alpha_1^2\alpha_2+\\
&\quad 4\Big(2u_3^2+12(u_2-u_3)u_3(-1+\alpha_0)+21(u_2-u_3)^2\Big(2(-1+\alpha_0)^2+\alpha_1^2\Big)\Big)\alpha_2^2+21(u_2-u_3)^2\alpha_2^4\Big)\alpha_3+\\
&30(u_2-u_3)\alpha_1\Big(2(u_2-u_3)(u_3+7(u_2-u_3)(-1+\alpha_0))\alpha_1^2+\\
&\quad\Big(4u_3^2+24(u_2-u_3)u_3(-1+\alpha_0)+21(u_2-u_3)^2\Big(4(-1+\alpha_0)^2+\alpha_1^2\Big)\Big)\alpha_2+\\
&\quad 6(u_2-u_3)(u_3+7(u_2-u_3)(-1+\alpha_0))\alpha_2^2+21(u_2-u_3)^2\alpha_2^3\Big)\alpha_3^2+\\
&2\Big(8u_3^3+40(u_2-u_3)u_3^2(-1+\alpha_0)+60(u_2-u_3)^2u_3\Big(2+2(-2+\alpha_0)\alpha_0+\alpha_1^2+\alpha_2^2\Big)+\\
&\quad 35(u_2-u_3)^3\Big(8(-1+\alpha_0)^3+12(-1+\alpha_0)\alpha_1^2+6\alpha_1^2\alpha_2+12(-1+\alpha_0)\alpha_2^2+3\alpha_2^3\Big)\Big)\alpha_3^3+\\
&525(u_2-u_3)^3\alpha_1\alpha_2\alpha_3^4+30(u_2-u_3)^2(u_3+7(u_2-u_3)(-1+\alpha_0))\alpha_3^5\Big)
\end{aligned}$$

AllCf[{α_0, α_1, α_2, α_3, α_4}, u_2, u_3][[10]]

$$\begin{aligned}
&\frac{1}{32\,u_3^8}(u_2-u_3)^4\Big(12(u_2-u_3)(u_3+7(u_2-u_3)(-1+\alpha_0))\alpha_2^5+240(u_2-u_3)(u_3+7(u_2-u_3)(-1+\alpha_0))\alpha_1\alpha_2^3\alpha_3+\\
&60(u_2-u_3)(u_3+7(u_2-u_3)(-1+\alpha_0))\alpha_2\alpha_3^2\Big(6\alpha_1^2+4\alpha_1\alpha_3+\alpha_3^2\Big)+\\
&105(u_2-u_3)^2\alpha_2^4\Big(\alpha_1^2+2\alpha_1\alpha_3+4\alpha_3^2\Big)+\\
&60\alpha_2^2\alpha_3\Big(7(u_2-u_3)^2\alpha_1^3+\Big(2u_3^2+12(u_2-u_3)u_3(-1+\alpha_0)+21(u_2-u_3)^2\Big(2(-1+\alpha_0)^2+\alpha_1^2\Big)\Big)\alpha_3+\\
&\quad 14(u_2-u_3)^2\alpha_1\alpha_3^2+7(u_2-u_3)^2\alpha_3^3\Big)+\\
&5\alpha_1\alpha_3^2\Big(21(u_2-u_3)^2\alpha_1^3+4\Big(4u_3^2+24(u_2-u_3)u_3(-1+\alpha_0)+21(u_2-u_3)^2\Big(4(-1+\alpha_0)^2+\alpha_1^2\Big)\Big)\alpha_3+\\
&\quad 21(u_2-u_3)^2\alpha_1\alpha_3^2+42(u_2-u_3)^2\alpha_3^3\Big)\Big)
\end{aligned}$$

AllCf[{α0, α1, α2, α3, α4}, u2, u3][[11]]

$$\frac{1}{16\,u_3^8}\,(u_2-u_3)^4\,\Big(21\,(u_2-u_3)^2\,\alpha_1\,\alpha_2^5+30\,(u_2-u_3)\,(u_3+7\,(u_2-u_3)\,(-1+\alpha_0))\,\alpha_2^4\,\alpha_3+180\,(u_2-u_3)\,(u_3+7\,(u_2-u_3)\,(-1+\alpha_0))\,\alpha_1\,\alpha_2^2\,\alpha_3^2+30\,(u_2-u_3)\,(u_3+7\,(u_2-u_3)\,(-1+\alpha_0))\,\alpha_1\,\alpha_3^3\,(2\,\alpha_1+\alpha_3)+210\,(u_2-u_3)^2\,\alpha_2^3\,\alpha_3\,\left(\alpha_1^2+\alpha_1\,\alpha_3+\alpha_3^2\right)+5\,\alpha_2\,\alpha_3^2\,\Big(42\,(u_2-u_3)^2\,\alpha_1^3+4\,\Big(2\,u_3^2+12\,(u_2-u_3)\,u_3\,(-1+\alpha_0)+21\,(u_2-u_3)^2\,\left(2\,(-1+\alpha_0)^2+\alpha_1^2\right)\Big)\,\alpha_3+21\,(u_2-u_3)^2\,\alpha_1\,\alpha_3^2+21\,(u_2-u_3)^2\,\alpha_3^3\Big)\Big)$$

AllCf[{α0, α1, α2, α3, α4}, u2, u3][[12]]

$$\frac{1}{32\,u_3^8}\,(u_2-u_3)^4\,\Big(7\,(u_2-u_3)^2\,\alpha_2^6+210\,(u_2-u_3)^2\,\alpha_1\,\alpha_2^4\,\alpha_3+30\,(u_2-u_3)\,\alpha_2^2\,\left(21\,(u_2-u_3)\,\alpha_1^2+4\,(u_3+7\,(u_2-u_3)\,(-1+\alpha_0))\,\alpha_2\right)\,\alpha_3^2+20\,(u_2-u_3)\,\alpha_1\,\left(7\,(u_2-u_3)\,\alpha_1^2+3\,\alpha_2\,(32\,u_3+7\,u_2\,(-4+4\,\alpha_0+\alpha_2)-7\,u_3\,(4\,\alpha_0+\alpha_2))\right)\,\alpha_3^3+10\,\Big(2\,u_3^2+12\,(u_2-u_3)\,u_3\,(-1+\alpha_0)+21\,(u_2-u_3)^2\,\left(2+2\,(-2+\alpha_0)\,\alpha_0+\alpha_1^2+\alpha_2^2\right)\Big)\,\alpha_3^4+42\,(u_2-u_3)^2\,\alpha_3^6\Big)$$

AllCf[{α0, α1, α2, α3, α4}, u2, u3][[13]]

$$\frac{1}{16\,u_3^8}\,3\,(u_2-u_3)^5\,\alpha_3\,\Big(7\,(u_2-u_3)\,\alpha_2^5+70\,(u_2-u_3)\,\alpha_1\,\alpha_2^3\,\alpha_3+20\,(u_3+7\,(u_2-u_3)\,(-1+\alpha_0))\,\alpha_2^2\,\alpha_3^2+10\,(u_3+7\,(u_2-u_3)\,(-1+\alpha_0))\,\alpha_1\,\alpha_3^3+7\,(u_2-u_3)\,\alpha_2\,\alpha_3^2\,\left(10\,\alpha_1^2+5\,\alpha_1\,\alpha_3+\alpha_3^2\right)\Big)$$

AllCf[{α0, α1, α2, α3, α4}, u2, u3][[14]]

$$\frac{1}{32\,u_3^8}\,3\,(u_2-u_3)^5\,\alpha_3^2\,\Big(35\,(u_2-u_3)\,\alpha_2^4+140\,(u_2-u_3)\,\alpha_1\,\alpha_2^2\,\alpha_3+20\,(u_3+7\,(u_2-u_3)\,(-1+\alpha_0))\,\alpha_2\,\alpha_3^2+7\,(u_2-u_3)\,\alpha_1\,\alpha_3^2\,(5\,\alpha_1+2\,\alpha_3)\Big)$$

AllCf[{α0, α1, α2, α3, α4}, u2, u3][[15]]

$$\frac{1}{16\,u_3^8}\,(u_2-u_3)^5\,\alpha_3^3\,\left(70\,(u_2-u_3)\,\alpha_2^3+105\,(u_2-u_3)\,\alpha_1\,\alpha_2\,\alpha_3+6\,(u_3+7\,(u_2-u_3)\,(-1+\alpha_0))\,\alpha_3^2\right)$$

AllCf[{α0, α1, α2, α3, α4}, u2, u3][[16]]

$$\frac{21\,(u_2-u_3)^6\,\alpha_3^4\,\left(5\,\alpha_2^2+2\,\alpha_1\,\alpha_3\right)}{32\,u_3^8}$$

AllCf[{α0, α1, α2, α3, α4}, u2, u3][[17]]

$$\frac{21\,(u_2-u_3)^6\,\alpha_2\,\alpha_3^5}{16\,u_3^8}$$

AllCf[{α0, α1, α2, α3, α4}, u2, u3][[18]]

$$\frac{7\,(u_2-u_3)^6\,\alpha_3^6}{32\,u_3^8}$$

C0f[{α0, α1, α2, α3, α4}, u2, u3]

$$
\begin{aligned}
&\frac{1}{32\,u_3^8}\Big(224\,(u_2-u_3)^6-192\,(u_2-u_3)^5\,u_3+160\,(u_2-u_3)^4\,u_3^2-128\,(u_2-u_3)^3\,u_3^3+96\,(u_2-u_3)^2\,u_3^4+\\
&32\,u_3^6+64\,u_3^5\,(-u_2+u_3)-1344\,(u_2-u_3)^6\,\alpha_0+960\,(u_2-u_3)^5\,u_3\,\alpha_0-640\,(u_2-u_3)^4\,u_3^2\,\alpha_0+\\
&384\,(u_2-u_3)^3\,u_3^3\,\alpha_0-192\,(u_2-u_3)^2\,u_3^4\,\alpha_0+64\,(u_2-u_3)\,u_3^5\,\alpha_0+3360\,(u_2-u_3)^6\,\alpha_0^2-\\
&1920\,(u_2-u_3)^5\,u_3\,\alpha_0^2+960\,(u_2-u_3)^4\,u_3^2\,\alpha_0^2-384\,(u_2-u_3)^3\,u_3^3\,\alpha_0^2+96\,(u_2-u_3)^2\,u_3^4\,\alpha_0^2-\\
&4480\,(u_2-u_3)^6\,\alpha_0^3+1920\,(u_2-u_3)^5\,u_3\,\alpha_0^3-640\,(u_2-u_3)^4\,u_3^2\,\alpha_0^3+128\,(u_2-u_3)^3\,u_3^3\,\alpha_0^3+\\
&3360\,(u_2-u_3)^6\,\alpha_0^4-960\,(u_2-u_3)^5\,u_3\,\alpha_0^4+160\,(u_2-u_3)^4\,u_3^2\,\alpha_0^4-1344\,(u_2-u_3)^6\,\alpha_0^5+\\
&192\,(u_2-u_3)^5\,u_3\,\alpha_0^5+224\,(u_2-u_3)^6\,\alpha_0^6+1680\,(u_2-u_3)^6\,\alpha_1^2-960\,(u_2-u_3)^5\,u_3\,\alpha_1^2+\\
&480\,(u_2-u_3)^4\,u_3^2\,\alpha_1^2-192\,(u_2-u_3)^3\,u_3^3\,\alpha_1^2+48\,(u_2-u_3)^2\,u_3^4\,\alpha_1^2-6720\,(u_2-u_3)^6\,\alpha_0\,\alpha_1^2+\\
&2880\,(u_2-u_3)^5\,u_3\,\alpha_0\,\alpha_1^2-960\,(u_2-u_3)^4\,u_3^2\,\alpha_0\,\alpha_1^2+192\,(u_2-u_3)^3\,u_3^3\,\alpha_0\,\alpha_1^2+10\,080\,(u_2-u_3)^6\,\alpha_0^2\,\alpha_1^2-\\
&2880\,(u_2-u_3)^5\,u_3\,\alpha_0^2\,\alpha_1^2+480\,(u_2-u_3)^4\,u_3^2\,\alpha_0^2\,\alpha_1^2-6720\,(u_2-u_3)^6\,\alpha_0^3\,\alpha_1^2+960\,(u_2-u_3)^5\,u_3\,\alpha_0^3\,\alpha_1^2+\\
&1680\,(u_2-u_3)^6\,\alpha_0^4\,\alpha_1^2+1260\,(u_2-u_3)^6\,\alpha_1^4-360\,(u_2-u_3)^5\,u_3\,\alpha_1^4+60\,(u_2-u_3)^4\,u_3^2\,\alpha_1^4-\\
&2520\,(u_2-u_3)^6\,\alpha_0\,\alpha_1^4+360\,(u_2-u_3)^5\,u_3\,\alpha_0\,\alpha_1^4+1260\,(u_2-u_3)^6\,\alpha_0^2\,\alpha_1^4+70\,(u_2-u_3)^6\,\alpha_1^6-\\
&3360\,(u_2-u_3)^6\,\alpha_1^2\,\alpha_2+1440\,(u_2-u_3)^5\,u_3\,\alpha_1^2\,\alpha_2-480\,(u_2-u_3)^4\,u_3^2\,\alpha_1^2\,\alpha_2+96\,(u_2-u_3)^3\,u_3^3\,\alpha_1^2\,\alpha_2+\\
&10\,080\,(u_2-u_3)^6\,\alpha_0\,\alpha_1^2\,\alpha_2-2880\,(u_2-u_3)^5\,u_3\,\alpha_0\,\alpha_1^2\,\alpha_2+480\,(u_2-u_3)^4\,u_3^2\,\alpha_0\,\alpha_1^2\,\alpha_2-\\
&10\,080\,(u_2-u_3)^6\,\alpha_0^2\,\alpha_1^2\,\alpha_2+1440\,(u_2-u_3)^5\,u_3\,\alpha_0^2\,\alpha_1^2\,\alpha_2+3360\,(u_2-u_3)^6\,\alpha_0^3\,\alpha_1^2\,\alpha_2-1680\,(u_2-u_3)^6\,\alpha_1^4\,\alpha_2+\\
&240\,(u_2-u_3)^5\,u_3\,\alpha_1^4\,\alpha_2+1680\,(u_2-u_3)^6\,\alpha_0\,\alpha_1^4\,\alpha_2+1680\,(u_2-u_3)^6\,\alpha_2^2-960\,(u_2-u_3)^5\,u_3\,\alpha_2^2+\\
&480\,(u_2-u_3)^4\,u_3^2\,\alpha_2^2-192\,(u_2-u_3)^3\,u_3^3\,\alpha_2^2+48\,(u_2-u_3)^2\,u_3^4\,\alpha_2^2-6720\,(u_2-u_3)^6\,\alpha_0\,\alpha_2^2+\\
&2880\,(u_2-u_3)^5\,u_3\,\alpha_0\,\alpha_2^2-960\,(u_2-u_3)^4\,u_3^2\,\alpha_0\,\alpha_2^2+192\,(u_2-u_3)^3\,u_3^3\,\alpha_0\,\alpha_2^2+10\,080\,(u_2-u_3)^6\,\alpha_0^2\,\alpha_2^2-\\
&2880\,(u_2-u_3)^5\,u_3\,\alpha_0^2\,\alpha_2^2+480\,(u_2-u_3)^4\,u_3^2\,\alpha_0^2\,\alpha_2^2-6720\,(u_2-u_3)^6\,\alpha_0^3\,\alpha_2^2+960\,(u_2-u_3)^5\,u_3\,\alpha_0^3\,\alpha_2^2+\\
&1680\,(u_2-u_3)^6\,\alpha_0^4\,\alpha_2^2+5040\,(u_2-u_3)^6\,\alpha_1^2\,\alpha_2^2-1440\,(u_2-u_3)^5\,u_3\,\alpha_1^2\,\alpha_2^2+240\,(u_2-u_3)^4\,u_3^2\,\alpha_1^2\,\alpha_2^2-\\
&10\,080\,(u_2-u_3)^6\,\alpha_0\,\alpha_1^2\,\alpha_2^2+1440\,(u_2-u_3)^5\,u_3\,\alpha_0\,\alpha_1^2\,\alpha_2^2+5040\,(u_2-u_3)^6\,\alpha_0^2\,\alpha_1^2\,\alpha_2^2+735\,(u_2-u_3)^6\,\alpha_1^4\,\alpha_2^2-\\
&2520\,(u_2-u_3)^6\,\alpha_1^2\,\alpha_2^3+360\,(u_2-u_3)^5\,u_3\,\alpha_1^2\,\alpha_2^3+2520\,(u_2-u_3)^6\,\alpha_0\,\alpha_1^2\,\alpha_2^3+1260\,(u_2-u_3)^6\,\alpha_2^4-\\
&360\,(u_2-u_3)^5\,u_3\,\alpha_2^4+60\,(u_2-u_3)^4\,u_3^2\,\alpha_2^4-2520\,(u_2-u_3)^6\,\alpha_0\,\alpha_2^4+360\,(u_2-u_3)^5\,u_3\,\alpha_0\,\alpha_2^4+\\
&1260\,(u_2-u_3)^6\,\alpha_0^2\,\alpha_2^4+630\,(u_2-u_3)^6\,\alpha_1^2\,\alpha_2^4+70\,(u_2-u_3)^6\,\alpha_2^6+1680\,(u_2-u_3)^6\,\alpha_1^3\,\alpha_3-\\
&480\,(u_2-u_3)^5\,u_3\,\alpha_1^3\,\alpha_3+80\,(u_2-u_3)^4\,u_3^2\,\alpha_1^3\,\alpha_3-3360\,(u_2-u_3)^6\,\alpha_0\,\alpha_1^3\,\alpha_3+480\,(u_2-u_3)^5\,u_3\,\alpha_0\,\alpha_1^3\,\alpha_3+\\
&1680\,(u_2-u_3)^6\,\alpha_0^2\,\alpha_1^3\,\alpha_3+210\,(u_2-u_3)^6\,\alpha_1^5\,\alpha_3-6720\,(u_2-u_3)^6\,\alpha_1\,\alpha_2\,\alpha_3+2880\,(u_2-u_3)^5\,u_3\,\alpha_1\,\alpha_2\,\alpha_3-\\
&960\,(u_2-u_3)^4\,u_3^2\,\alpha_1\,\alpha_2\,\alpha_3+192\,(u_2-u_3)^3\,u_3^3\,\alpha_1\,\alpha_2\,\alpha_3+20\,160\,(u_2-u_3)^6\,\alpha_0\,\alpha_1\,\alpha_2\,\alpha_3-\\
&5760\,(u_2-u_3)^5\,u_3\,\alpha_0\,\alpha_1\,\alpha_2\,\alpha_3+960\,(u_2-u_3)^4\,u_3^2\,\alpha_0\,\alpha_1\,\alpha_2\,\alpha_3-20\,160\,(u_2-u_3)^6\,\alpha_0^2\,\alpha_1\,\alpha_2\,\alpha_3+\\
&2880\,(u_2-u_3)^5\,u_3\,\alpha_0^2\,\alpha_1\,\alpha_2\,\alpha_3+6720\,(u_2-u_3)^6\,\alpha_0^3\,\alpha_1\,\alpha_2\,\alpha_3-5040\,(u_2-u_3)^6\,\alpha_1^3\,\alpha_2\,\alpha_3+\\
&720\,(u_2-u_3)^5\,u_3\,\alpha_1^3\,\alpha_2\,\alpha_3+5040\,(u_2-u_3)^6\,\alpha_0\,\alpha_1^3\,\alpha_2\,\alpha_3+5040\,(u_2-u_3)^6\,\alpha_1\,\alpha_2^2\,\alpha_3-\\
&1440\,(u_2-u_3)^5\,u_3\,\alpha_1\,\alpha_2^2\,\alpha_3+240\,(u_2-u_3)^4\,u_3^2\,\alpha_1\,\alpha_2^2\,\alpha_3-10\,080\,(u_2-u_3)^6\,\alpha_0\,\alpha_1\,\alpha_2^2\,\alpha_3+\\
&1440\,(u_2-u_3)^5\,u_3\,\alpha_0\,\alpha_1\,\alpha_2^2\,\alpha_3+5040\,(u_2-u_3)^6\,\alpha_0^2\,\alpha_1\,\alpha_2^2\,\alpha_3+2100\,(u_2-u_3)^6\,\alpha_1^3\,\alpha_2^2\,\alpha_3-\\
&5040\,(u_2-u_3)^6\,\alpha_1\,\alpha_2^3\,\alpha_3+720\,(u_2-u_3)^5\,u_3\,\alpha_1\,\alpha_2^3\,\alpha_3+5040\,(u_2-u_3)^6\,\alpha_0\,\alpha_1\,\alpha_2^3\,\alpha_3+\\
&840\,(u_2-u_3)^6\,\alpha_1\,\alpha_2^4\,\alpha_3+1680\,(u_2-u_3)^6\,\alpha_3^2-960\,(u_2-u_3)^5\,u_3\,\alpha_3^2+480\,(u_2-u_3)^4\,u_3^2\,\alpha_3^2-\\
&192\,(u_2-u_3)^3\,u_3^3\,\alpha_3^2+48\,(u_2-u_3)^2\,u_3^4\,\alpha_3^2-6720\,(u_2-u_3)^6\,\alpha_0\,\alpha_3^2+2880\,(u_2-u_3)^5\,u_3\,\alpha_0\,\alpha_3^2-\\
&960\,(u_2-u_3)^4\,u_3^2\,\alpha_0\,\alpha_3^2+192\,(u_2-u_3)^3\,u_3^3\,\alpha_0\,\alpha_3^2+10\,080\,(u_2-u_3)^6\,\alpha_0^2\,\alpha_3^2-2880\,(u_2-u_3)^5\,u_3\,\alpha_0^2\,\alpha_3^2+\\
&480\,(u_2-u_3)^4\,u_3^2\,\alpha_0^2\,\alpha_3^2-6720\,(u_2-u_3)^6\,\alpha_0^3\,\alpha_3^2+960\,(u_2-u_3)^5\,u_3\,\alpha_0^3\,\alpha_3^2+1680\,(u_2-u_3)^6\,\alpha_0^4\,\alpha_3^2+\\
&5040\,(u_2-u_3)^6\,\alpha_1^2\,\alpha_3^2-1440\,(u_2-u_3)^5\,u_3\,\alpha_1^2\,\alpha_3^2+240\,(u_2-u_3)^4\,u_3^2\,\alpha_1^2\,\alpha_3^2-10\,080\,(u_2-u_3)^6\,\alpha_0\,\alpha_1^2\,\alpha_3^2+\\
&1440\,(u_2-u_3)^5\,u_3\,\alpha_0\,\alpha_1^2\,\alpha_3^2+5040\,(u_2-u_3)^6\,\alpha_0^2\,\alpha_1^2\,\alpha_3^2+630\,(u_2-u_3)^6\,\alpha_1^4\,\alpha_3^2-5040\,(u_2-u_3)^6\,\alpha_1^2\,\alpha_2\,\alpha_3^2+\\
&720\,(u_2-u_3)^5\,u_3\,\alpha_1^2\,\alpha_2\,\alpha_3^2+5040\,(u_2-u_3)^6\,\alpha_0\,\alpha_1^2\,\alpha_2\,\alpha_3^2+5040\,(u_2-u_3)^6\,\alpha_2^2\,\alpha_3^2-1440\,(u_2-u_3)^5\,u_3\,\alpha_2^2\,\alpha_3^2+\\
&240\,(u_2-u_3)^4\,u_3^2\,\alpha_2^2\,\alpha_3^2-10\,080\,(u_2-u_3)^6\,\alpha_0\,\alpha_2^2\,\alpha_3^2+1440\,(u_2-u_3)^5\,u_3\,\alpha_0\,\alpha_2^2\,\alpha_3^2+\\
&5040\,(u_2-u_3)^6\,\alpha_0^2\,\alpha_2^2\,\alpha_3^2+3150\,(u_2-u_3)^6\,\alpha_1^2\,\alpha_2^2\,\alpha_3^2-840\,(u_2-u_3)^6\,\alpha_2^3\,\alpha_3^2+120\,(u_2-u_3)^5\,u_3\,\alpha_2^3\,\alpha_3^2+\\
&840\,(u_2-u_3)^6\,\alpha_0\,\alpha_2^3\,\alpha_3^2+630\,(u_2-u_3)^6\,\alpha_2^4\,\alpha_3^2+420\,(u_2-u_3)^6\,\alpha_1^3\,\alpha_3^3-5040\,(u_2-u_3)^6\,\alpha_1\,\alpha_2\,\alpha_3^3+\\
&720\,(u_2-u_3)^5\,u_3\,\alpha_1\,\alpha_2\,\alpha_3^3+5040\,(u_2-u_3)^6\,\alpha_0\,\alpha_1\,\alpha_2\,\alpha_3^3+1260\,(u_2-u_3)^6\,\alpha_1\,\alpha_2^2\,\alpha_3^3+1260\,(u_2-u_3)^6\,\alpha_3^4-\\
&360\,(u_2-u_3)^5\,u_3\,\alpha_3^4+60\,(u_2-u_3)^4\,u_3^2\,\alpha_3^4-2520\,(u_2-u_3)^6\,\alpha_0\,\alpha_3^4+360\,(u_2-u_3)^5\,u_3\,\alpha_0\,\alpha_3^4+\\
&1260\,(u_2-u_3)^6\,\alpha_0^2\,\alpha_3^4+630\,(u_2-u_3)^6\,\alpha_1^2\,\alpha_3^4+630\,(u_2-u_3)^6\,\alpha_2^2\,\alpha_3^4+70\,(u_2-u_3)^6\,\alpha_3^6\Big)
\end{aligned}
$$

(* $r^2[\phi]$ *)

$$\text{RKvadrat}[\phi\_] := \text{Function}\Big[\{a, \epsilon\},\ \lambda = \frac{1}{2}\sqrt{a\left(1-\epsilon^2\right)};\ \eta = -\frac{1}{2\,a};\ \lambda i = \frac{1}{\lambda};$$

$$qq = \frac{3}{2}\,\frac{1}{\left(-3\,\lambda i^2+1\right)^{3/2}}\left(\sqrt{\left(\left(24\,\eta+12\,\eta^2\right)+\left(3-108\,\eta-378\,\eta^2-324\,\eta^3-81\,\eta^4\right)\lambda i^2-12\,\lambda i^4\right)}\right)\lambda i;$$

$$\Psi = -\text{ArcSin}[qq];$$

$$U1 = \sqrt{1-3/\lambda^2} + \frac{1/\lambda^2}{1+\sqrt{1-3/\lambda^2}} - \frac{4}{3}\sqrt{1-3/\lambda^2}\ \text{Sin}\left[\frac{\Psi}{6}\right]^2;$$

$$U2 = \frac{1}{3}\left(\frac{3/\lambda^2}{1+\sqrt{1-3/\lambda^2}} - \sqrt{3}\,\sqrt{1-3/\lambda^2}\ \text{Sin}\left[\frac{\Psi}{3}\right] + 2\sqrt{1-3/\lambda^2}\ \text{Sin}\left[\frac{\Psi}{6}\right]^2\right);$$

$$U3 = \frac{1}{3}\left(\frac{3/\lambda^2}{1+\sqrt{1-3/\lambda^2}} + \sqrt{3}\,\sqrt{1-3/\lambda^2}\ \text{Sin}\left[\frac{\Psi}{3}\right] + 2\sqrt{1-3/\lambda^2}\ \text{Sin}\left[\frac{\Psi}{6}\right]^2\right);$$

$$na = \frac{1}{\sqrt{U1-U3}};\ ma = \frac{U2-U3}{U1-U3};$$

$$A0123 = \Big\{\frac{1}{2}\left(\frac{\pi}{2\,\text{EllipticK}[ma]}\right)^2\left(1+\frac{3\,ma}{8}-\frac{7\,ma^2}{64}\right),\ \frac{1}{2}\left(\frac{\pi}{2\,\text{EllipticK}[ma]}\right)^2\left(1+\frac{ma}{2}+\frac{ma^2}{256}\right),$$
$$\frac{1}{2}\left(\frac{\pi}{2\,\text{EllipticK}[ma]}\right)^2\left(\frac{ma}{8}+\frac{ma^2}{8}\right),\ \frac{1}{2}\left(\frac{\pi}{2\,\text{EllipticK}[ma]}\right)^2\frac{ma^2\,3}{256},\ 0\Big\};$$

$$KKK = \text{Prepend}[\text{AllCf}[A0123, U2, U3], \text{C0f}[A0123, U2, U3]];$$

$$\text{Do}\big[s = \text{If}\big[\text{Abs}[KKK[[i]]\,/\,KKK[[1]]] > 10^{-18}, i, s\big], \{i, 2, 18\}\big];$$

$$ven = KKK[[1]] + \text{Sum}\left[(-1)^i\, KKK[[i+1]]\ \text{Cos}\left[\left(\frac{\pi\,\phi}{2\,\text{EllipticK}[ma]\ na}\right) i\right], \{i, s\}\right]\Big];$$

(* End $r^2[\phi]$ *)

$$\mathbf{InvFun}[x\tau\_, \{a0\_, a1\_, a2\_, a3\_, a4\_, a5\_, a6\_, a7\_, a8\_, a9\_, a10\_\}] :=$$

$$\frac{x\tau}{a0} + \frac{1}{737\,280} \left(-a1^9 + 16\, a1^7\, (5 + a2) - 336\, a1^6\, a3 + 96\, a1^5 \left(-10\, a2 + 7\, a2^2 + 8\, (-5 + a4)\right) -\right.$$
$$3840\, a1^3 \left(-24 + 5\, a2^2 + a2^3 + 6\, a3^2 + 4\, a4 - 8\, a2\, (1 + a4)\right) -$$
$$960\, a1^4\, ((-10 + a2)\, a3 + 2\, a5) - 0\; 11\,520\, a1^2 \left(a3 \left(8 - 4\, a2 + a2^2 - 4\, a4\right) + 4\, a2\, a5\right) +$$
$$46\,080 \left(a2^3\, a3 + 4\, a2\, a3\, (-2 + a4) + 2\, a2^2\, (a3 - a5) - 8\, a4\, (a3 + a5)\right) -$$
$$\left.11\,520\, a1 \left(-16\, a2^2 - 4\, a2^3 + a2^4 - 8\, a2 \left(-4 + a3^2 - 2\, a4\right) - 16 \left(-4 + a3^2 + a4^2 - a3\, a5\right)\right)\right) \mathrm{Sin}\left[\frac{x\tau}{a0}\right] +$$

$$\frac{1}{17\,280} \left(8640\, a1^2 - 2880\, a1^4 + 360\, a1^6 - 24\, a1^8 + a1^{10} - 17\,280\, a2 + 17\,280\, a1^2\, a2 - 3600\, a1^4\, a2 +\right.$$
$$336\, a1^6\, a2 - 18\, a1^8\, a2 - 4320\, a1^2\, a2^2 + 1440\, a1^4\, a2^2 - 168\, a1^6\, a2^2 + 8640\, a2^3 - 8640\, a1^2\, a2^3 +$$
$$1680\, a1^4\, a2^3 + 720\, a1^2\, a2^4 - 1440\, a2^5 - 17\,280\, a1\, a3 + 8640\, a1^3\, a3 - 1584\, a1^5\, a3 + 144\, a1^7\, a3 +$$
$$17\,280\, a1\, a2\, a3 - 2880\, a1^3\, a2\, a3 + 8640\, a1\, a2^2\, a3 - 2880\, a1^3\, a2^2\, a3 - 11\,520\, a1\, a2^3\, a3 -$$
$$8640\, a1^2\, a3^2 + 3240\, a1^4\, a3^2 + 17\,280\, a2\, a3^2 - 12\,960\, a1^2\, a2\, a3^2 + 4320\, a2^2\, a3^2 +$$
$$8640\, a1\, a3^3 - 8640\, a1^2\, a4 + 2880\, a1^4\, a4 - 336\, a1^6\, a4 - 17\,280\, a2\, a4 + 17\,280\, a1^2\, a2\, a4 -$$
$$4320\, a1^4\, a2\, a4 + 8640\, a1^2\, a2^2\, a4 + 5760\, a2^3\, a4 + 17\,280\, a1\, a3\, a4 - 5760\, a1^3\, a3\, a4 +$$
$$8640\, a3^2\, a4 - 8640\, a1^2\, a4^2 + 17\,280\, a2\, a4^2 - 2880\, a1^3\, a5 + 720\, a1^5\, a5 - 17\,280\, a1\, a2\, a5 +$$
$$8640\, a1^3\, a2\, a5 + 8640\, a1\, a2^2\, a5 - 17\,280\, a3\, a5 + 17\,280\, a1^2\, a3\, a5 + 17\,280\, a1\, a4\, a5 -$$
$$\left.720\, a1^4\, a6 - 8640\, a1^2\, a2\, a6 - 8640\, a2^2\, a6 - 17\,280\, a1\, a3\, a6 - 17\,280\, a4\, a6\right) \mathrm{Sin}\left[\frac{2\, x\tau}{a0}\right] +$$

$$\frac{1}{40\,960} \left(243\, a1^9 - 1944\, a1^7\, (1 + 2\, a2) + 13\,608\, a1^6\, a3 + 864\, a1^5\, (10 + 27\, a2 - 30\, a4) -\right.$$
$$4320\, a1^4\, (3\, (4 + a2)\, a3 - 8\, a5) - 5760\, a1^2 \left(a3 \left(-16 + 27\, a2^2 + 12\, a4\right) + 8\, (1 - 3\, a2)\, a5\right) +$$
$$1920\, a1^3 \left(-8 - 9\, a2^2 + 36\, a2^3 + 27\, a3^2 + 36\, a4 - 36\, a2\, (1 + a4) - 12\, a6\right) -$$
$$3840\, a1 \left(18\, a2^3 + 9\, a2^4 - 12\, a2^2\, (1 + 3\, a4) + 8\, (2\, a4 - 3\, a3\, a5) + 2\, a2 \left(-8 + 9\, a3^2 - 12\, a4 + 12\, a6\right)\right) -$$
$$\left.2560 \left(-18\, a3^3 + 24\, a2\, a5 + a3 \left(16 - 36\, a2^2 + 9\, a2^3 - 36\, a2\, a4 + 24\, a6\right)\right)\right) \mathrm{Sin}\left[\frac{3\, x\tau}{a0}\right] +$$

$$\frac{1}{945} \left(315\, a1^4 - 252\, a1^6 + 84\, a1^8 - 16\, a1^{10} - 1890\, a1^2\, a2 + 2520\, a1^4\, a2 - 1176\, a1^6\, a2 +\right.$$
$$288\, a1^8\, a2 + 945\, a2^2 - 3780\, a1^2\, a2^2 + 2520\, a1^4\, a2^2 - 672\, a1^6\, a2^2 + 2520\, a1^2\, a2^3 - 3360\, a1^4\, a2^3 -$$
$$1260\, a2^4 + 5040\, a1^2\, a2^4 + 1890\, a1\, a3 - 3780\, a1^3\, a3 + 2520\, a1^5\, a3 - 864\, a1^7\, a3 + 3780\, a1\, a2\, a3 -$$
$$5040\, a1^3\, a2\, a3 + 3024\, a1^5\, a2\, a3 - 7560\, a1\, a2^2\, a3 + 10\,080\, a1^3\, a2^2\, a3 - 5040\, a1\, a2^3\, a3 +$$
$$1890\, a1^2\, a3^2 - 3780\, a1^4\, a3^2 + 1890\, a2\, a3^2 - 3780\, a2^2\, a3^2 - 3780\, a1\, a3^3 - 945\, a4 +$$
$$3780\, a1^2\, a4 - 3780\, a1^4\, a4 + 1680\, a1^6\, a4 + 3780\, a2^2\, a4 - 15\,120\, a1^2\, a2^2\, a4 + 5040\, a1^3\, a3\, a4 +$$
$$3780\, a3^2\, a4 - 1890\, a1\, a5 + 3780\, a1^3\, a5 - 2520\, a1^5\, a5 + 3780\, a1\, a2\, a5 - 5040\, a1^3\, a2\, a5 +$$
$$7560\, a1\, a2^2\, a5 - 3780\, a1^2\, a3\, a5 + 3780\, a2\, a3\, a5 - 1890\, a1^2\, a6 + 2520\, a1^4\, a6 - 1890\, a2\, a6 +$$
$$\left.7560\, a1^2\, a2\, a6 + 3780\, a1\, a3\, a6 - 1260\, a1^3\, a7 - 3780\, a1\, a2\, a7 - 1890\, a3\, a7\right) \mathrm{Sin}\left[\frac{4\, x\tau}{a0}\right] +$$

$$\frac{1}{516\,096} \left(-78\,125\, a1^9 + 25\,000\, a1^7\, (7 + 50\, a2) - 2\,625\,000\, a1^6\, a3 -\right.$$
$$84\,000\, a1^5 \left(2 + 25\, a2 + 50\, a2^2 - 50\, a4\right) + 420\,000\, a1^4\, ((8 + 25\, a2)\, a3 - 12\, a5) +$$

$$336000\, a1^{3} \left(15\, a2^{2} + a2\, (4 - 20\, a4) - 3 \left(5\, a3^{2} + 4\, a4 - 4\, a6\right)\right) + 26880\, a1$$
$$\left(-50\, a2^{3} + 125\, a2^{4} - 60\, a2^{2}\, (1 + 5\, a4) + 12 \left(5\, a3^{2} + 4\, a4 - 4\, a6\right) - 30\, a2 \left(5\, a3^{2} - 4\, (a4 + a6)\right)\right) +$$
$$32256 \left(-125\, a2^{3}\, a3 - 16\, a5 + 100\, a2^{2}\, a5 + 20\, a2\, (a3\, (2 + 5\, a4) - 2\, a7)\right) +$$
$$201600\, a1^{2} \left(a3 \left(-8 - 40\, a2 + 25\, a2^{2} + 20\, a4\right) + 16\, a5 - 8\, a7\right)\Big)\, \text{Sin}\left[\frac{5\, x\tau}{a0}\right] +$$

$$\frac{1}{8960} \Big(3024\, a1^{6} - 3888\, a1^{8} + 2187\, a1^{10} - 30240\, a1^{4}\, a2 + 54432\, a1^{6}\, a2 - 39366\, a1^{8}\, a2 +$$
$$60480\, a1^{2}\, a2^{2} - 181440\, a1^{4}\, a2^{2} + 176904\, a1^{6}\, a2^{2} - 13440\, a2^{3} + 120960\, a1^{2}\, a2^{3} - 136080\, a1^{4}\, a2^{3} -$$
$$136080\, a1^{2}\, a2^{4} + 30240\, a2^{5} + 40320\, a1^{3}\, a3 - 90720\, a1^{5}\, a3 + 81648\, a1^{7}\, a3 - 80640\, a1\, a2\, a3 +$$
$$362880\, a1^{3}\, a2\, a3 - 489888\, a1^{5}\, a2\, a3 - 120960\, a1\, a2^{2}\, a3 + 181440\, a1^{3}\, a2^{2}\, a3 + 362880\, a1\, a2^{3}\, a3 +$$
$$13440\, a3^{2} - 120960\, a1^{2}\, a3^{2} + 272160\, a1^{4}\, a3^{2} - 120960\, a2^{2}\, a3^{2} - 40320\, a1^{2}\, a4 + 120960\, a1^{4}\, a4 -$$
$$136080\, a1^{6}\, a4 + 26880\, a2\, a4 - 241920\, a1^{2}\, a2\, a4 + 453600\, a1^{4}\, a2\, a4 + 181440\, a1^{2}\, a2^{2}\, a4 -$$
$$120960\, a2^{3}\, a4 + 80640\, a1\, a3\, a4 - 362880\, a1^{3}\, a3\, a4 - 241920\, a1\, a2\, a3\, a4 + 60480\, a1^{2}\, a4^{2} +$$
$$40320\, a2\, a4^{2} + 26880\, a1\, a5 - 120960\, a1^{3}\, a5 + 181440\, a1^{5}\, a5 + 80640\, a1\, a2\, a5 - 241920\, a1^{3}\, a2\, a5 -$$
$$241920\, a1\, a2^{2}\, a5 + 120960\, a1^{2}\, a3\, a5 + 80640\, a2\, a3\, a5 - 8960\, a6 + 80640\, a1^{2}\, a6 - 181440\, a1^{4}\, a6 +$$
$$80640\, a2^{2}\, a6 - 26880\, a1\, a7 + 120960\, a1^{3}\, a7 + 80640\, a1\, a2\, a7 - 40320\, a1^{2}\, a8 - 26880\, a2\, a8\Big)$$
$$\text{Sin}\left[\frac{6\, x\tau}{a0}\right] + \frac{1}{1474560} \Big(823543\, a1^{9} - 268912\, a1^{7}\, (2 + 49\, a2) + 22588608\, a1^{6}\, a3 +$$
$$1613472\, a1^{5} \left(4\, a2 + 35\, a2^{2} - 20\, a4\right) - 9219840\, a1^{4}\, (a3 + 14\, a2\, a3 - 4\, a5) -$$
$$1317120\, a1^{3} \left(14\, a2^{2} + 49\, a2^{3} - 42\, a3^{2} - 8\, a4 - 84\, a2\, a4 + 24\, a6\right) +$$
$$2257920\, a1^{2} \left(49\, a2^{2}\, a3 + 14\, a2\, (a3 - 2\, a5) - 4\, (7\, a3\, a4 + a5 - 2\, a7)\right) +$$
$$184320 \left(-49\, a2^{2}\, a3 + 28\, a3\, a4 + 28\, a2\, a5 - 8\, a7\right) + 26880\, a1 \Big(392\, a2^{3} + 343\, a2^{4} - 1176\, a2^{2}\, a4 -$$
$$168\, a2 \left(7\, a3^{2} + 4\, a4 - 4\, a6\right) - 48 \left(7\, a3^{2} - 7\, a4^{2} - 14\, a3\, a5 - 4\, a6 + 4\, a8\right)\Big)\Big)\, \text{Sin}\left[\frac{7\, x\tau}{a0}\right] +$$

$$\frac{1}{2835} \Big(1152\, a1^{8} - 2048\, a1^{10} - 16128\, a1^{6}\, a2 + 36864\, a1^{8}\, a2 + 60480\, a1^{4}\, a2^{2} - 193536\, a1^{6}\, a2^{2} -$$
$$60480\, a1^{2}\, a2^{3} + 322560\, a1^{4}\, a2^{3} + 7560\, a2^{4} - 120960\, a1^{2}\, a2^{4} + 24192\, a1^{5}\, a3 - 64512\, a1^{7}\, a3 -$$
$$120960\, a1^{3}\, a2\, a3 + 483840\, a1^{5}\, a2\, a3 + 90720\, a1\, a2^{2}\, a3 - 725760\, a1^{3}\, a2^{2}\, a3 + 120960\, a1\, a2^{3}\, a3 +$$
$$45360\, a1^{2}\, a3^{2} - 241920\, a1^{4}\, a3^{2} - 22680\, a2\, a3^{2} + 362880\, a1^{2}\, a2\, a3^{2} - 30240\, a1\, a3^{3} -$$
$$30240\, a1^{4}\, a4 + 96768\, a1^{6}\, a4 + 90720\, a1^{2}\, a2\, a4 - 483840\, a1^{4}\, a2\, a4 - 22680\, a2^{2}\, a4 +$$
$$362880\, a1^{2}\, a2^{2}\, a4 - 45360\, a1\, a3\, a4 + 362880\, a1^{3}\, a3\, a4 - 181440\, a1\, a2\, a3\, a4 + 5670\, a4^{2} -$$
$$90720\, a1^{2}\, a4^{2} + 30240\, a1^{3}\, a5 - 120960\, a1^{5}\, a5 - 45360\, a1\, a2\, a5 + 362880\, a1^{3}\, a2\, a5 -$$
$$90720\, a1\, a2^{2}\, a5 + 11340\, a3\, a5 - 181440\, a1^{2}\, a3\, a5 + 45360\, a1\, a4\, a5 - 22680\, a1^{2}\, a6 +$$
$$120960\, a1^{4}\, a6 + 11340\, a2\, a6 - 181440\, a1^{2}\, a2\, a6 + 45360\, a1\, a3\, a6 + 11340\, a1\, a7 -$$
$$90720\, a1^{3}\, a7 + 45360\, a1\, a2\, a7 - 2835\, a8 + 45360\, a1^{2}\, a8 - 11340\, a1\, a9\Big)\, \text{Sin}\left[\frac{8\, x\tau}{a0}\right] +$$

$$\frac{1}{1146880} \Big(-531441\, a1^{9} + 8503056\, a1^{7}\, a2 - 13226976\, a1^{6}\, a3 - 4408992\, a1^{5} \left(9\, a2^{2} - 4\, a4\right) +$$
$$9797760\, a1^{4}\, (9\, a2\, a3 - 2\, a5) + 2177280\, a1^{3} \left(27\, a2^{3} - 18\, a3^{2} - 36\, a2\, a4 + 8\, a6\right) -$$
$$1451520\, a1^{2} \left(81\, a2^{2}\, a3 - 36\, a3\, a4 - 36\, a2\, a5 + 8\, a7\right) -$$
$$80640\, a1 \left(243\, a2^{4} - 648\, a2^{2}\, a4 - 72\, a2 \left(9\, a3^{2} - 4\, a6\right) + 16 \left(9\, a4^{2} + 18\, a3\, a5 - 4\, a8\right)\right) +$$

$$
71680 \left(243\, a2^3\, a3 - 54\, a3^3 - 324\, a2\, a3\, a4 - 162\, a2^2\, a5 + 72\, a4\, a5 + 72\, a3\, a6 + 72\, a2\, a7 - 16\, a9\right)\Big)
$$

$$
\mathrm{Sin}\left[\frac{9\, x\tau}{a0}\right] + \left(\frac{78125\, a1^{10}}{145152} - a10 - \frac{78125\, a1^8\, a2}{8064} + \frac{15625\, a1^7\, a3}{1008} + \frac{3125}{288}\, a1^6 \left(5\, a2^2 - 2\, a4\right) - \right.
$$

$$
\frac{625}{24}\, a1^5\, (5\, a2\, a3 - a5) - \frac{625}{144}\, a1^4 \left(25\, a2^3 - 15\, a3^2 - 30\, a2\, a4 + 6\, a6\right) +
$$

$$
\frac{125}{12}\, a1^3 \left(25\, a2^2\, a3 - 10\, a2\, a5 + 2\, (-5\, a3\, a4 + a7)\right) - \frac{5}{24} \left(25\, a2^5 - 100\, a2^3\, a4 - \right.
$$

$$
\left. 30\, a2^2 \left(5\, a3^2 - 2\, a6\right) + 12 \left(5\, a3^2\, a4 - a5^2 - 2\, a4\, a6 - 2\, a3\, a7\right) + 12\, a2 \left(5\, a4^2 + 10\, a3\, a5 - 2\, a8\right)\right) +
$$

$$
\frac{25}{48}\, a1^2 \left(125\, a2^4 - 300\, a2\, a3^2 - 300\, a2^2\, a4 + 60\, a4^2 + 120\, a3\, a5 + 120\, a2\, a6 - 24\, a8\right) - \frac{5}{6}\, a1 \left(125\right.
$$

$$
\left.\left. a2^3\, a3 - 25\, a3^3 - 150\, a2\, a3\, a4 - 75\, a2^2\, a5 + 30\, a4\, a5 + 30\, a3\, a6 + 30\, a2\, a7 - 6\, a9\right)\right)\, \mathrm{Sin}\left[\frac{10\, x\tau}{a0}\right];
$$

(* $\phi[\tau]$ *)

$$\mathtt{\Phi od\tau[t\tau\_]} := \mathtt{Function}\Big[\{a, \epsilon\},\ \lambda = \frac{1}{2}\sqrt{a\left(1-\epsilon^{2}\right)}\ ;\ \eta = -\frac{1}{2\,a}\ ;\ \lambda i = \frac{1}{\lambda}\ ;$$

$$qq = \frac{3}{2}\,\frac{1}{\left(-3\,\lambda i^{2}+1\right)^{3/2}}\left(\sqrt{\left(\left(24\,\eta+12\,\eta^{2}\right)+\left(3-108\,\eta-378\,\eta^{2}-324\,\eta^{3}-81\,\eta^{4}\right)\lambda i^{2}-12\,\lambda i^{4}\right)}\right)\lambda i;$$

$$\Psi = -\mathtt{ArcSin}[qq];$$

$$U1 = \sqrt{1-3/\lambda^{2}} + \frac{1/\lambda^{2}}{1+\sqrt{1-3/\lambda^{2}}} - \frac{4}{3}\sqrt{1-3/\lambda^{2}}\ \mathtt{Sin}\left[\frac{\Psi}{6}\right]^{2};$$

$$U2 = \frac{1}{3}\left(\frac{3/\lambda^{2}}{1+\sqrt{1-3/\lambda^{2}}} - \sqrt{3}\,\sqrt{1-3/\lambda^{2}}\ \mathtt{Sin}\left[\frac{\Psi}{3}\right] + 2\sqrt{1-3/\lambda^{2}}\ \mathtt{Sin}\left[\frac{\Psi}{6}\right]^{2}\right);$$

$$U3 = \frac{1}{3}\left(\frac{3/\lambda^{2}}{1+\sqrt{1-3/\lambda^{2}}} + \sqrt{3}\,\sqrt{1-3/\lambda^{2}}\ \mathtt{Sin}\left[\frac{\Psi}{3}\right] + 2\sqrt{1-3/\lambda^{2}}\ \mathtt{Sin}\left[\frac{\Psi}{6}\right]^{2}\right);$$

$$na = \frac{1}{\sqrt{U1-U3}}\ ;\ ma = \frac{U2-U3}{U1-U3};$$

$$A0123 = \left\{\frac{1}{2}\left(\frac{\pi}{2\,\mathtt{EllipticK}[ma]}\right)^{2}\left(1+\frac{3\,ma}{8}-\frac{7\,ma^{2}}{64}\right),\ \frac{1}{2}\left(\frac{\pi}{2\,\mathtt{EllipticK}[ma]}\right)^{2}\left(1+\frac{ma}{2}+\frac{ma^{2}}{256}\right),\right.$$
$$\left.\frac{1}{2}\left(\frac{\pi}{2\,\mathtt{EllipticK}[ma]}\right)^{2}\left(\frac{ma}{8}+\frac{ma^{2}}{8}\right),\ \frac{1}{2}\left(\frac{\pi}{2\,\mathtt{EllipticK}[ma]}\right)^{2}\frac{ma^{2}\,3}{256},\ 0\right\};$$

$$KKK = \mathtt{Prepend}[\mathtt{AllCf}[A0123, U2, U3], \mathtt{C0f}[A0123, U2, U3]];$$

$$aaa = \mathtt{Table}\left[(-1)^{i}\,\frac{KKK[[i+1]]}{KKK[[1]]}\,\frac{1}{i},\ \{i, 10\}\right];\ Cf = \mathtt{Prepend}[aaa, 1];$$

$$ven = \frac{2\,\mathtt{EllipticK}[ma]\,na}{\pi}\ \mathtt{InvFun}\left[t\tau\,\frac{\lambda\,\pi}{4\,\mathtt{EllipticK}[ma]\,na\,KKK[[1]]},\ Cf\right]\Big];$$

(* End $\phi[\tau]$ *)

```
kκ[κ_, σ_] = (κ + σ)/2;
sκ[κ_, σ_] = (-κ + σ)/2;
Dodaj[sss_] = If[Mod[sss, 2] == 0, 0, 1];
Produkt = Function[{KT, KS},
   Vsotaκ[σ_, KTi_, KSi_] :=
     Sum[KTi[[1 + kκ[2 i + Dodaj[σ], σ]]] KSi[[1 + sκ[2 i + Dodaj[σ], σ]]] 1/2,
      {i, -Abs[IntegerPart[σ / 2]] - Dodaj[σ], Abs[IntegerPart[σ / 2]]}];
   Vsotaσ[κ_, KTj_, KSj_] := Sum[KTj[[1 + kκ[κ, 2 i + Dodaj[κ]]]]
       KSj[[1 + sκ[κ, 2 i + Dodaj[κ]]]] 1/2, {i, Abs[IntegerPart[κ / 2]],
       IntegerPart[Min[Length[KT], Length[KS]] / 2] - Dodaj[κ]}];
ven = Table[Vsotaκ[i, KT, KS] + If[i == 0, Vsotaσ[i, KT, KS],
        Vsotaσ[i, KT, KS] + Vsotaσ[-i, KT, KS]], {i, 0, Min[Length[KT], Length[KS]] - 1}];
```

(* t[ϕ] *)

$$\text{SchwTime} := \text{Function}\Big[\{a, \epsilon\},\ \lambda = \frac{1}{2}\sqrt{a\left(1-\epsilon^2\right)};$$

$$\eta = -\frac{1}{2a};$$

$$\lambda i = \frac{1}{\lambda};$$

$$qq = \frac{3}{2}\frac{1}{\left(-3\lambda i^2+1\right)^{3/2}}\left(\sqrt{\left(\left(24\eta+12\eta^2\right)+\left(3-108\eta-378\eta^2-324\eta^3-81\eta^4\right)\lambda i^2-12\lambda i^4\right)}\right)\lambda i;$$

$$\Psi = -\text{ArcSin}[qq];$$

$$U1 = \sqrt{1-3/\lambda^2}+\frac{1/\lambda^2}{1+\sqrt{1-3/\lambda^2}}-\frac{4}{3}\sqrt{1-3/\lambda^2}\ \text{Sin}\left[\frac{\Psi}{6}\right]^2;$$

$$U2 = \frac{1}{3}\left(\frac{3/\lambda^2}{1+\sqrt{1-3/\lambda^2}}-\sqrt{3}\sqrt{1-3/\lambda^2}\ \text{Sin}\left[\frac{\Psi}{3}\right]+2\sqrt{1-3/\lambda^2}\ \text{Sin}\left[\frac{\Psi}{6}\right]^2\right);$$

$$U3 = \frac{1}{3}\left(\frac{3/\lambda^2}{1+\sqrt{1-3/\lambda^2}}+\sqrt{3}\sqrt{1-3/\lambda^2}\ \text{Sin}\left[\frac{\Psi}{3}\right]+2\sqrt{1-3/\lambda^2}\ \text{Sin}\left[\frac{\Psi}{6}\right]^2\right);$$

$$na = \frac{1}{\sqrt{U1-U3}};$$

$$ma = \frac{U2-U3}{U1-U3};$$

$$A0123 = \left\{\frac{1}{2}\left(\frac{\pi}{2\,\text{EllipticK}[ma]}\right)^2\left(1+\frac{3\,ma}{8}-\frac{7\,ma^2}{64}\right),\ \frac{1}{2}\left(\frac{\pi}{2\,\text{EllipticK}[ma]}\right)^2\left(1+\frac{ma}{2}+\frac{ma^2}{256}\right),\ \frac{1}{2}\left(\frac{\pi}{2\,\text{EllipticK}[ma]}\right)^2\left(\frac{ma}{8}+\frac{ma^2}{8}\right),\ \frac{1}{2}\left(\frac{\pi}{2\,\text{EllipticK}[ma]}\right)^2\frac{ma^2\,3}{256},\ 0\right\};$$

KSQ = Prepend[AllCf[A0123, U2, U3], C0f[A0123, U2, U3]]; Kkm = EllipticK[ma];

$$qm = e^{-\pi\,\text{EllipticK}[1-ma]/Kkm};\ Energ = 1+\eta;\ Ktim =$$

$$\Big\{Energ+\Big(Energ\left(Kkm^2\,ma\left(1+qm\left(-1+qm+qm^4-qm^5+qm^6\right)\right)^2 U2-2\pi^2\,qm\left(1+qm\,(1+(-1+qm)\,qm)\right)\left(-4+qm\left(1+qm^2\right)(7+qm\,(-9+qm\,(8+qm\,(-7+qm\,(6+(-3+qm)\,qm)))))\right)\right)$$

$$(\mathrm{U2}-\mathrm{U3})))\Big/\left(\mathrm{Kkm}^2\,\mathrm{ma}\,(1+\mathrm{qm}\,(-1+\mathrm{qm}+\mathrm{qm}^4-\mathrm{qm}^5+\mathrm{qm}^6))^2\right)+$$

$$\frac{1}{\mathrm{Kkm}^4\,\mathrm{ma}^2\,(1+\mathrm{qm}^3)^4\,(1-\mathrm{qm}+\mathrm{qm}^2-\mathrm{qm}^3+\mathrm{qm}^4)^4}\,\mathrm{Energ}\,(\mathrm{Kkm}^4\,\mathrm{ma}^2\,(1-\mathrm{qm}+\mathrm{qm}^2+\mathrm{qm}^5-\mathrm{qm}^6+\mathrm{qm}^7)^4$$

$$\mathrm{U2}^2-4\,\mathrm{Kkm}^2\,\mathrm{ma}\,\pi^2\,\mathrm{qm}\,(1-\mathrm{qm}+\mathrm{qm}^2+\mathrm{qm}^5-\mathrm{qm}^6+\mathrm{qm}^7)^2\,(1-4\,\mathrm{qm}+11\,\mathrm{qm}^2-20\,\mathrm{qm}^3+31\,\mathrm{qm}^4-$$

$$40\,\mathrm{qm}^5+45\,\mathrm{qm}^6-40\,\mathrm{qm}^7+31\,\mathrm{qm}^8-20\,\mathrm{qm}^9+11\,\mathrm{qm}^{10}-4\,\mathrm{qm}^{11}+\mathrm{qm}^{12})\,\mathrm{U2}\,(\mathrm{U2}-\mathrm{U3})+$$

$$2\,\pi^4\,\mathrm{qm}^2\,(3-20\,\mathrm{qm}+92\,\mathrm{qm}^2-296\,\mathrm{qm}^3+777\,\mathrm{qm}^4-1716\,\mathrm{qm}^5+3340\,\mathrm{qm}^6-5764\,\mathrm{qm}^7+$$

$$8941\,\mathrm{qm}^8-12\,480\,\mathrm{qm}^9+15\,816\,\mathrm{qm}^{10}-18\,204\,\mathrm{qm}^{11}+19\,095\,\mathrm{qm}^{12}-18\,204\,\mathrm{qm}^{13}+15\,816\,\mathrm{qm}^{14}-$$

$$12\,480\,\mathrm{qm}^{15}+8941\,\mathrm{qm}^{16}-5764\,\mathrm{qm}^{17}+3340\,\mathrm{qm}^{18}-1716\,\mathrm{qm}^{19}+777\,\mathrm{qm}^{20}-296\,\mathrm{qm}^{21}+92\,\mathrm{qm}^{22}-$$

$$20\,\mathrm{qm}^{23}+3\,\mathrm{qm}^{24})\,(\mathrm{U2}-\mathrm{U3})^2),\ -\frac{2\,\mathrm{Energ}\,\pi^2\,\mathrm{qm}\,(1+\mathrm{qm}+\mathrm{qm}^2+\mathrm{qm}^3+\mathrm{qm}^4)\,(\mathrm{U2}-\mathrm{U3})}{\mathrm{Kkm}^2\,\mathrm{ma}\,(1+\mathrm{qm})^2\,(1-\mathrm{qm}+\mathrm{qm}^2-\mathrm{qm}^3+\mathrm{qm}^4)}-$$

$$(4\,\mathrm{Energ}\,\pi^2\,\mathrm{qm}\,(\mathrm{Kkm}^2\,\mathrm{ma}\,(1+\mathrm{qm}+\mathrm{qm}^2+\mathrm{qm}^3+\mathrm{qm}^4)\,(1-\mathrm{qm}+\mathrm{qm}^2+\mathrm{qm}^5-\mathrm{qm}^6+\mathrm{qm}^7)^2\,\mathrm{U2}-$$

$$2\,\pi^2\,\mathrm{qm}\,(1-2\,\mathrm{qm}+7\,\mathrm{qm}^2-7\,\mathrm{qm}^3+13\,\mathrm{qm}^4-9\,\mathrm{qm}^5+12\,\mathrm{qm}^6-\mathrm{qm}^7+7\,\mathrm{qm}^8-\mathrm{qm}^9+12\,\mathrm{qm}^{10}-$$

$$9\,\mathrm{qm}^{11}+13\,\mathrm{qm}^{12}-7\,\mathrm{qm}^{13}+7\,\mathrm{qm}^{14}-2\,\mathrm{qm}^{15}+\mathrm{qm}^{16})\,(\mathrm{U2}-\mathrm{U3}))\,(\mathrm{U2}-\mathrm{U3}))\Big/$$

$$(\mathrm{Kkm}^4\,\mathrm{ma}^2\,(1+\mathrm{qm})^4\,(1-\mathrm{qm}+\mathrm{qm}^2)^2\,(1-\mathrm{qm}+\mathrm{qm}^2-\mathrm{qm}^3+\mathrm{qm}^4)^3),$$

$$-\frac{4\,\mathrm{Energ}\,\pi^2\,\mathrm{qm}^2\,(1+\mathrm{qm}^4)\,(\mathrm{U2}-\mathrm{U3})}{\mathrm{Kkm}^2\,\mathrm{ma}\,(1+\mathrm{qm}^3+\mathrm{qm}^5+\mathrm{qm}^8)}+$$

$$(2\,\mathrm{Energ}\,\pi^2\,\mathrm{qm}^2\,(-4\,\mathrm{Kkm}^2\,\mathrm{ma}\,(1+\mathrm{qm}^4)\,(1-\mathrm{qm}+\mathrm{qm}^2+\mathrm{qm}^5-\mathrm{qm}^6+\mathrm{qm}^7)^2\,\mathrm{U2}+\pi^2\,(1+6\,\mathrm{qm}-21\,\mathrm{qm}^2+$$

$$67\,\mathrm{qm}^3-108\,\mathrm{qm}^4+184\,\mathrm{qm}^5-245\,\mathrm{qm}^6+333\,\mathrm{qm}^7-331\,\mathrm{qm}^8+353\,\mathrm{qm}^9-331\,\mathrm{qm}^{10}+333\,\mathrm{qm}^{11}-$$

$$245\,\mathrm{qm}^{12}+184\,\mathrm{qm}^{13}-108\,\mathrm{qm}^{14}+67\,\mathrm{qm}^{15}-21\,\mathrm{qm}^{16}+6\,\mathrm{qm}^{17}+\mathrm{qm}^{18})\,(\mathrm{U2}-\mathrm{U3}))\,(\mathrm{U2}-\mathrm{U3}))\Big/$$

$$(\mathrm{Kkm}^4\,\mathrm{ma}^2\,(1+\mathrm{qm})^4\,(1-\mathrm{qm}+\mathrm{qm}^2)^3\,(1-\mathrm{qm}+\mathrm{qm}^2-\mathrm{qm}^3+\mathrm{qm}^4)^3),$$

$$-\frac{2\,\mathrm{Energ}\,\pi^2\,\mathrm{qm}^3\,(3-5\,\mathrm{qm}+7\,\mathrm{qm}^2-5\,\mathrm{qm}^3+3\,\mathrm{qm}^4)\,(\mathrm{U2}-\mathrm{U3})}{\mathrm{Kkm}^2\,\mathrm{ma}\,(1+\mathrm{qm}^3)^2\,(1-\mathrm{qm}+\mathrm{qm}^2-\mathrm{qm}^3+\mathrm{qm}^4)}+$$

$$(4\,\mathrm{Energ}\,\pi^2\,\mathrm{qm}^3\,(-\mathrm{Kkm}^2\,\mathrm{ma}\,(3-5\,\mathrm{qm}+7\,\mathrm{qm}^2-5\,\mathrm{qm}^3+3\,\mathrm{qm}^4)\,(1-\mathrm{qm}+\mathrm{qm}^2+\mathrm{qm}^5-\mathrm{qm}^6+\mathrm{qm}^7)^2\,\mathrm{U2}+$$

$$2\,\pi^2\,(1-9\,\mathrm{qm}^2+47\,\mathrm{qm}^3-126\,\mathrm{qm}^4+264\,\mathrm{qm}^5-442\,\mathrm{qm}^6+642\,\mathrm{qm}^7-792\,\mathrm{qm}^8+856\,\mathrm{qm}^9-$$

$$792\,\mathrm{qm}^{10}+642\,\mathrm{qm}^{11}-442\,\mathrm{qm}^{12}+264\,\mathrm{qm}^{13}-126\,\mathrm{qm}^{14}+47\,\mathrm{qm}^{15}-9\,\mathrm{qm}^{16}+\mathrm{qm}^{18})\,(\mathrm{U2}-\mathrm{U3}))$$

$$(\mathrm{U2}-\mathrm{U3}))\Big/\,(\mathrm{Kkm}^4\,\mathrm{ma}^2\,(1+\mathrm{qm}^3)^4\,(1-\mathrm{qm}+\mathrm{qm}^2-\mathrm{qm}^3+\mathrm{qm}^4)^3),$$

$$(4\,\mathrm{Energ}\,\pi^2\,\mathrm{qm}^4\,(-2\,\mathrm{Kkm}^2\,\mathrm{ma}\,(1-\mathrm{qm}+\mathrm{qm}^2+\mathrm{qm}^5-\mathrm{qm}^6+\mathrm{qm}^7)^2\,\mathrm{U2}+$$

$$\pi^2\,(5-8\,\mathrm{qm}+9\,\mathrm{qm}^2+11\,\mathrm{qm}^3-33\,\mathrm{qm}^4+76\,\mathrm{qm}^5-107\,\mathrm{qm}^6+134\,\mathrm{qm}^7-107\,\mathrm{qm}^8+$$

$$76\,\mathrm{qm}^9-33\,\mathrm{qm}^{10}+11\,\mathrm{qm}^{11}+9\,\mathrm{qm}^{12}-8\,\mathrm{qm}^{13}+5\,\mathrm{qm}^{14})\,(\mathrm{U2}-\mathrm{U3}))\,(\mathrm{U2}-\mathrm{U3}))\Big/$$

$$(\mathrm{Kkm}^4\,\mathrm{ma}^2\,(1+\mathrm{qm})^4\,(1-\mathrm{qm}+\mathrm{qm}^2)^3\,(1-\mathrm{qm}+\mathrm{qm}^2-\mathrm{qm}^3+\mathrm{qm}^4)^3)+\frac{4\,\mathrm{Energ}\,\pi^2\,\mathrm{qm}^4\,(-\mathrm{U2}+\mathrm{U3})}{\mathrm{Kkm}^2\,\mathrm{ma}\,(1+\mathrm{qm}^3+\mathrm{qm}^5+\mathrm{qm}^8)},$$

$$(4\,\mathrm{Energ}\,\pi^2\,\mathrm{qm}^5\,(-\mathrm{Kkm}^2\,\mathrm{ma}\,(1-\mathrm{qm}+\mathrm{qm}^2)^3\,(1+\mathrm{qm}^5)^2\,\mathrm{U2}+$$

$$2\,\pi^2\,(4-13\,\mathrm{qm}+28\,\mathrm{qm}^2-41\,\mathrm{qm}^3+53\,\mathrm{qm}^4-54\,\mathrm{qm}^5+50\,\mathrm{qm}^6-38\,\mathrm{qm}^7+36\,\mathrm{qm}^8-38\,\mathrm{qm}^9+$$

```
50 qm^10 - 54 qm^11 + 53 qm^12 - 41 qm^13 + 28 qm^14 - 13 qm^15 + 4 qm^16) (U2 - U3)) (U2 - U3)) /
  (Kkm^4 ma^2 (1 - qm + qm^2)^3 (1 + qm^5)^4) + (2 Energ π^2 qm^5 (-U2 + U3))/(Kkm^2 ma (1 + qm^5)^2), 0, 0, 0};
Kff = Produkt[KSQ, Ktim] 2 / λ; ss = 0; Do[ss = If[Abs[Kff[[l]] / Kff[[1]]] > 10^-18, l, ss],
  {l, Length[Kff]}]; Funx = Prepend[Table[(-1)^s 2 (Kkm na)/(s π) Sin[s (π ϕ)/(2 na Kkm)], {s, ss}], ϕ];
ven = Sum[Kff[[i]] Funx[[i]], {i, ss}]];
```

(* End t[ϕ] *)

B From mutual to global constants of motion

```
(*
To calculate {t , t'} for two satellites
 moving on orbits with parameters
 MC1 and MC2 (MC={a,ϵ,ι,Ω,ω,t_peri})
*)
RotZ[Ome_] := {{Cos[Ome], -Sin[Ome], 0}, {Sin[Ome], Cos[Ome], 0}, {0, 0, 1}}
RotX[Ome_] := {{1, 0, 0}, {0, Cos[Ome], -Sin[Ome]}, {0, Sin[Ome], Cos[Ome]}}
RM[A_] := RotZ[A[[4]]].RotX[A[[3]]].RotZ[A[[5]]]
Orbita[A_, ϕ_] := RM[A].{A[[1]] (Cos[ϕ] - A[[2]]), A[[1]] Sqrt[1 - A[[2]]^2] Sin[ϕ], 0}
r[ϕ_, {a_, ϵ_, ι_, Ω_, ω_, tret_}] = Orbita[{a, ϵ, ι, Ω, ω}, ϕ];

δr[MoKo1_, MoKo2_, ϕi_, ψi_] =
  ((r[ϕi, MoKo1] - r[ψi, MoKo2]).(r[ϕi, MoKo1] - r[ψi, MoKo2]))^(1/2);
(* eccentric anomaly Ψ as a function of average anomaly M *)
Ψ[M_, ϵ_] := M + Sum[2/k BesselJ[k, k ϵ] Sin[k M], {k, 5}];
Δr = Function[{t, tp, MotionConst1, MotionConst2},
   Clear[ϕa, ψa]; ϕa = Ψ[(t - MotionConst1[[6]])/MotionConst1[[1]]^(3/2), MotionConst1[[2]]];
   ψa = Ψ[(tp - MotionConst2[[6]])/MotionConst2[[1]]^(3/2), MotionConst2[[2]]];
   ven = δr[MotionConst1, MotionConst2, ϕa, ψa]];
Ret = Function[{t, MotionConst1, MotionConst2},
   τ0 = Δr[t - MotionConst1[[6]], t - MotionConst2[[6]], MotionConst1, MotionConst2];
   res = FindRoot[Δr[t, t - τ, MotionConst1, MotionConst2] == c τ,
     {τ, τ0}, WorkingPrecision → 52]; ven = τ /. res];

(*
If MotionConst1 and MotionConst2 are
 constants of motion of satellites 1 and 2,
Casi will generate the pairs
 {t,t'} along eight orbits
*)

Casi =
```

```
Function[{MotionConst1, MotionConst2}, vm = (1/MotionConst1[[1]]^(3/2) + 1/MotionConst2[[1]]^(3/2));
  ven = Table[{(2 π i)/(vm 50), (2 π i)/(vm 50) - Ret[(2 π i)/(vm 50), MotionConst1, MotionConst2]}, {i, 400}]];
```

(* -- *)

(* Solve for orbital parameters from {t,t'} *)

(* distance with respect to mutual constants *)

```
δR[{a_, ap_, ϵ_, ϵp_, ι_, Ω_, ω_, t0_}, ϕ_, ψ_] :=
  Sqrt[(ap^2 Sin[ι]^2 (Sqrt[1 - ϵp^2] Cos[ω] Sin[ψ] + (-ϵp + Cos[ψ]) Sin[ω])^2 +
     (a Sqrt[1 - ϵ^2] Sin[ϕ] + ap (ϵp - Cos[ψ]) (Cos[ι] Cos[Ω] Sin[ω] + Cos[ω] Sin[Ω]) -
       ap Sqrt[1 - ϵp^2] Sin[ψ] (Cos[ι] Cos[ω] Cos[Ω] - Sin[ω] Sin[Ω]))^2 +
     (a (-ϵ + Cos[ϕ]) + ap Sqrt[1 - ϵp^2] Sin[ψ] (Cos[Ω] Sin[ω] + Cos[ι] Cos[ω] Sin[Ω]) +
       ap (ϵp - Cos[ψ]) (Cos[ω] Cos[Ω] - Cos[ι] Sin[ω] Sin[Ω]))^2)];

ΔR = Function[{t, tp, MotionConst}, Clear[ϕ, ψ];
  ϕ = Ψ[t/MotionConst[[1]]^(3/2), MotionConst[[3]]];
  ψ = Ψ[(tp - MotionConst[[8]])/MotionConst[[2]]^(3/2), MotionConst[[4]]]; ven = δR[MotionConst, ϕ, ψ]];
```

(* Identities: *)

```
Simplify[
 δR[{a, ap, -ϵ, -ϵp, ι, Ω + π, ω + π, to}, F + π, P + π]^2 - δR[{a, ap, ϵ, ϵp, ι, Ω, ω, to}, F, P]^2]

Simplify[δR[{a, ap, ϵ, ϵp, -ι, Ω, ω, to}, F, P]^2 - δR[{a, ap, ϵ, ϵp, ι, Ω, ω, to}, F, P]^2]
```

```
Simplify[δR[{a, ap, -ϵ, ϵp, ι, Ω, ω + π, to}, F + π, P]^2 - δR[{a, ap, ϵ, ϵp, ι, Ω, ω, to}, F, P]^2]

Simplify[δR[{a, ap, ϵ, -ϵp, ι, Ω + π, ω, to}, F, P + π]^2 - δR[{a, ap, ϵ, ϵp, ι, Ω, ω, to}, F, P]^2]

(* Action *)
Akcija =
  Function[{VsiCasi, tper1, InMC}, SetPrecision[Sum[((VsiCasi[[i, 1]] - VsiCasi[[i, 2]]) c -
        ΔR[VsiCasi[[i, 1]] - tper1, VsiCasi[[i, 2]], InMC])^2, {i, Length[VsiCasi]}], 32]];
(* angular momentum and Runge–Lenz vectors –
  Cartezian components *)
nλ[MC_] := Sqrt[MC[[1]] (1 - MC[[2]]^2)]
   {Sin[MC[[3]]] Sin[MC[[4]]], -Cos[MC[[4]]] Sin[MC[[3]]], Cos[MC[[3]]]};
nR[MC_] := MC[[1]] (1 - MC[[2]]^2) MC[[2]]
   {Cos[MC[[5]]] Cos[MC[[4]]] - Cos[MC[[3]]] Sin[MC[[5]]] Sin[MC[[4]]],
    Cos[MC[[3]]] Cos[MC[[4]]] Sin[MC[[5]]] + Cos[MC[[5]]] Sin[MC[[4]]],
    Sin[MC[[3]]] Sin[MC[[5]]]};
(*  Redu reduces periastron passage time to
  within the nearest periode of t=0,
RedT calculates Cartesian components of
  angular momentum and Runge–Lenz vector *)
Redu = Function[{A}, a1 = α /. A[[2]]; a2 = αp /.A[[2]]; T1 = π a1^(3/2); T2 = π a2^(3/2);
   tp1 = (x /. A[[2]]); tp2 = (tper /. A[[2]]); ven = {Mod[tp1, T1], Mod[tp2, T2]}];

(*RedT=Function[{A},a1=α/.A[[2]];a2=αp/.A[[2]];
   T1=π a1^(3/2);T2=π a2^(3/2);ϵ1=ϵ/.A[[2]];ϵ2=ϵp/.A[[2]];tp1=(x/.A[[2]]);
   tp2=(tper/.A[[2]]);Ome=Ω/.A[[2]];ome=ω/.A[[2]];MO1={a1,ϵ1,0,0,0,tp1};
   MO2={a2,ϵ2,ι/.A[[2]],Ome,ome,tper/.A[[2]]};
   ven={{(*Sqrt[a1(1-ϵ1^2)] *)nλ[MO1],(*a1(1-ϵ1^2)ϵ1*) nR[MO1],(*Sqrt[a2(1-ϵ2^2)] *)
      nλ[MO2],(*a2(1-ϵ2^2)ϵ2*) nR[MO2],{Mod[tp1,T1],Mod[tp2,T2]}}}];*)

RedTn = Function[{A}, a1 = α /. A[[2]]; a2 = αp /.A[[2]]; T1 = π a1^(3/2); T2 = π a2^(3/2);
   ϵ1 = ϵ /. A[[2]]; ϵ2 = ϵp /. A[[2]]; tp1 = (x /. A[[2]]); tp2 = (tper /. A[[2]]);
   Ome = Ω /. A[[2]]; ome = ω /. A[[2]]; Selectn = {ϵ1, ϵ2, ι, Ome, ome, tp1, tp2};
   NewSelectn = If[ϵ1 < 0, If[ϵ2 < 0, {-ϵ1, -ϵ2, ι, Ome + π, ome + π, tp1 + T1 / 2, tp2 + T2 / 2},
       {-ϵ1, ϵ2, ι, Ome, ome + π, tp1 + T1 / 2, tp2}],
     If[ϵ2 < 0, {ϵ1, -ϵ2, ι, Ome + π, ome, tp1, tp2 + T2 / 2}, {ϵ1, ϵ2, ι, Ome, ome, tp1, tp2}]];
   MO1 = {a1, NewSelectn[[1]], 0, 0, 0, NewSelectn[[6]]};
   MO2 =
    {a2, NewSelectn[[2]], ι /. A[[2]], NewSelectn[[4]], NewSelectn[[5]], NewSelectn[[7]]};
```

```
ven = {{(*√(a1(1-ϵ1²)) *)nλ[MO1], (*a1(1-ϵ1²)ϵ1*) nR[MO1], (*√(a2(1-ϵ2²)) *)
    nλ[MO2], (*a2(1-ϵ2²)ϵ2*) nR[MO2], {Mod[tp1, T1], Mod[tp2, T2]}}}];
(* Resitev calculates mutual constants of
 motion {α,αp,ϵ,ϵp,ι,Ω,ω,tper};
the first guess values don't seem to be too important,
but if they are too far from the correct
 solution one might get a bad solution,
which will show as a large action*)
Resitev = Function[{TimTb}, Res = FindMinimum[
    Akcija[TimTb, x, {α, αp, ϵ, ϵp, ι, Ω, ω, tper}], {α, 1.0}, {αp, 1.0}, {ϵ, 0.01},
    {ϵp, 0.01}, {ι, 0.7}, {Ω, 0.2}, {ω, 0.6}, {tper, 0}, {x, 0}]; ven = {Res, Redu[Res]}];
(* In addition to the output of Resitev the Cartesian
  components of the angular momenta and Runge–
 Lenz vectors are given in a frame where the angular
  momentum of satellite 1 and its Runge–Lenz vector
  are in the directions {0,0,1} and {1,0,0} respectively*)
ResitevKart =  Function[{TimTb, InitialGuess}, aG = InitialGuess[[1]];
  aGp = InitialGuess[[2]]; ϵG = InitialGuess[[3]]; ϵGp = InitialGuess[[4]];
  ιG = InitialGuess[[5]]; ΩG = InitialGuess[[6]]; ωG = InitialGuess[[7]];
  tperG = InitialGuess[[8]]; xG = InitialGuess[[9]];
  Res = FindMinimum[Akcija[TimTb, x, {α, αp, ϵ, ϵp, ι, Ω, ω, tper}], {α, aG},
    {αp, aGp}, {ϵ, ϵG}, {ϵp, ϵGp}, {ι, ιG}, {Ω, ΩG}, {ω, ωG}, {tper, tperG}, {x, xG},
    StepMonitor :→ Print[{α, αp, ϵ, ϵp, ι, Ω, ω, tper}]]; ven = {Res, RedTn[Res]}];
(*  ResitevKart output:
    ven[[1,1]] .... Akcija
                  ven[[1,2]]....{α→a,αp→a',ϵ→,ϵp→,ι→,Ω→,ω→,tper→t_per^2,x→t_per^2}
              ven[[2]][[1,1]]....λ1 (cartezian components ... λ1={0,0,√(a(1-ϵ²)) })
              ven[[2]][[1,2]]....R1 (cartezian components ... R1={aϵ(1-ϵ²),0,0})
              ven[[2]][[1,3]]....λ2 2
              ven[[2]][[1,4]].... R2
              ven[[2]][[1,5]]....{t_peri^1,t_peri^2}
*)

(* calculates constants of motion a,ϵ,ι,Ω,
ω from Cartesian components of λ and R *)
FromKart = Function[{Nλ, NR}, r0 = Nλ.Nλ;
  Nλn = Nλ / √r0 ;
```

```
Rn = Sqrt[NR.NR];
ϵps = Rn / r0;
NRn = NR / Rn;
NNN = Cross[Nλn, NRn];
ιnc = ArcCos[Nλ[[3]] / Sqrt[r0]];
Ωme = Arg[(Nλ[[2]] - ⅈ Nλ[[1]])] + π;
ωme = Arg[-(NNN[[3]] + ⅈ NRn[[3]])] + π; out = {r0/(1 - ϵps^2), ϵps, ιnc, Ωme, ωme, 0}];
```

```
MC = {a, ϵ, ι, Ω, ω, t_peri}
```

(* Set example constants and tests *)

```
MC2 = SetPrecision[{1.05, 0.001, 10 π/180, 35 π/180, 27 π/180, 2/10}, 60];
MC1 = SetPrecision[{1, 0.002, 40 π/180, 60 π/180, 47 π/180, 3/10}, 60];
MC3 = SetPrecision[{1, 0.0015, 40 π/180, 60 π/180, 47 π/180, 7/10}, 60];
c = 86000;
Plot[δr[MC1, MC2, ϕ, ϕ], {ϕ, 0, 8 π}]
(*  test retarded time  *)


TestRet = Function[{tm1}, dtret = Ret[tm1, MC1, MC2];
   Δr[tm1, tm1 - dtret, MC1, MC2]; Δr[tm1, tm1 - dtret, MC1, MC2] - c dtret];
TestRet[3.00000000000000000000000000000000000000000000000000000000000000]
TimTbl12 = Casi[MC1, MC2];
TimTbl21 = Casi[MC2, MC1];
TimTbl13 = Casi[MC1, MC3];
TimTbl31 = Casi[MC3, MC1];
TimTbl23 = Casi[MC2, MC3];
TimTbl32 = Casi[MC3, MC2];
ListPlot[{TimTbl12.{1, 0} - TimTbl12.{0, 1}, TimTbl21.{1, 0} - TimTbl21.{0, 1}}]
ListPlot[
 {TimTbl12.{1, 0} - TimTbl12.{0, 1} - TimTbl21.{1, 0} + TimTbl21.{0, 1}}, Joined → True]
```

```
(*  rotate the Cartesian vectors λ=λ{0,0,1},
R=R{1,0,0}, λ'=..., R'=... given by the solution of
 ResitevKart into the frame in which satellite's
 1 has angular constants of motion are ι, Ω, ω *)
ReduceToBaseFrameOftFrame =
  Function[{MIn, Soln}, RRR = RM[MIn]; ven = Table[RRR.Soln[[2]][[1, i]], {i, 4}]];

(*Test that constants of motion as found by
 minimization procedure give the original values*)
B12 = ResitevKart[TimTbl12, {1, 1.05, 0.0019, 0.001, -0.54, 0.1, -.1, 0.3, 0.2}]
FromKart[B12[[2]][[1, 1]], B12[[2]][[1, 2]]]
FromKart[B12[[2]][[1, 3]], B12[[2]][[1, 4]]]
BaseCart12 = ReduceToBaseFrameOftFrame[MC1, B12]
Faktor = {1, 500, 1, 500}
Sl1 = Show[Table[
    Graphics3D[{Red, Dashed, Arrow[{{0, 0, 0}, Faktor[[i]] BaseCart12[[i]]}]}], {i, 4}]];
Fig12 = Show[Graphics3D[{Blue, Arrow[{{0, 0, 0}, nλ[MC1]}]}],
  Graphics3D[{Blue, Arrow[{{0, 0, 0}, 500 nR[MC1]}]}],
  Graphics3D[{Blue, Arrow[{{0, 0, 0}, nλ[MC2]}]}],
  Graphics3D[{Blue, Arrow[{{0, 0, 0}, 500 nR[MC2]}]}], Sl1, ViewPoint → {5, 2, 1}]
BaseCart12[[1]] - nλ[MC1]
BaseCart12[[2]] - nR[MC1]
BaseCart12[[3]] - nλ[MC2]
BaseCart12[[4]] - nR[MC2]
```

{{5.87848 × 10^{-27}, {α → 1., αp → 1.05, ∈ → -0.002, ∈p → -0.001,
ι → -0.54415, Ω → 21.3131, ω → -28.3555, tper → -30.2212, x → -21.6911}},
{{{0., 0., 0.999998}, {0.00199999, 0., 0.}, {0.332761, 0.413127, 0.876695},
{0.00076934, -0.000713211, 0.0000440746}, {0.3, 0.2}}}}

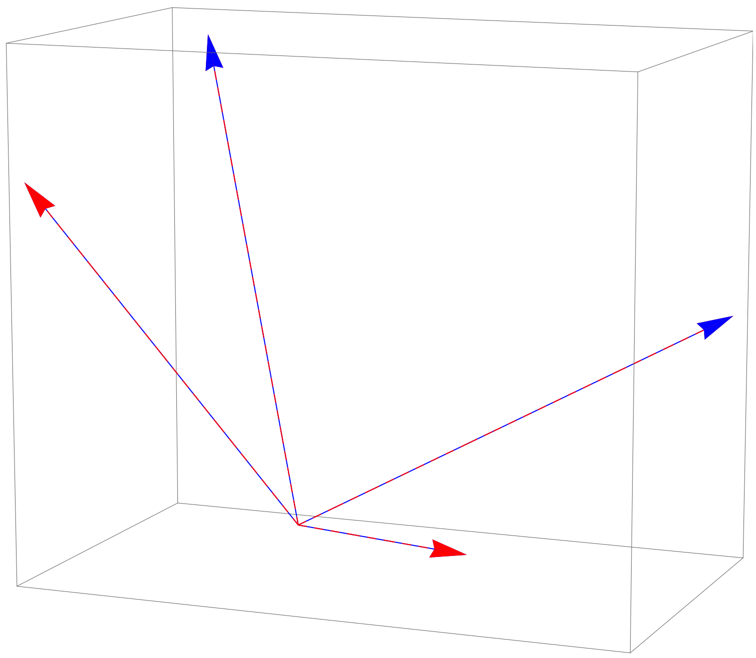

$\{-1.11022\times10^{-16},\ 0.,\ -1.11022\times10^{-16}\}$

$\{2.16678\times10^{-16},\ -1.30863\times10^{-15},\ -7.06358\times10^{-16}\}$

$\{-1.16226\times10^{-13},\ -2.64594\times10^{-13},\ -2.64233\times10^{-14}\}$

$\{3.41524\times10^{-16},\ -1.36609\times10^{-15},\ 6.91314\times10^{-17}\}$

```
err = FromKart[BaseCart12[[1]], BaseCart12[[2]]] - MC1
```

$\{-4.44089\times10^{-16},\ -1.50227\times10^{-15},\ 1.11022\times10^{-16},\ -4.44089\times10^{-16},$
$0.,\ -0.300000000000000000000000000000000000000000000000000000000000000\}$

```
err = FromKart[BaseCart12[[3]], BaseCart12[[4]]] - MC2
```

$\{0.,\ -9.82287\times10^{-16},\ 1.49214\times10^{-13},\ -1.388\times10^{-12},\ 4.96048\times10^{-13},$
$-0.200000000000000000000000000000000000000000000000000000000000000\}$

```
B21 = ResitevKart[TimTbl21, {1.05, 1.0, 0.001, 0.002, -0.5, 0, 0, 0.2, 0.3}]
FromKart[B21[[2]][[1, 1]], B21[[2]][[1, 2]]]
FromKart[B21[[2]][[1, 3]], B21[[2]][[1, 4]]]
BaseCart21 = ReduceToBaseFrameOftFrame[MC2, B21]
Faktor = {1, 500, 1, 500}
Sl2 = Show[Table[
    Graphics3D[{Red, Dashed, Arrow[{{0, 0, 0}, Faktor[[i]] BaseCart21[[i]]}]}], {i, 4}]];
Fig21 = Show[Graphics3D[{Blue, Arrow[{{0, 0, 0}, nλ[MC1]}]}],
  Graphics3D[{Blue, Arrow[{{0, 0, 0}, 500 nR[MC1]}]}],
  Graphics3D[{Blue, Arrow[{{0, 0, 0}, nλ[MC2]}]}],
  Graphics3D[{Blue, Arrow[{{0, 0, 0}, 500 nR[MC2]}]}], Sl2, ViewPoint → {5, 2, 1}]
BaseCart21[[1]] - nλ[MC2]
BaseCart21[[2]] - nR[MC2]
BaseCart21[[3]] - nλ[MC1]
BaseCart21[[4]] - nR[MC1]
```

$\{\{3.84374\times10^{-25}, \{\alpha\to1.05, \alpha p\to1., \epsilon\to0.001, \epsilon p\to-0.002,$
$\iota\to-0.54415, \Omega\to31.4971, \omega\to-21.3131, \text{tper}\to-21.6911, \text{x}\to-33.6013\}\},$
$\{\{\{0., 0., 1.02469\}, \{0.00105, 0., 0.\}, \{0.0419758, -0.515986, 0.855566\},$
$\{0.00146541, 0.00119613, 0.000649482\}, \{0.2, 0.3\}\}\}\}$

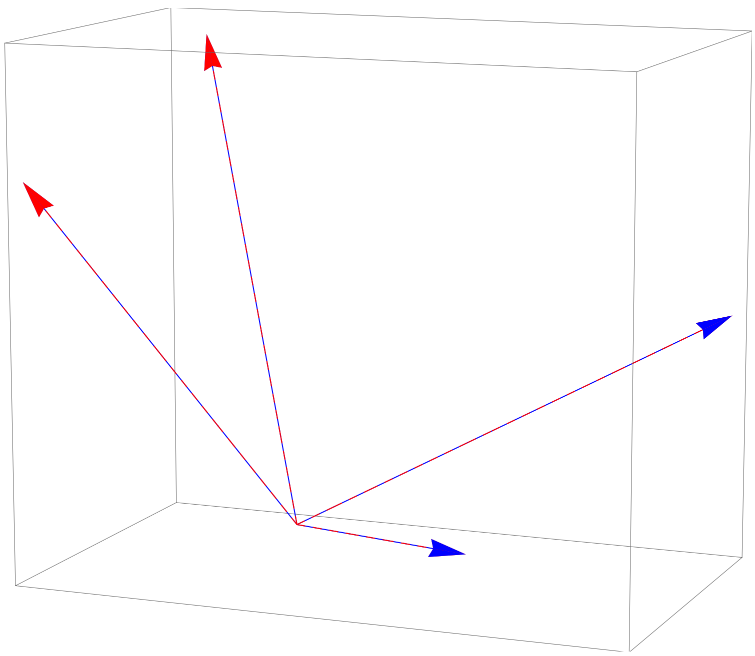

$\{0., 2.77556\times10^{-17}, 0.\}$

$\{-9.87058\times10^{-16}, -1.82905\times10^{-15}, -1.64365\times10^{-16}\}$

$\{2.76446\times10^{-14}, 6.14508\times10^{-14}, 5.66214\times10^{-15}\}$

$\{-1.25148\times10^{-14}, -2.51719\times10^{-14}, -1.60288\times10^{-15}\}$

```
err = FromKart[BaseCart21[[1]], BaseCart21[[2]]] - MC2
```

$\{-2.22045\times10^{-16}, -1.98539\times10^{-15}, 2.22045\times10^{-16}, -2.22045\times10^{-16},$
$0., -0.2000000000000000000000000000000000000000000000000000000000000\}$

```
err = FromKart[BaseCart21[[3]], BaseCart21[[4]]] - MC1
```

$\{-2.22045\times10^{-16}, -2.08674\times10^{-14}, -8.77076\times10^{-15}, 1.03917\times10^{-13},$
$9.37206\times10^{-12}, -0.3000000000000000000000000000000000000000000000000000000000000\}$

```
B13 = ResitevKart[TimTbl13, {1.0, 1.00001, 0.0021, 0.0015, 0.0001, 0.5, -0.5, 0.2, 0.7}]
FromKart[B13[[2]][[1, 1]], B13[[2]][[1, 2]]]
FromKart[B13[[2]][[1, 3]], B13[[2]][[1, 4]]]
BaseCart13 = ReduceToBaseFrameOftFrame[MC1, B13]
Faktor = {1, 500, 1, 500}
S13 = Show[Table[
    Graphics3D[{Red, Dashed, Arrow[{{0, 0, 0}, Faktor[[i]] BaseCart13[[i]]}]}], {i, 4}]];
Fig13 = Show[Graphics3D[{Blue, Arrow[{{0, 0, 0}, nλ[MC1]}]}],
  Graphics3D[{Blue, Arrow[{{0, 0, 0}, 500 nR[MC1]}]}],
  Graphics3D[{Blue, Arrow[{{0, 0, 0}, nλ[MC3]}]}],
  Graphics3D[{Blue, Arrow[{{0, 0, 0}, 500 nR[MC3]}]}], S13, ViewPoint → {5, 2, 1}]
BaseCart13[[1]] - nλ[MC1]
BaseCart13[[2]] - nR[MC1]
BaseCart13[[3]] - nλ[MC3]
BaseCart13[[4]] - nR[MC3]
```

$\{\{6.9104\times10^{-27}, \{\alpha\to1., \alpha p\to1., \epsilon\to0.00150002, \epsilon p\to0.00200003,$
$\iota\to4.13764\times10^{-6}, \Omega\to112.242, \omega\to-112.242, \text{tper}\to0.299994, x\to0.700006\}\},$
$\{\{\{0., 0., 0.999999\}, \{0.00150001, 0., 0.\}, \{-3.12299\times10^{-6}, -2.71421\times10^{-6}, 0.999998\},$
$\{0.00200002, -3.92977\times10^{-9}, 6.24604\times10^{-9}\}, \{0.700006, 0.299994\}\}\}$

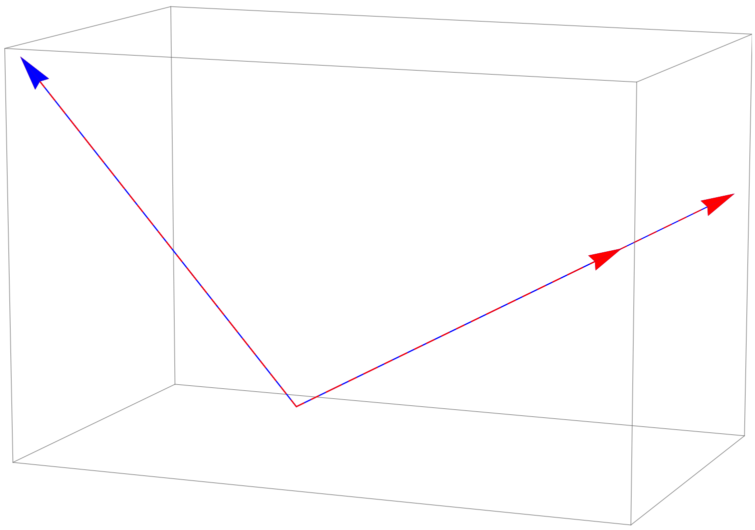

$\{4.87073\times10^{-7}, -2.81212\times10^{-7}, 6.70271\times10^{-7}\}$

$\{0.0000720925, -0.000435358, -0.000235043\}$

$\{2.18374\times10^{-6}, -1.42802\times10^{-6}, -3.32833\times10^{-6}\}$

$\{-0.0000720922, 0.000435396, 0.000235067\}$

```
err = FromKart[BaseCart13[[1]], BaseCart13[[2]]] - MC1
```

$\{-6.65024\times10^{-14}, -0.000499983, 1.11022\times10^{-16}, 0., -4.44089\times10^{-16},$
$-0.30000000000000000000000000000000000000000000000000000000000\}$

```
err = FromKart[BaseCart13[[3]], BaseCart13[[4]]] - MC3
```

$\{-6.66134\times10^{-14},\ 0.000500028,\ 4.1351\times10^{-6},\ -2.25308\times10^{-7},\ -1.79226\times10^{-6},$
$-0.7000000000000000000000000000000000000000000000000000000000000\}$

```
B31 = ResitevKart[TimTbl31, {1.0, 1.00001, 0.00021, 0.0014, 0.001, -0.5, 0.5, 0.2, 0.7}]
FromKart[B31[[2]][[1, 1]], B31[[2]][[1, 2]]]
FromKart[B31[[2]][[1, 3]], B31[[2]][[1, 4]]]
BaseCart31 = ReduceToBaseFrameOftFrame[MC3, B31]
Faktor = {1, 500, 1, 500}
S31 = Show[Table[
    Graphics3D[{Red, Dashed, Arrow[{{0, 0, 0}, Faktor[[i]] BaseCart31[[i]]}]}], {i, 4}]];
Fig31 = Show[Graphics3D[{Blue, Arrow[{{0, 0, 0}, nλ[MC1]}]}],
  Graphics3D[{Blue, Arrow[{{0, 0, 0}, 500 nR[MC1]}]}],
  Graphics3D[{Blue, Arrow[{{0, 0, 0}, nλ[MC3]}]}],
  Graphics3D[{Blue, Arrow[{{0, 0, 0}, 500 nR[MC3]}]}], S31, ViewPoint → {5, 2, 1}]
BaseCart31[[1]] - nλ[MC3]
BaseCart31[[2]] - nR[MC3]
BaseCart31[[3]] - nλ[MC1]
BaseCart31[[4]] - nR[MC1]
```

$\{\{1.88779\times10^{-27},\ \{\alpha\to1.,\ \alpha p\to1.,\ \epsilon\to0.0015,\ \epsilon p\to0.002,$
$\iota\to-3.30441\times10^{-7},\ \Omega\to0.618641,\ \omega\to-0.618641,\ tper\to0.3,\ x\to0.7\}\},$
$\{\{\{0.,\ 0.,\ 0.999999\},\ \{0.0015,\ 0.,\ 0.\},\ \{-1.91632\times10^{-7},\ 2.69199\times10^{-7},\ 0.999998\},$
$\{0.00199999,\ 3.12162\times10^{-12},\ 3.83263\times10^{-10}\},\ \{0.7,\ 0.3\}\}\}\}$

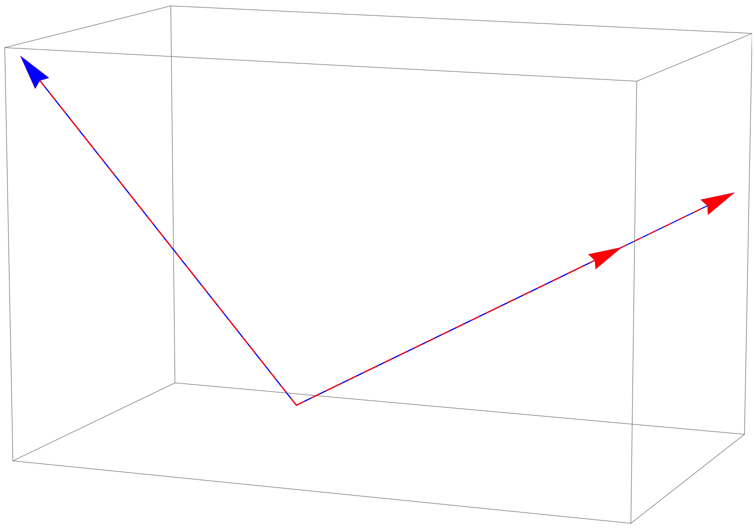

$\{-5.85088\times10^{-14},\ 3.37508\times10^{-14},\ -8.06022\times10^{-14}\}$

$\{-1.02261\times10^{-11},\ 6.1754\times10^{-11},\ 3.334\times10^{-11}\}$

$\{-1.92607\times10^{-7},\ -2.67046\times10^{-7},\ 2.79242\times10^{-8}\}$

$\{2.01641\times10^{-10},\ -6.90478\times10^{-11},\ 3.24816\times10^{-10}\}$

```
err = FromKart[BaseCart31[[1]], BaseCart31[[2]]] - MC3
```

$\{2.66454\times10^{-15}, 7.09207\times10^{-11}, 1.11022\times10^{-16}, -4.44089\times10^{-16},$
$0., -0.700000000000000000000000000000000000000000000000000000000000\}$

```
err = FromKart[BaseCart31[[3]], BaseCart31[[4]]] - MC1
```

$\{2.44249\times10^{-15}, 6.35002\times10^{-11}, -4.34426\times10^{-8}, -5.09613\times10^{-7}, 3.91947\times10^{-7},$
$-0.300000000000000000000000000000000000000000000000000000000000\}$

```
GraphicsArray[{{Fig12, Fig21}, {Fig13, Fig31}}]
```

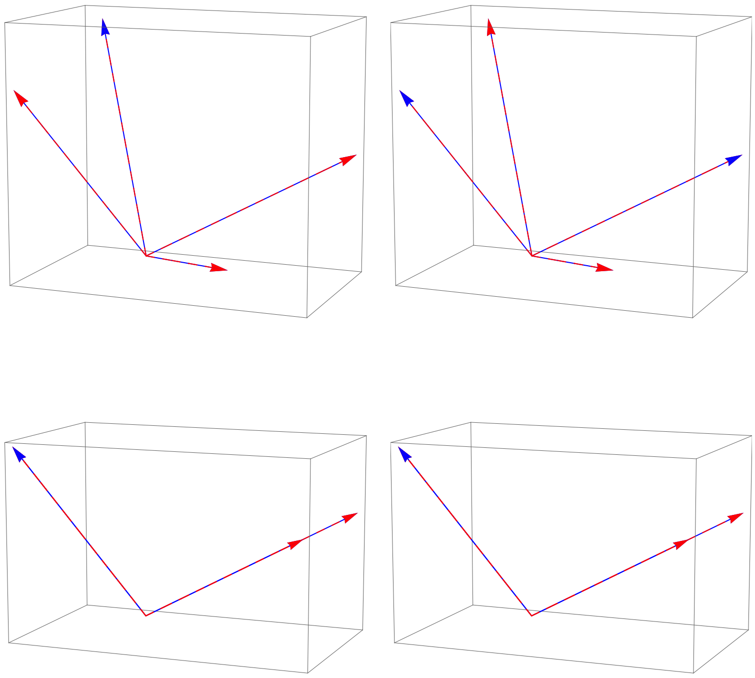

Bibliography

L. Arona, J. Pulido, F. Soualle, A. Fernández, and M. Sánchez-Nogales. GNSSPLUS, Final Report. GNSSPLUS-DMS-TEC-FIR01-11-E-R, 2006. URL http://esamultimedia.esa.int/docs/gsp/completed/C20105ExS.Pdf.

B. Coll and J. M. Pozo. Relativistic positioning systems: the emission coordinates. *Class. Quantum Grav.*, 23:7395–7416, 2006. doi: 10.1088/0264-9381/23/24/012.

B. Coll, J. J. Ferrando, and J. A. Morales-Lladosa. Newtonian and relativistic emission coordinates. *Phys. Rev. D*, 80(6):064038, 2009. doi: 10.1103/PhysRevD.80.064038.

B. Coll, J. J. Ferrando, and J. A. Morales-Lladosa. Positioning systems in Minkowski space-time: from emission to inertial coordinates. *Classical and Quantum Gravity*, 27(6):065013, 2010a. doi: 10.1088/0264-9381/27/6/065013.

B. Coll, J. J. Ferrando, and J. A. Morales-Lladosa. Positioning in a flat two-dimensional space-time: The delay master equation. *Phys. Rev. D*, 82(8):084038, 2010b. doi: 10.1103/PhysRevD.82.084038.

P. Delva, U. Kostić, and A. Čadež. Numerical modeling of a Global Navigation Satellite System in a general relativistic framework. *Advances in Space Research*, 47:370–379, 2011.

G. Petit, B. Luzum, and et al. IERS Conventions (2010). *IERS Technical Note*, 36:1, 2010. URL http://www.iers.org/nn_11216/SharedDocs/Publikationen/EN/IERS/Publications/tn/TechnNote36/tn36,templateId=raw,property=publicationFile.pdf/tn36.pdf.

I. Rodríguez-Pérez, C. García-Serrano, C. Catalán Catalán, A. M. García, P. Tavella, L. Galleani, and F. Amarillo. Inter-satellite links for satellite autonomous integrity monitoring. *Advances in Space Research*, 47:197–212, 2011.

A. Čadež, U. Kostić, and P. Delva. Mapping the Spacetime Metric with a Global Navigation Satellite System - Final Report, 2010. URL http://www.esa.int/gsp/ACT/doc/ARI/ARI Study Report/ACT-RPT-PHY-ARI-09-1301-MappingSpacetime-Ljubljana.pdf.